

THEORY OF THE HIGH ALTITUDE
ELECTROMAGNETIC PULSE

THESIS

GNE/PH/74-7

John R. Lillis
2Lt. USAF

Approved for public release; distribution unlimited.

UNCLASSIFIED

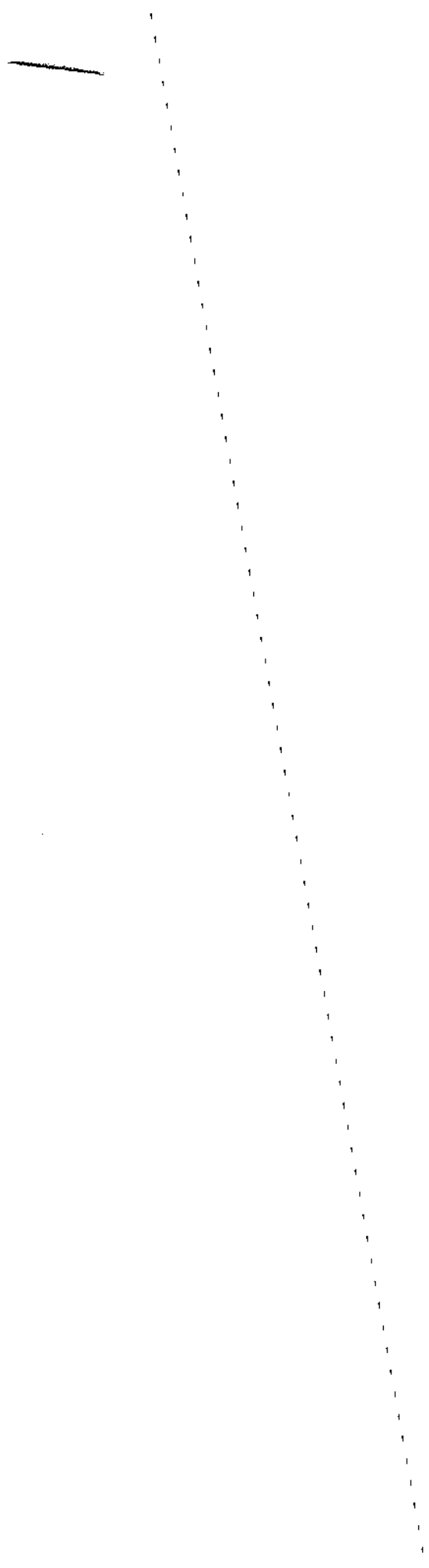
SECURITY CLASSIFICATION OF THIS PAGE (When Data Entered)

REPORT DOCUMENTATION PAGE		READ INSTRUCTIONS BEFORE COMPLETING FORM
1. REPORT NUMBER GNE/PH/74-7 ✓	2. GOVT ACCESSION NO.	3. RECIPIENT'S CATALOG NUMBER AD 777 846
4. TITLE (and Subtitle) THEORY OF THE HIGH ALTITUDE ELECTROMAGNETIC PULSE		5. TYPE OF REPORT & PERIOD COVERED M.S. Thesis
		6. PERFORMING ORG. REPORT NUMBER
7. AUTHOR(s) John R. Lillis 2nd Lt.		8. CONTRACT OR GRANT NUMBER(s)
9. PERFORMING ORGANIZATION NAME AND ADDRESS Air Force Institute of Technology (AFIT-EN) Wright Patterson AFB, Ohio 45433		10. PROGRAM ELEMENT, PROJECT, TASK AREA & WORK UNIT NUMBERS
11. CONTROLLING OFFICE NAME AND ADDRESS Air Force Institute Of Technology/ EMP Wright-Patterson AFB, Ohio 45433		12. REPORT DATE March 1974
		13. NUMBER OF PAGES 118
14. MONITORING AGENCY NAME & ADDRESS (if different from Controlling Office) Air Force Weapons Laboratory/ EL Kirtland AFB, New Mexico 87117		15. SECURITY CLASS. (of this report) Unclassified
		15a. DECLASSIFICATION/DOWNGRADING SCHEDULE
16. DISTRIBUTION STATEMENT (of this Report) Approved for public release, distribution unlimited		
17. DISTRIBUTION STATEMENT (of the abstract entered in Block 20, if different from Report) Reproduced by NATIONAL TECHNICAL INFORMATION SERVICE U S Department of Commerce Springfield VA 22151 Reproduced from best available copy. 		
18. SUPPLEMENTARY NOTES Approved for public release, IAW-APR 190-17 Jerry C. Hill, Captain, USAF Director of Information PRICES SUBJECT TO CHANGE		
19. KEY WORDS (Continue on reverse side if necessary and identify by block number) High Altitude Electromagnetic Pulse Compton Scatter Synchrotron Radiation Electrons Nuclear Weapon Effect Microscopic EMP Model		
20. ABSTRACT (Continue on reverse side if necessary and identify by block number) This thesis constitutes a microscopic approach to the electro- magnetic pulse (EMP) caused by a high altitude nuclear weapon burst. This approach involves the detailed calculations for the time- dependent electromagnetic fields of a single relativistic, Compton electron created in the upper atmosphere by the gamma radiation from the weapon detonation. The effect of all such electrons created is superimposed to obtain the net effect or the EMP measured by an observer. The basic theory developed ignores the conductivity which		

DD FORM 1473 1 JAN 73 EDITION OF 1 NOV 65 IS OBSOLETE

UNCLASSIFIED

SECURITY CLASSIFICATION OF THIS PAGE (When Data Entered)



THEORY OF THE HIGH ALTITUDE
ELECTROMAGNETIC PULSE

THESIS

Presented to the Faculty of the School of Engineering
of the Air Force Institute of Technology

Air University

in Partial Fulfillment of the
Requirements for the Degree of
Master of Science

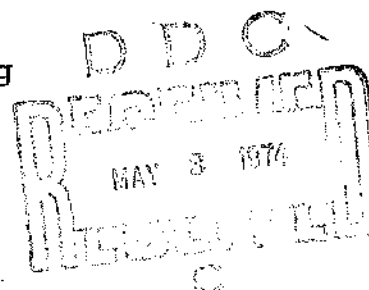
by

John R. Lillis

2Lt. USAF

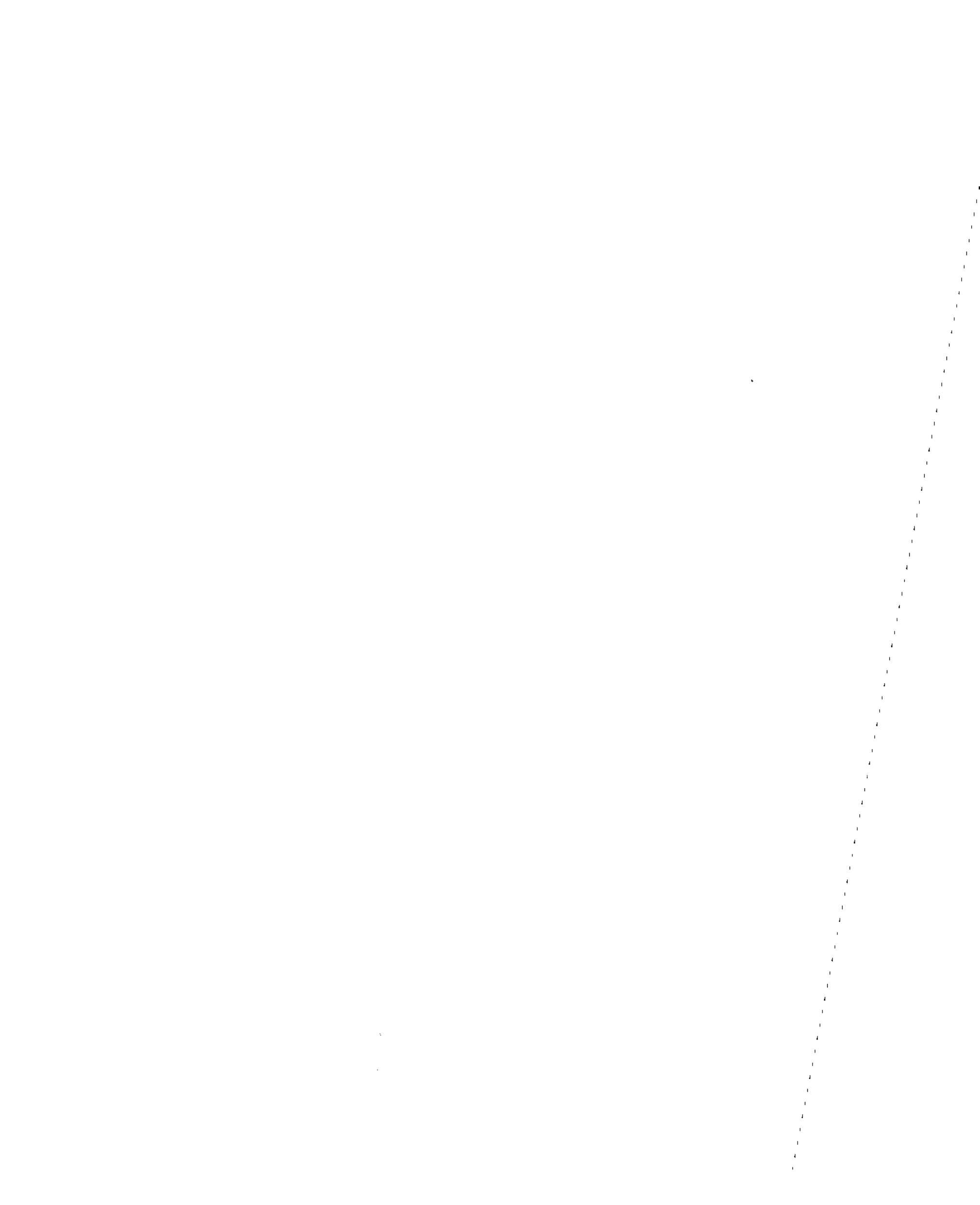
Graduate Nuclear Engineering

March 1974



Approved for public release; distribution unlimited.

ic



Preface

The purpose of this thesis has been to present a self-contained text explaining the fundamentals of the high altitude electromagnetic pulse in a manner which would provide a basic understanding of the phenomenon for the first year graduate student of Engineering. I would like to emphasize the fact that it has not been the purpose of this thesis to provide "state of the art" threat levels for the fields of the electromagnetic pulse. Rather, the calculations concerning these levels which are included in this report are meant only to show order of magnitude agreement of the model developed here with accepted theories. Although some of the results of derivations in the report involve advanced electromagnetic theory, I have attempted to develop these derivations in a manner that requires only a familiarity with integral and vector calculus, Maxwell's equations, and a few basic precepts of modern physics.

I would like to express my sincere appreciation to Major Carl T. Case for the many hours of guidance and advice which he devoted to this effort. I would also like to thank Dr. Charles J. Bridgman for his encouragement and interest in the project. Finally, I would like to acknowledge my wife's patience and support, without which I could not have completed this thesis.

1
2
3
4
5
6
7
8
9
10
11
12
13
14
15
16
17
18
19
20
21
22
23
24
25
26
27
28
29
30
31
32
33
34
35
36
37
38
39
40
41
42
43
44
45
46
47
48
49
50
51
52
53
54
55
56
57
58
59
60
61
62
63
64
65
66
67
68
69
70
71
72
73
74
75
76
77
78
79
80
81
82
83
84
85
86
87
88
89
90
91
92
93
94
95
96
97
98
99
100

Contents

	Page
Preface	ii
List of Figures	v
List of Tables	vi
Abstract	vii
I. Introduction	1
Definition	1
History	2
High Altitude EMP Source	3
Microscopic Versus Macroscopic	4
Overview	5
II. Review of Nuclear Weapon Physics and Effects	9
Origin and Nature of Radiation	9
Transport of Radiation Through the Environment	11
Creation of Electrons	17
Summary	23
III. Electromagnetic Theory of the High Altitude EMP	26
General Field Equations for a Single Electron	26
Electron Kinematics in the Atmosphere	31
Perpendicular Acceleration	32
Parallel Acceleration	36
Electron Trajectory	40
Fields for Electron Moving in Specific Manner	44
The Net Effect of Many Electrons	52
Line-of-Sight Effect	52
Superimposing Effect	56
IV. Sample Calculations	59
Line-of-Sight Area	59
Integration Over Absorption Layer	65
Discussion of Results	66
V. Effects of Air Conductivity	74
Formation and Buildup of Conductivity	74
Relative Significance of Conductivity	79
Field Equations for a Conducting Media	82
VI. Final Remarks	84
Bibliography	85

<u>Contents</u> <u>continued</u>	Page
Appendix A: Gamma Ray Interaction with Matter	87
Appendix B: Derivation of E and B for an Accelerated Electron	92
Appendix C: Derivation of the Green's Function for Conducting Media	105
Vita	108

List of Figures

Figure		Page
1	Generation of the High Altitude EMP	1
2	Empirical Time Dependence for Gamma Yield	12
3	EMP as Line-of-Sight Phenomenon	14
4	Geometry of High Altitude EMP	16
5	Mass Attenuation Coefficients for Photons in Air	18
6	Geometry of Compton Collision	20
7	Number Density of Primary Electrons Versus Altitude	24
8	Geometry for a Single Electron Source	30
9	Electron Moving in a Magnetic Field	33
10	Trajectory of an Electron in a Uniform Magnetic Field	35
11	Approximation of Continuous Slowing Down of Electron	39
12	Velocity Versus Time for Electron in Air	41
13	Electron Trajectory in Atmosphere	44
14	Geometry for Angular Distribution of Electron Radiation	48
15	E-Field for Single Electron Measured by Line-of-Sight Observer	51
16	Radiation Pattern for Electron in Circular Motion	53
17	Time Phasing for EM Fields for High Altitude EMP	53
18	Iso-power Lines for Electrons in Three Different Configurations Relative to Observer	62
19	Geometry for Finding the Line-of-Sight Radius	63
20	Line-of-Sight Radius as a Function of Altitude	64

<u>List of Figures continued</u>		Page
21	Top View of Electron in Line-of-Sight Area . . .	66
22	EMP Measured at Ground as a Function of Time . .	68
23	Effect of the Earth's Magnetic Field Orientation on the High Altitude EMP	70
24	The Horizon-to-Horizon Nature of the EMP	70
25	EMP Measured at Ground as a Function of Time . .	71
26	EMP Measured at Ground as a Function of Time . .	72
27	EMP Measured at Ground as a Function of Time . .	73
28	Conductivity as a Function of Altitude for a Fixed Time	80
29	Spherical Geometry for Attenuation Law	89

List of Tables

Table		Page
1	Calculations for Electron Trajectory	43
2	Comparison of $\frac{dP_L}{d\Omega}$ and $\frac{dP_C}{d\Omega}$ for Electron at 40 Km	49
3	Difference of Total Power Received for Electrons Off Line-of-Sight	61
4	Conductivity as a Function of Time	78

Abstract

This thesis constitutes a microscopic approach to the electromagnetic pulse (EMP) caused by a high altitude nuclear weapon burst. This approach involves the detailed calculations for the time-dependent electromagnetic fields of a single relativistic, Compton electron created in the upper atmosphere by the gamma radiation from the weapon detonation. The effect of all such electrons created is superimposed to obtain the net effect or the EMP measured by an observer. The basic theory developed ignores the conductivity which builds up in the surrounding air. This is shown to be a relatively good assumption for weapons with gamma radiation yields less than a kiloton. A brief section is included to indicate the derivations necessary for the EMP in a conducting media.

THEORY OF THE HIGH ALTITUDE
ELECTROMAGNETIC PULSE

I. Introduction

With the advent of nuclear weapons several previously unsuspected phenomena emerged as possible system damage mechanisms. One such phenomenon is the interaction of the radiation from a nuclear weapon with the environment in such a manner as to cause the motion of electric charges. The motion of these charges in turn causes a pulse of electric and magnetic fields which can be very intense and can be radiated for great distances. The nature of these fields varies according to the altitude at which the weapon is detonated. This thesis will concern only those fields associated with weapon detonations which occur at exoatmospheric altitudes. With the development of weapon systems involving highly sensitive electronics, the electric and magnetic fields of the electromagnetic pulse (EMP) associated with high altitude bursts constitute a phenomenon which should be fully understood by defense planners.

Definition

The EMP can be defined as a long range nuclear weapon effect wherein a high intensity, radio-frequency electromagnetic pulse is generated (Ref 9, chap X). There are several other similar nuclear effects which should not be confused with EMP. These include the Argus effect, the blackout phenomenon, and transient effect on electronics

(TREE). The Argus effect is the phenomenon whereby the electrons produced by a nuclear burst are trapped in the earth's magnetic field thereby creating a potential radiation hazard for personnel and electronic equipment (Ref 2, pg 1). The blackout phenomenon relates to the ionization produced by a nuclear detonation in or above the atmosphere and the subsequent radio frequency interference (BLACKOUT) resulting from the attenuating, reflecting, cluttering and scattering of radar and radio signals (Ref 2, pg 1). TREE refers to the direct effects of radiation on electronic systems and components (see also Ref 14, pp 1-3).

History

Although it has been said that Enrico Fermi predicted the EMP before the Trinity explosion on 16 July 1945 (Ref 14, pg 4), the high frequency component of this signal associated with high altitude weapon detonations did not become a seriously studied problem until the early 1960's. There are several reasons for the recent interest in this problem. One of these is the fact that the electronics in weapons systems have become more sensitive to extraneous electrical fields. Furthermore, it has been shown that the high altitude EMP can serve as a "signature" for a weapon detonation, thereby allowing for greater control of the ban on atmospheric testing. Also, there has been a greater understanding of the impact of the effect on systems previously thought hardened by defense planners.

Some of the first serious studies of the problem of the

high altitude EMP began in 1961 with theoretical studies by W. J. Karzas and R. Latter (Ref 12). These studies provided theoretical models and mechanisms for describing what was then the unconfirmed high frequency component of the high altitude EMP. The existence of this component was confirmed in the 1962 Pacific tests in which "a component of the 'radio flash' which depends on the magnetic bearing of the nuclear detonation from the observation point" was observed (Ref 20, pg 3). From the early 1960's until the present, the EMP, and more specifically the high altitude, high frequency EMP, has received a great deal of theoretical and experimental study.

High Altitude EMP Source

The EMP which results from a high altitude weapons burst is generated by electrons which are created in the upper atmosphere. These electrons are created by energetic photons (γ -rays) from the weapon which undergo collisions with the molecules of the air, ejecting atomic electrons. These scattered electrons are very energetic and radiate by means which will be described in a later chapter.

It should be noted that electromagnetic signals can arise from a nuclear burst from sources other than that mentioned above. An example of one such signal is the case signal which is associated with assymetries in the weapon casing. Another involves the electromagnetic fields generated within a system by the interaction of the weapon radiation with the materials of the system itself (System-

Generated EMP or SGEMP). A third example concerns the electrostatic fields in the near vicinity of the burst caused by charge separation due to ionization (Close-In EMP). The relative threats of these other effects are small as compared to the high altitude EMP.

Microscopic Versus Macroscopic

When calculating field strengths associated with the high altitude EMP, the general approach is "macroscopic" in nature. That is, one solves Maxwell's equations for electromagnetism using expressions for the "current" of electrons created in the upper atmosphere. Calculations are made based on the "current density" or the amount of charge passing through a unit area in a unit time interval. If one can find an expression for the current density, then, in principle, one can compute the electric and magnetic fields associated with this current.

Although the approach described above has been used with much success to obtain actual values for field strengths associated with the EMP, it is not an enlightening approach for one who is interested in the physical processes which are involved in the generation of the EMP. There is a considerable amount of physics "buried" in this macroscopic approach to the EMP. For this reason, it is the purpose of this thesis to develop a microscopic model of the high altitude EMP. Rather than calculating the EMP field strengths based on a current density, the fields for a single, accelerated electron have been calculated in great detail. The effect of all the

electrons created are then superimposed to obtain the overall or net field strength of the generated EMP. It is hoped that this microscopic approach will enable the serious student of the EMP to have a more basic and satisfying understanding of the high altitude EMP.

Overview

The first chronological step in the generation of the high altitude EMP is the production of gamma rays resulting from a nuclear burst. These gamma rays travel through the upper atmosphere depositing energy through Compton collisions thereby creating energetic electrons (See Figure 1). In Chapter II, which deals with the nature of the weapon gamma radiation and its transport through the atmosphere, it is shown that the number density of Compton electrons, N_{pri} , at a distance R from a burst occurring at an altitude of HOB is given by

$$(II-17) \quad N_{pri}(R, t) = \lambda(R) \frac{\exp\{\mu_0 Z_0 e^{-HOB/Z_0} (1 - e^{-R/Z_0})\}}{4\pi R^2} \\ \times \left\{ \frac{Y_\gamma}{E_\gamma} \int_0^t f(t' - \frac{R}{c}) dt' \right\}$$

where λ is the Compton macroscopic cross section, μ_0 is the total macroscopic cross section at sea level, Z_0 is the scale height, Y_γ is the total gamma yield, E_γ is the average gamma ray energy, $f(t)$ is the time dependence of the yield, and an exponential atmosphere has been assumed.

The Compton electrons are turned by the earth's magnetic field which causes them to radiate. It is shown

in Chapter III that, for a given observer, the radiated fields which he measures result from only those electrons moving within a small cross-sectional area centered about his line-of-sight with the weapon burst (see Figure 1). Further, it is shown that, for the periods when its radiation is significant, the electron has essentially a constant speed. The power radiated by such an electron is primarily in the forward direction (see Figures 15 and 16) as is indicated by the following formula (developed in Chapter III) for the power radiated per solid angle $\left(\frac{dP}{d\Omega}\right)_C$:

$$(III-40) \quad \frac{dP}{d\Omega}_C = \frac{1}{C\epsilon_v} \left(\frac{e\dot{\beta}}{4\pi}\right)^2 \frac{1}{(1-\beta \cos \psi)^3} \left\{1 - \frac{\sin^2 \psi \cos^2 \eta}{\gamma^2 (1-\beta \cos \psi)^2}\right\}$$

where C , ϵ_v , e are the speed of light, free space permittivity, and electron charge respectively, β is the electron's relative speed, $\dot{\beta}$ is its relative acceleration, and ψ and η are angles defined in Figure 14. If $A(R)$ represents the cross-sectional area which encloses electrons contributing to the EMP measured by an observer located at a distance X from the burst, then the time dependent fields which he observes are given by:

$$(III-46) \quad E(X,t) = \frac{Y}{E} \frac{X}{Y} \int_0^X dR \frac{A(R)\lambda(R)F(R)}{(X-R)} \int_0^{t-\frac{(X-R)}{C}} dT'' f(T'') E_e(t-T'')$$

where $F(R)$ is the R dependence given by the exponential term divided by $4\pi R^2$ in (II-17) above and $E_e(t)$ is the general time dependence of the field strengths radiated by a single electron and measured by the observer. This equation is developed in Chapter III.

Determining the size of $A(R)$ is one of the key cal-

culations in this approach. Chapter IV illustrates how to obtain this variable and also gives some results of the EMP which an observer would measure. These calculations were performed assuming that the conductivity of the air was zero. The range of validity for this assumption is checked in Chapter V and it is indicated how one might proceed when air conductivity is significant. The equations above and the developments which follow are relativistically correct.

Reproduced from
best available copy.

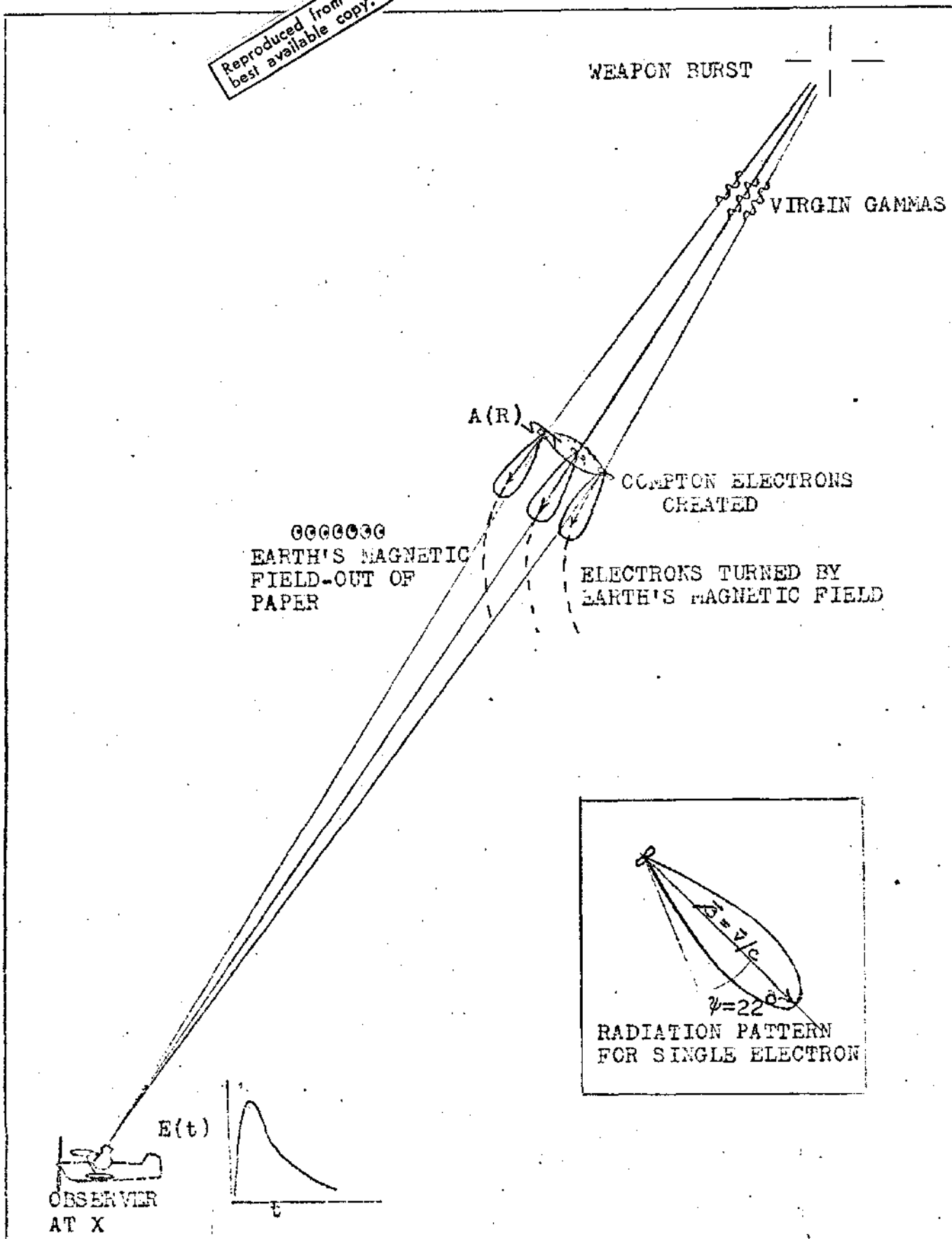


Figure 1. Generation of the High Altitude EMP.

II. Review of Nuclear Weapon Physics and Effects

Since the EMP depends upon the radiation emitted from a nuclear weapon, it is the purpose of this chapter, to present a brief discussion of the physics involved in the creation and transport of the radiation produced from a nuclear weapon detonation.

The chapter will encompass three main areas relating to weapon radiation. The first area will involve the origin and nature of the radiation that is produced within the initial weapon burst. Secondly, the transport of this radiation through the surrounding atmosphere will be considered. Finally, the interaction of the radiation with the atmosphere to create energetic electrons (Compton effect) will be investigated. Key derivations are included in the Appendices and are referenced throughout the main body of the text.

Origin and Nature of Radiation

With regard to the high altitude EMP the important portion of the weapon output is the radiation in the form of gamma rays and x-rays. For weapon detonations occurring below 100 or so kilometers, the primary source of the EMP involves only the electrons created by the gamma rays. One reason for this is that at these altitudes the range of the electrons created by the x-rays is too short to cause an appreciable current. Furthermore, for detonations at these altitudes, the x-rays are absorbed in a relatively small region about the burst point. This region has been

made conducting by ionization from the earlier emission of gamma rays and hence the weak radiation from the electrons created by the x-rays is effectively damped out (Ref 11, pp 40-5). Since the basic physics for the creation of the EMP is essentially the same for x-rays and gamma rays, only the EMP generated by gamma rays will be considered in this thesis.

There are two main characteristics of the gamma radiation output of the weapon which must be considered with respect to the EMP. First it is necessary to know the energy of the gamma rays and second, one must know the time dependence of the radiation yield of the weapon. The energy of the gamma rays produced in a typical theoretical fission device range from under 1.0 MeV up to around 5.0 MeV, with an average energy of approximately 1.5 MeV.¹ For simplicity, in any calculations which follow it shall be assumed that the spectrum of gamma rays emitted from a weapon is monoenergetic such that all gamma rays have an energy of 1.5 MeV. The time dependence of the radiation yield of a hypothetical weapon is characterized by a sharp rise followed by a decay both of which are generally described as exponential in nature. The physical reasons for the time dependence of the radiation output is beyond the scope of this study, however, the interested reader is referred to The Physics of Nuclear

¹Information concerning the average energy was obtained in private correspondence with Dr. C. J. Bridgman, Physics Dept., AFIT.

Explosives which is a set of class notes by Dr. C. J. Bridgman (Ref 1).

There have been several attempts to analytically describe the time dependence of weapon yield. One such attempt which is an empirical model for the time dependence presents the following formula.

$$(II-1) \quad f(t) = \frac{(\alpha+\beta)\exp\{\alpha(t-t_0)\}}{N(\beta+\alpha \exp\{(\alpha+\beta)(t-t_0)\})} \quad (\text{Ref 18})$$

where α and β are weapon parameters, t_0 represents the time t at which the time dependence $f(t)$ is a maximum and N is a normalization parameter chosen such that

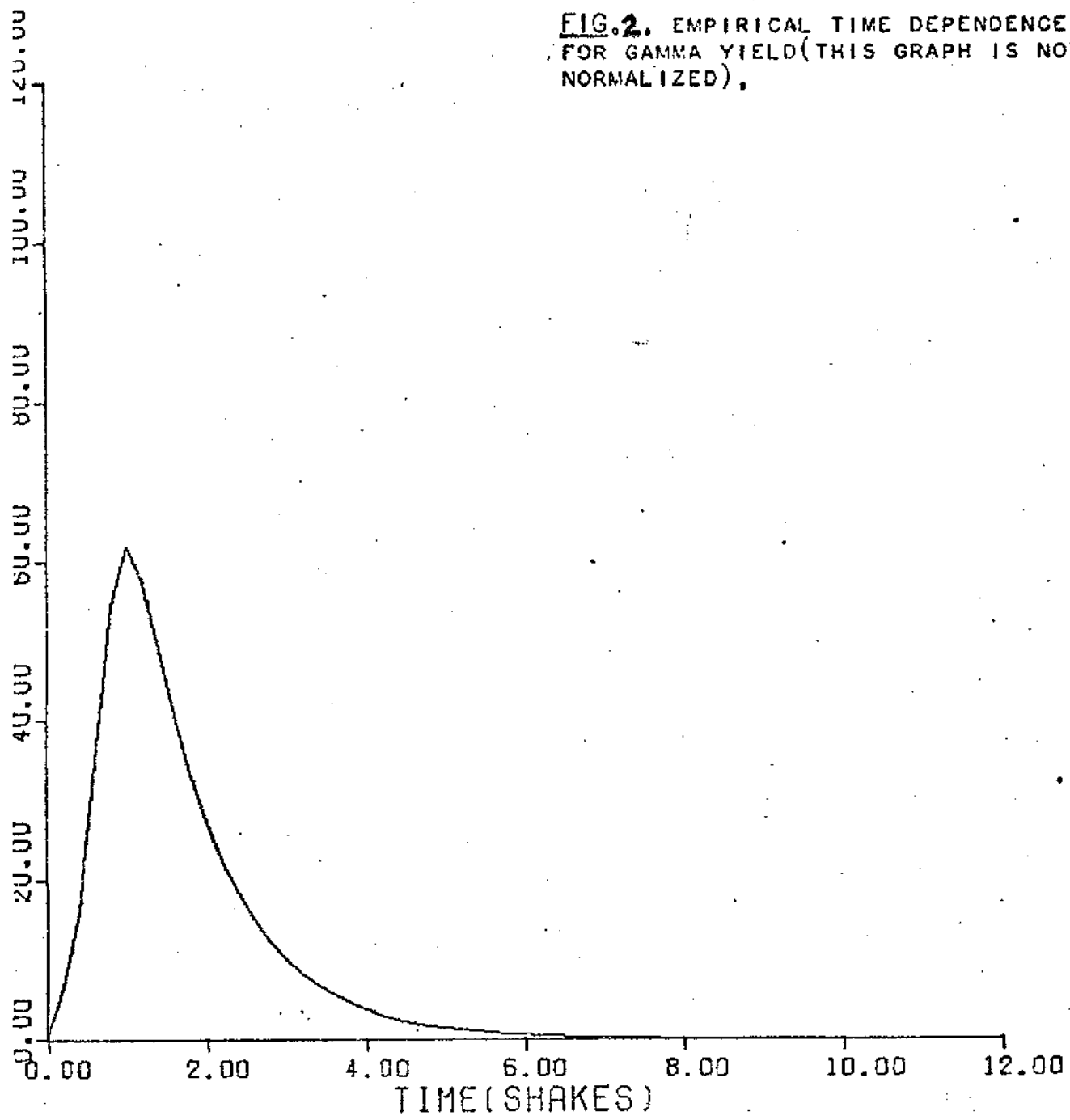
$$(II-2) \quad \int_0^{\infty} f(t) dt = 1.$$

A graph of this particular time dependence is given in Figure 2 using typical values of α and β .

Transport of Radiation Through the Environment

After one has an understanding of the nature (energy and time dependence) of the radiation emitted from a nuclear weapon, it is necessary to gain an understanding of how this radiation is transported through the surrounding environment. That is, if there is a given amount of radiation produced at the weapon burst, how much of this radiation will reach some point which is a known distance away.

If the gamma ray pulse emitted from a nuclear detonation can be described with respect to time by a function $f(t)$ as mentioned in the previous section then at any time t the number of gammas produced per second is given by (next page) . . .



$$(II-3) \quad \frac{dN_{\gamma}(t)}{dt} = \frac{Y_{\gamma} f(t)}{E_{\gamma}}$$

where Y_{γ} is the gamma yield of the explosion (in MeV), E_{γ} is the average photon energy (in MeV - assuming a monoenergetic source), and $N_{\gamma}(t)$ is the number of gamma rays. It can be shown (see Appendix A) that if the weapon burst is assumed to be a point source of gamma's then at a distance R from this source the number of unreacted or virgin gammas passing through a unit area per unit length of time (the virgin intensity - ϕ) is given by²

$$(II-4) \quad \phi(R,t) = \frac{dN_{\gamma}(t-\frac{R}{c})}{dt} \frac{e^{-\int_0^R \mu(r)dr}}{4\pi R^2}$$

where $\mu(r)$ is the total macroscopic cross section (see Appendix A) for photon reaction with the environment and c is the speed of light. As is evidenced by (II-4), when considering high altitude EMP one is concerned only with those gammas that arrive at a point R without having been scattered or acted upon by the environment in any manner (virgin intensity - ϕ). The reason for this is that the high frequency EMP associated with high altitude bursts is essentially a "line-of-sight" phenomenon. That is, if an observer is below the burst, then only those electrons that are traveling directly on the "line-of-sight" between the observer and the weapon burst will contribute significantly to the EMP that the observer measures (see Figure 3). This will be more

²The $\frac{R}{c}$ in the argument of N_{γ} accounts for time delay due to transport of γ - pulse over distance R .

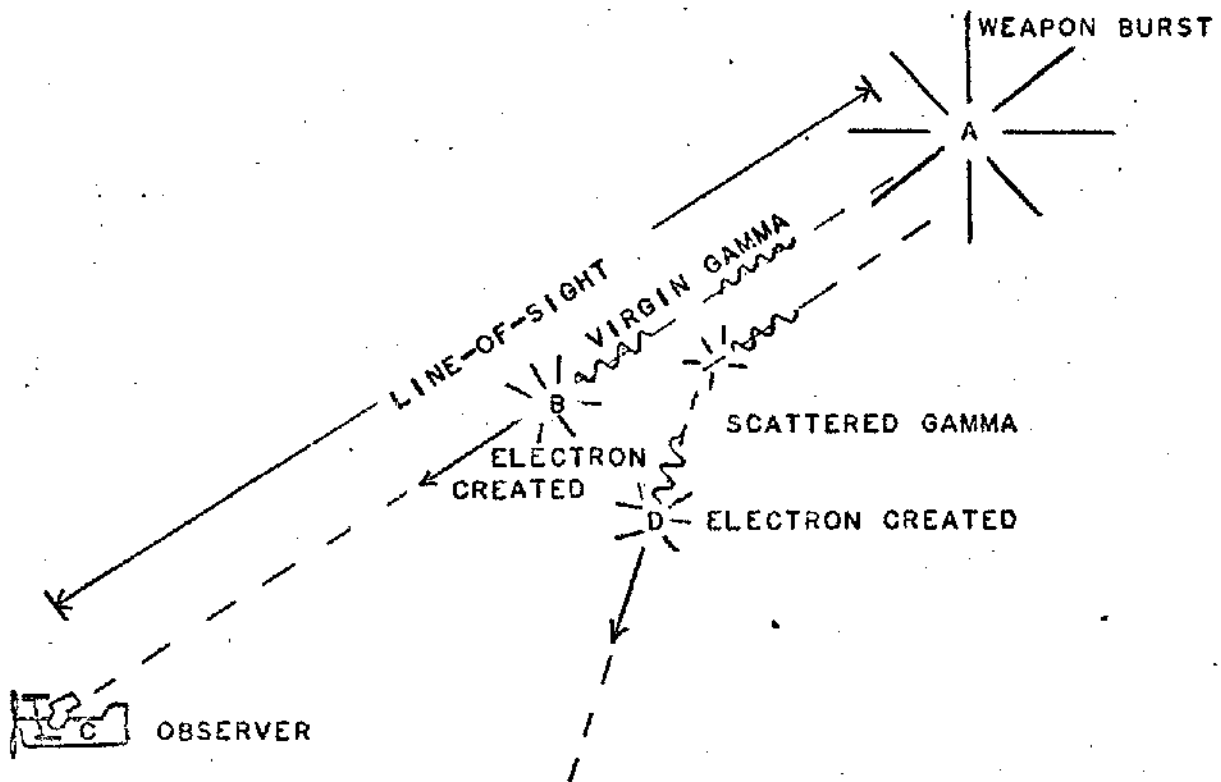


Figure 3. EMP as Line-of-Sight Phenomenon. The fields from the electron created at (B) will contribute to the EMP measured at (C) whereas the electron created at (D) will make no contribution.

fully explained in Chapter III. Although it is possible that a gamma photon which was not originally on the "line-of-sight" could be scattered onto the "line-of-sight" thereby creating an electron which could possibly contribute to the EMP, the chances for this are small enough that it will be ignored in the rest of this development.

Although (II-4) provides a formalistic solution to the problem of the transport of virgin gamma photons, it is desirable to have a form of $\Phi(R,t)$ with which one can obtain actual numerical values. The main problem with this in (II-4) is the following integral in the exponential term:

$$(II-5) \quad \int_0^R \mu(r) dr$$

In order to obtain a closed solution of this integral, it is necessary to make some approximations concerning the nature of the function $\mu(r)$. First it shall be assumed that the macroscopic cross section $\mu(r)$ varies with r only as the density of the media through which the gamma photons are being transported varies with r . In air, a good approximation is to let the density vary exponentially with the altitude Z above sea level (see Figure 4) such that

$$(II-6) \quad \rho(Z) = \rho_0 e^{-Z/Z_0}$$

where $\rho(Z)$ is the density of air at an altitude Z , ρ_0 is the density of air at sea level, and Z_0 is a scaling factor (if Z is measured in kilometers then $Z_0 \approx 7$). If one lets μ_0 represent the macroscopic cross section at sea level and makes the substitution $Z = HOB - r$ then using the approximations outlined above $\mu(r)$ becomes

$$(II-7) \quad \mu(r) = \mu_0 e^{-(HOB-r)/Z_0}$$

The integral in (II-5) can now be evaluated using (II-7) such that

$$(II-8) \quad \int_0^R \mu(r) dr = \int_0^R \mu_0 e^{-(HOB-r)/Z_0} dr$$

Upon integrating, the right hand side of the above becomes

$$\int_0^R \mu_0 e^{-(HOB-r)/Z_0} dr = \mu_0 Z_0 e^{-HOB/Z_0} \left(e^{r/Z_0} \Big|_0^R \right)$$

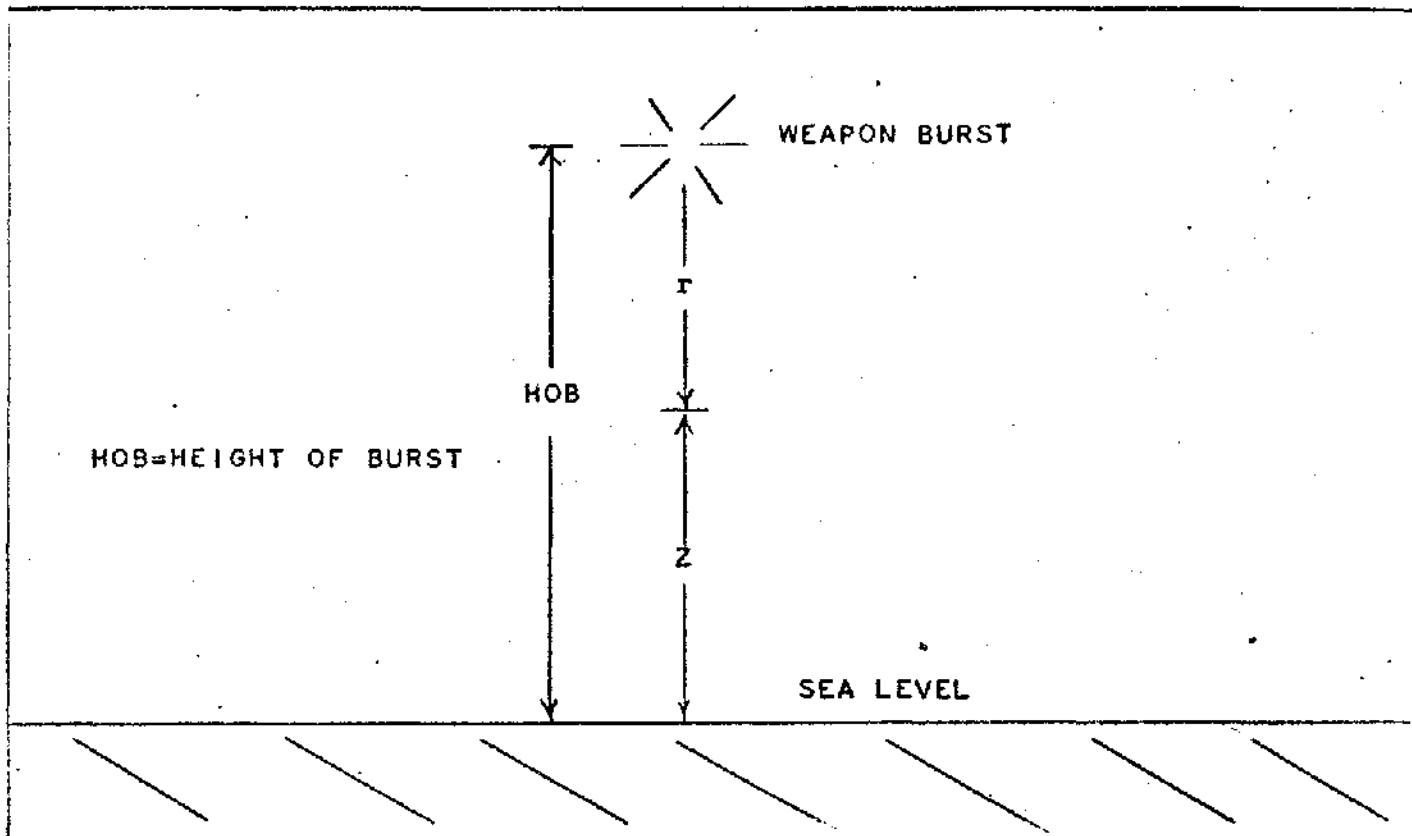


Figure 4. Geometry of High Altitude EMP.

or

$$(II-9) \quad \int_0^R \mu(r) dr = \mu_0 z_0 e^{-HOB/z_0} (e^{R/z_0} - 1) \quad (3)$$

Substituting (II-9) into (II-4) one has a closed solution for the virgin intensity of gamma photons at a distance R such that

$$(II-10) \quad \phi(R,t) = \frac{dN_\gamma(t - \frac{R}{C})}{dt} \frac{\exp\{\mu_0 z_0 e^{-HOB/z_0} (1 - e^{R/z_0})\}}{4\pi R^2}$$

Using the expression for $\frac{dN_\gamma}{dt}$ given in (II-3) the virgin

³The approximations made in solving this integral were obtained through private correspondence with Capt. Terry C. Chapman, GNE-74M, AFIT.

intensity can be written as

$$(II-11) \quad \Phi(R, t) = \frac{Y}{E_{\gamma}} f(t) \frac{\exp\{\mu_0 z_0 e^{-HOB/z_0} (1 - e^{-R/z_0})\}}{4\pi R^2}$$

The reader should be aware that it has been tacitly assumed that the macroscopic cross section $\mu(r)$ is independent of time. For early time periods following a weapon burst this is a safe assumption. The air chemistry involved in late time calculations concerning $\mu(r)$ are beyond the scope of this thesis.

Creation of Electrons

There are several ways in which gamma photons can interact with the molecules of air to produce electrons. These processes include the photoelectric effect, pair production, and the Compton effect. The probability of any one of these events occurring to a given gamma photon depends upon the energy of that photon and the material through which it is traveling. This fact is illustrated in Figure 5 on the following page which is a graph of the mass attenuation coefficients⁴ corresponding to the various processes as a function of the energy of the photon in air. The curve corresponding to total attenuation is the overall sum of all the individual effects. With respect to Figure 5 one can see that for relatively low energies (<0.1 MeV) the photoelectric effect is the predominant factor in the total

⁴The mass attenuation coefficient is the macroscopic cross section (see Appendix A) divided by the density of the photon environment.

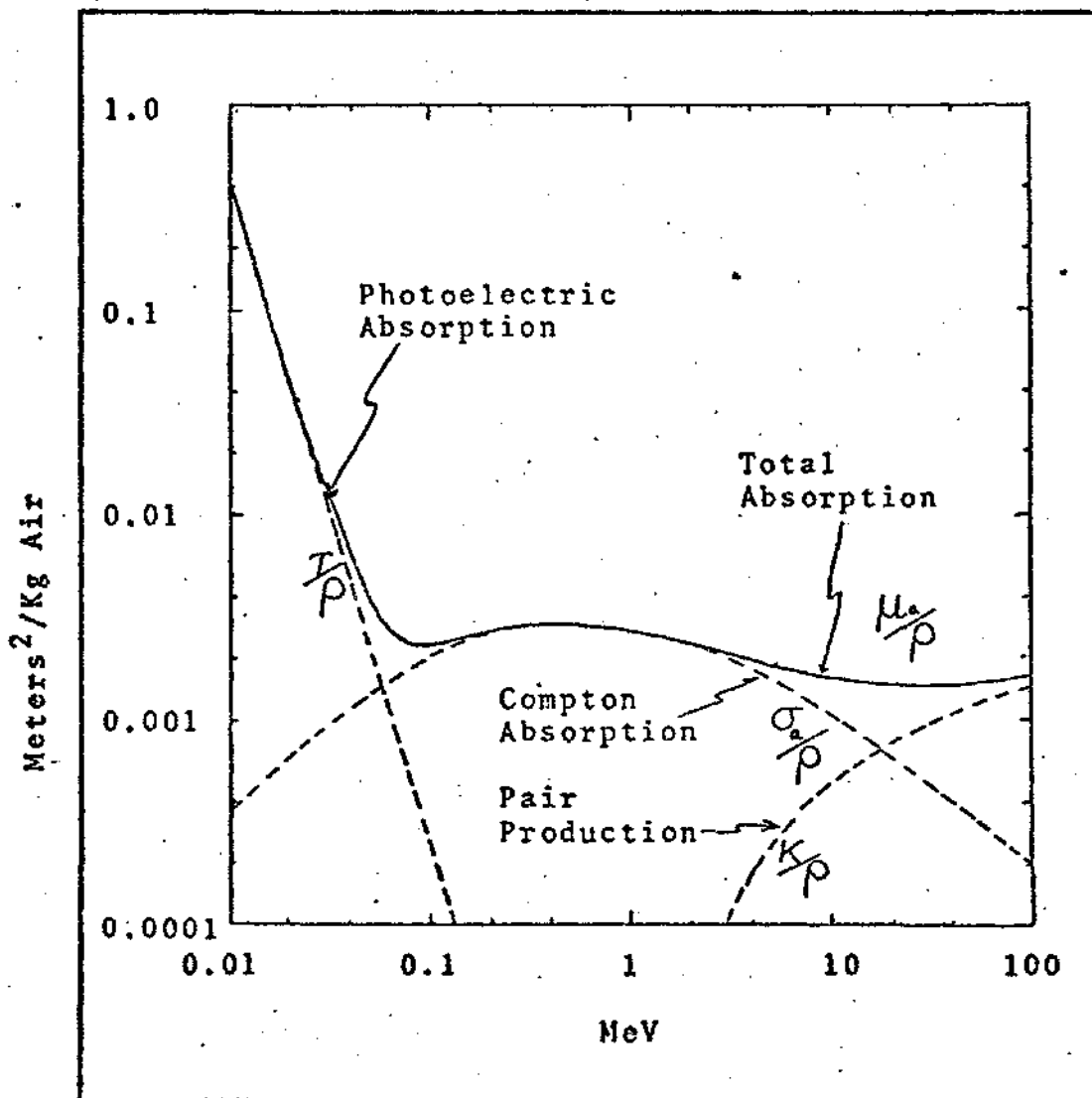


Fig. 5. Mass Attenuation Coefficients for Photons in Air. The curve marked "total absorption" is $(\mu_a/\rho) = (\sigma_a/\rho) + (\tau/\rho) + (\kappa/\rho)$ where σ_a , τ and κ are the corresponding linear coefficients for Compton absorption, photoelectric absorption, and pair production; ρ is the air density. For example at 1.5 MeV the Compton absorption is 2.4×10^{-5} meter²/kg of air; at 0° C and 760 mm Hg pressure, the density of air is $\rho = 1.293$ kg/m³. (Ref. 14, p.40)

attenuation whereas for relatively high photon energies (>10 MeV) pair production provides the major contribution. However, for the intermediate photon energies (between 0.1 and 10 MeV) the Compton effect is the predominant interaction for photon attenuation. Therefore, since weapon gamma radiation consists of photons with energies between 1 MeV and 5 MeV the Compton process is the effect which shall be considered with respect to the creation of electrons.

The Compton effect (scatter) is the process whereby a gamma photon is scattered by an atomic electron such that the energy of the gamma photon is decreased and the electron, which will be assumed to be initially at rest, is ionized and set into motion. For gamma photons of 1.5 MeV the atomic electrons, because of their relatively low binding energy, may be considered as free electrons which are at rest. The geometry of the situation is illustrated in Figure 6. If E_γ is the incident photon energy then one can easily show (see Appendix A) that the energy of the scatter photon is given by the relation

$$(II-12) \quad E'_\gamma = \frac{E_\gamma}{1 + (1 - \cos \theta) E_\gamma / m_0 c^2}$$

where θ is the angle between the direction of the incident and scattered photon (see Figure 6), m_0 is the electron rest mass, and c is the speed of light in a vacuum. The kinetic energy of the scattered electron T_e can be easily found using the conservation of energy (assuming elastic

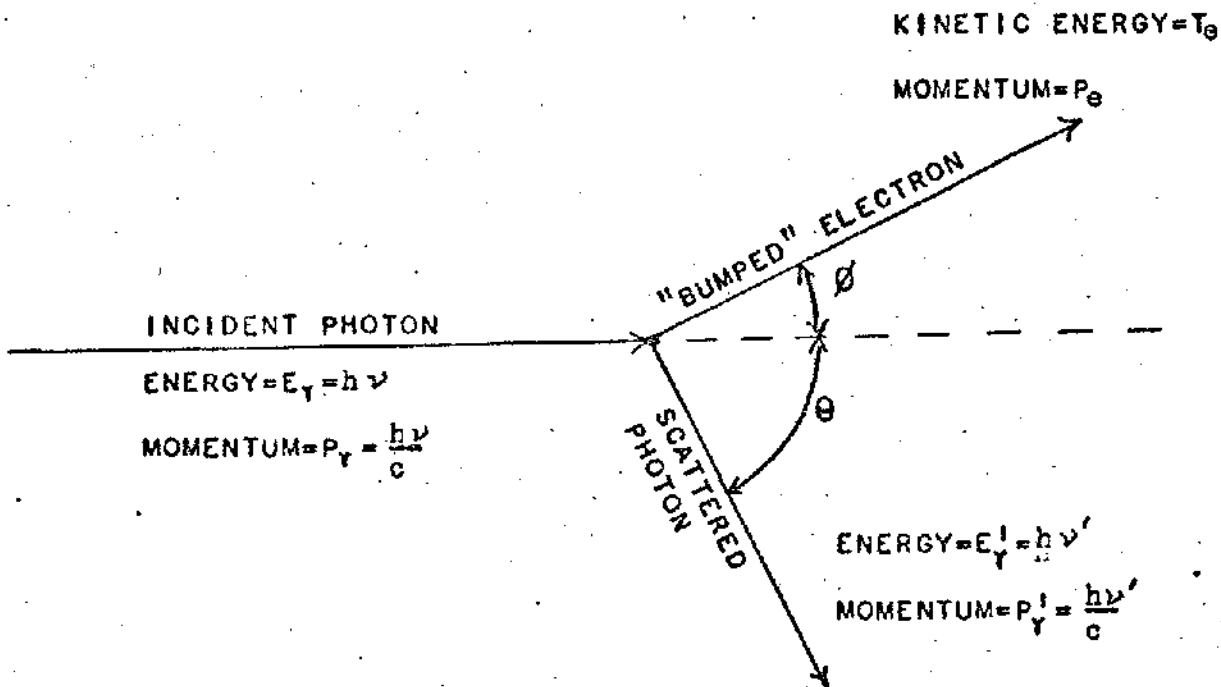


Figure 6. Geometry of Compton Collision. (h is Planck's constant and ν is the photons' frequency)

collision). That is

$$(II-13) \quad T_e = E_Y - E'_Y = E_Y \left\{ \frac{(1 - \cos \theta) E_Y / m_0 c^2}{1 + (1 - \cos \theta) E_Y / m_0 c^2} \right\}$$

As was mentioned earlier, the only electrons which are of interest with respect to the high altitude EMP are those which are moving on the "line-of-sight" that is, those electrons corresponding to $\phi = 0$. This is not entirely true. It will be shown that electrons which vary slightly off the "line-of-sight" do contribute to the EMP. Although the majority of electrons scattered by 1.5 MeV gamma photons are in the "line-of-sight" direction ($\phi = 0$), one can show that there is a distribution of directions for the scattered electrons ranging from $\phi = 0^\circ$ to $\phi = 90^\circ$ (Ref 17, pp 16-9). It is possible to account for those electrons scattered off

the "line-of-sight" but which still contribute to the EMP. However, this is a secondary effect and will be ignored in this thesis. Therefore it will be assumed that all the electrons created by the gamma photons travel in the initial direction of the gamma photon ($\theta=0^\circ$). To find T_e for these electrons, one uses (II-13) with $\theta=180^\circ$ since momentum must be conserved. Thus

$$(II-14) \quad T_{e-LoS} = \frac{E_\gamma}{1 + m_0 c^2 / 2E_\gamma}$$

where T_{e-LoS} is the kinetic energy for the "line-of-sight" electrons.

Since it will be necessary later to superimpose the individual effects of these Compton electrons, it is desirable to know how many of these are created at various distances from the burst. A quantity which is needed in determining this is the reaction rate or the number of Compton events which occur in a unit volume over a unit time period. If λ is the macroscopic cross section for the Compton interaction and $\phi(r,t)$ is the virgin intensity of gamma photons at a distance r from the burst, then the reaction rate for Compton scatter of virgin photons is given by the relation

$$(II-15) \quad R_C(r,t) = \lambda(r) \phi(r,t)$$

where R_C is the reaction rate. If one assumes that each one of these events creates an energetic electron which contributes to the EMP (it's motion is on the "line-of-sight") then the time rate of change of the number density

of these "primary" electrons would be given by the relation

$$\frac{dN_{\text{pri}}(r,t)}{dt} = R_c(r,t)$$

or

$$(II-16) \quad \frac{dN_{\text{pri}}(r,t)}{dt} = \lambda(r) \phi(r,t)$$

where N_{pri} is the primary electron number density. Therefore, at any time t after the detonation and at any distance R from the point of detonation, the number density of primary electrons is

$$N_{\text{pri}}(R,t) = \lambda(R) \int_0^t \phi(R,t') dt'$$

or using equation (II-10) and (II-4)

$$(II-17) \quad N_{\text{pri}}(R,t) = \lambda(R) \frac{\exp\{\mu_0 Z_0 e^{-H_0 B/Z_0} (1 - e^{-R/Z_0})\}}{4\pi R^2} \\ \times \left\{ \frac{Y}{E_\gamma} \int_0^t f\left(t' - \frac{R}{C}\right) dt' \right\}$$

To see physically what is represented by (II-17) one should understand how the gamma energy is deposited throughout the atmosphere with respect to distance from the burst. This can be done by considering (II-17) for late times ($t \rightarrow \infty$). If one assumes a normalized time function then in the limit as t approaches ∞ the expression for N_{pri} becomes

$$(II-18) \quad N_{\text{pri}}(R,t \rightarrow \infty) = \lambda(R) \frac{Y}{E_\gamma} \frac{\exp\{\mu_0 Z_0 e^{-H_0 B/Z_0} (1 - e^{-R/Z_0})\}}{4\pi R^2}$$

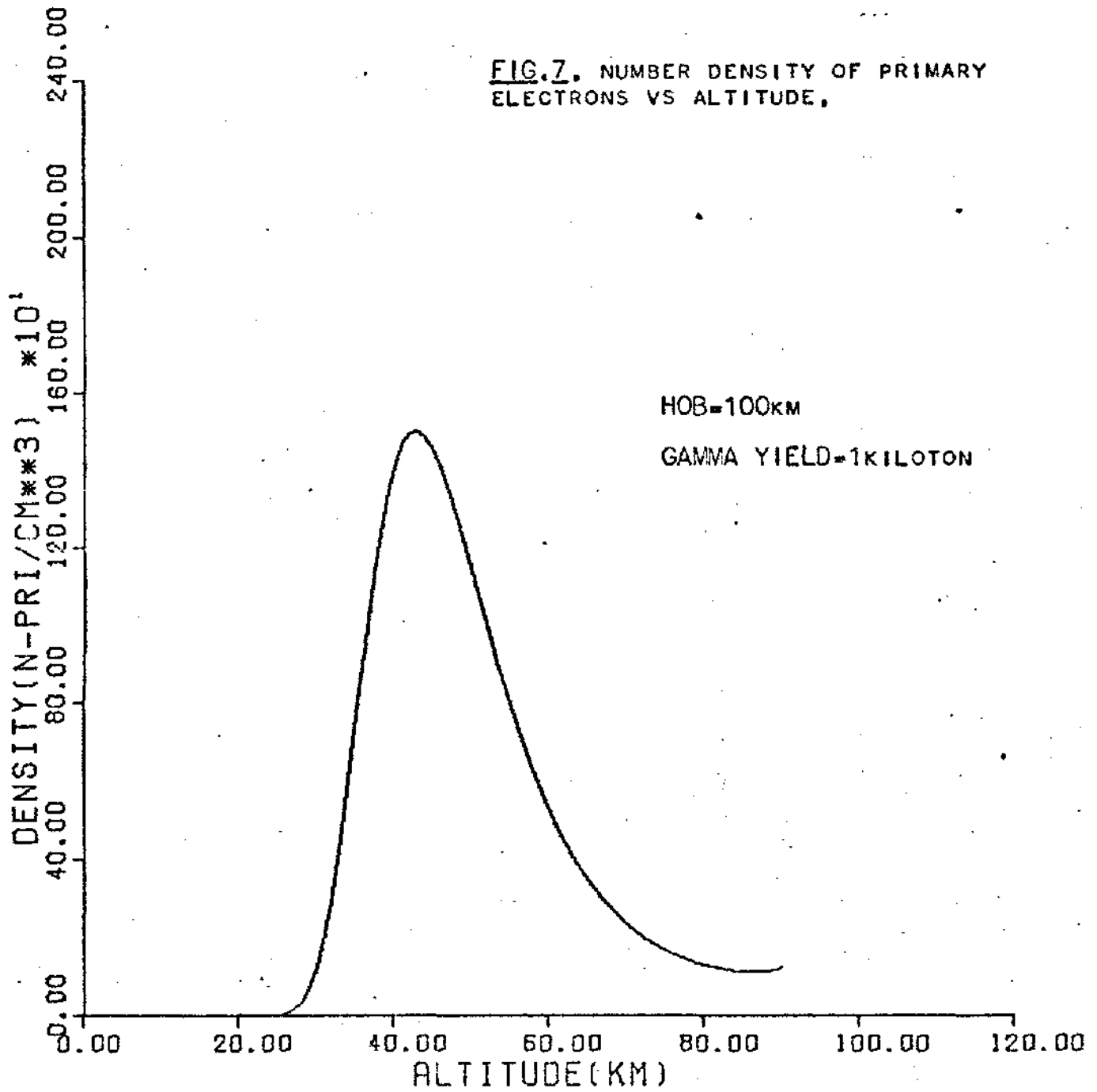
The function $\lambda(R)$ can be approximated using the exponential approximation illustrated in equation (II-7). A graph of

$N_{pri}(R, t \rightarrow \infty)$ is given in Figure 7 on the following page where μ_0 , which is the total attenuation cross section, has been taken to be equal to the cross section for the Compton interaction.⁵ It should be noted that it is a rather common practice in much of the technical literature concerning the high altitude EMP to use λ for μ_0 in the above expression since the Compton effect is a predominant interaction in the energy ranges of interest. This is seen to be a valid assumption if one refers to Figure 5 which shows that the total attenuation coefficient is due almost entirely to Compton attenuation for 1.5 MeV gamma photons. With regard to Figure 7, it is obvious that most of the primary electrons are created in a layer of air between thirty and fifty kilometers. For this reason, when speaking of the high altitude EMP, one often refers to the "absorption layer" which is that portion of the atmosphere in which most of the gamma energy is absorbed and most of the primary electrons are created as described above.

Summary

There have been several assumptions and points made in this chapter which should be reiterated at this time. First, although the gamma photons which emanate from a nuclear weapon burst have an energy spectrum ranging from around 1.0 MeV to 5.0 MeV, it will be assumed for the remainder of this study that the gamma spectrum is mono-

⁵These values were obtained from the American Institute of Physics Handbook (Ref. 5, p. 8-93).



energetic with an energy of 1.5 MeV. With respect to the creation of primary electrons it has been asserted that only the virgin or unscattered gamma photons are important for the high frequency EMP. Finally, the attenuation of the virgin photons with energy of 1.5 MeV has been assumed to be due to the Compton effect and all other processes have been ignored.

III. Electromagnetic Theory of the High Altitude EMP

The purpose of this chapter is to describe and to develop the microscopic model. Difficult and unwieldy derivations appear in the Appendices and are referenced in the body of the chapter.

The first section of this chapter is devoted to the general field equations as developed from Maxwell's equations for a single electron. This is followed by a section concerning the equations of motion of an electron in the upper atmosphere. The results of the first two sections are then combined in the third section to obtain the field equations for an electron moving in a specific manner. The effects of all those electrons which contribute to the high altitude EMP are then summed up in the fourth section. The effects of air conductivity are ignored in this chapter but are discussed in Chapter V.

General Field Equations for a Single Electron

The most basic equations in electromagnetic theory are Maxwell's equations. They are presented here without justification or derivation as follows⁶

$$\begin{aligned}
 \nabla \times \vec{E}(\vec{r}, t) &= - \frac{\partial \vec{B}(\vec{r}, t)}{\partial t} \\
 \nabla \times \vec{B}(\vec{r}, t) &= \mu_v \vec{J}(\vec{r}, t) + \mu_v \epsilon_v \frac{\partial \vec{E}(\vec{r}, t)}{\partial t} \\
 \nabla \cdot \vec{E}(\vec{r}, t) &= \frac{\rho_c(\vec{r}, t)}{\epsilon_v} \\
 \nabla \cdot \vec{B}(\vec{r}, t) &= 0
 \end{aligned}
 \tag{III-1}$$

⁶The interested reader is referred to the text Electromagnetic Fields and Waves by Lorrain and Corson.

where \vec{E} is the electric field, \vec{B} is the magnetic field, ρ_c is the charge density, \vec{J} is the current density, μ_v is permeability of vacuum, ϵ_v is the permittivity of vacuum, r is the position at which the fields are measured, and t is the time at which they are measured.

If one defines the quantities $\vec{A}(r,t)$ and $V(r,t)$ such that⁷

$$\begin{aligned} \vec{E}(\vec{r},t) &= -\nabla V(\vec{r},t) - \frac{\partial \vec{A}(\vec{r},t)}{\partial t} \\ \text{(III-2)} \quad \vec{B}(\vec{r},t) &= \nabla \times \vec{A}(\vec{r},t) \end{aligned}$$

and then manipulates the equations (III-1) using the above substitutions, the following relations are obtained (see Appendix B):

$$\text{(III-3)} \quad \nabla^2 V(\vec{r},t) + \frac{\partial}{\partial t} \{ \nabla \cdot \vec{A}(\vec{r},t) \} = - \frac{\rho_c(\vec{r},t)}{\epsilon_v}$$

$$\begin{aligned} \text{(III-4)} \quad \nabla^2 \vec{A}(\vec{r},t) - \mu_v \epsilon_v \frac{\partial^2 \vec{A}(\vec{r},t)}{\partial t^2} &= - \mu_v \epsilon_v \vec{J}(\vec{r},t) \\ &+ \nabla(\nabla \cdot \vec{A}(\vec{r},t)) + \nabla \left\{ \mu_v \epsilon_v \frac{\partial V(\vec{r},t)}{\partial t} \right\} \end{aligned}$$

Since a vector field is not uniquely defined unless one specifies both its curl and divergence and since only the curl of \vec{A} has been specified in the above, one can "choose" the following relationship concerning the divergence of \vec{A}

$$\text{(III-5)} \quad \nabla \cdot \vec{A}(\vec{r},t) = - \mu_v \epsilon_v \frac{\partial V(\vec{r},t)}{\partial t}$$

This procedure is known as picking the gauge of \vec{A} and the particular gauge chosen above is called the Lorentz gauge. Upon substituting (III-5) into (III-3) and (III-4) one

⁷ \vec{A} is often called the vector potential and V the scalar potential.

obtains the following wave equations⁸:

$$\nabla^2 \mathbf{v}(\bar{\mathbf{r}}, t) - \frac{1}{c^2} \frac{\partial^2 \mathbf{v}(\bar{\mathbf{r}}, t)}{\partial t^2} = - \frac{\rho_c(\bar{\mathbf{r}}, t)}{\epsilon_v}$$

and

$$\nabla^2 \bar{\mathbf{A}}(\bar{\mathbf{r}}, t) - \frac{1}{c^2} \frac{\partial^2 \bar{\mathbf{A}}(\bar{\mathbf{r}}, t)}{\partial t^2} = - \mu_v \bar{\mathbf{J}}(\bar{\mathbf{r}}, t)$$

which can be written in the following abbreviated manner.

$$(III-6) \quad \left(\nabla^2 - \frac{1}{c^2} \frac{\partial^2}{\partial t^2} \right) \begin{vmatrix} \bar{\mathbf{A}}(\bar{\mathbf{r}}, t) \\ \mathbf{v}(\bar{\mathbf{r}}, t) \end{vmatrix} = \begin{vmatrix} -\mu_v \bar{\mathbf{J}}(\bar{\mathbf{r}}, t) \\ -\frac{1}{\epsilon_v} \rho_c(\bar{\mathbf{r}}, t) \end{vmatrix}$$

or

$$(III-7) \quad \hat{L}_{t,r} \begin{vmatrix} \bar{\mathbf{A}}(\bar{\mathbf{r}}, t) \\ \mathbf{v}(\bar{\mathbf{r}}, t) \end{vmatrix} = \begin{vmatrix} -\mu_v \bar{\mathbf{J}}(\bar{\mathbf{r}}, t) \\ -\frac{1}{\epsilon_v} \rho_c(\bar{\mathbf{r}}, t) \end{vmatrix}$$

The solution to equation (III-7) can be written formally as follows:

$$(III-8) \quad \begin{vmatrix} \bar{\mathbf{A}}(\bar{\mathbf{r}}, t) \\ \mathbf{v}(\bar{\mathbf{r}}, t) \end{vmatrix} = \int d^3\bar{\mathbf{r}}' \int dt' G(\bar{\mathbf{r}}, t | \bar{\mathbf{r}}'; t') \begin{vmatrix} -\mu_v \bar{\mathbf{J}}(\bar{\mathbf{r}}'; t') \\ -\frac{1}{\epsilon_v} \rho_c(\bar{\mathbf{r}}'; t') \end{vmatrix}$$

where $G(\bar{\mathbf{r}}, t | \bar{\mathbf{r}}'; t')$ is the Green's function associated with the operator $\hat{L}_{t,r}$ and which must satisfy the following equation

$$(III-9) \quad \hat{L}_{t,r} G(\bar{\mathbf{r}}, t | \bar{\mathbf{r}}'; t') = \delta(\bar{\mathbf{r}} - \bar{\mathbf{r}}') \delta(t - t')$$

where δ is the Dirac delta function.

In order to obtain a closed form solution to (III-8) one must find the form of the Green's function which is determined by (III-9). This can be easily done (see Appendix B) using Laplace Transform techniques to obtain the following solution for $G(\bar{\mathbf{r}}, t | \bar{\mathbf{r}}'; t')$:

$$(III-10) \quad G(\bar{\mathbf{r}}, t | \bar{\mathbf{r}}'; t') = - \frac{1}{4\pi} \frac{\delta(t' - (t - \frac{|\bar{\mathbf{r}} - \bar{\mathbf{r}}'|}{c}))}{|\bar{\mathbf{r}} - \bar{\mathbf{r}}'|}$$

⁸The relation $\mu_v \epsilon_v = \frac{1}{c^2}$ has been used.

Another requirement for a closed form solution to (III-8) is a functional form for $\bar{J}(\bar{r}, t)$ and $\rho_c(\bar{r}, t)$. The current source which is considered in this study is a single electron traveling with a velocity $\bar{v}(\bar{x}, t)$ located at some point \bar{x} at time t . Thus, since this source is localized rather than distributed through space the current density, as well as the charge density, can be represented using the Dirac delta function such that

$$(III-11) \quad \bar{J}(\bar{r}; t') = ec\bar{\beta}(\bar{r}')\delta\{\bar{r}' - \bar{x}(t')\}$$

and

$$(III-12) \quad \rho_c(\bar{r}; t') = e\delta\{\bar{r}' - \bar{x}(t')\}$$

where $\bar{\beta} = \frac{\bar{v}}{c}$, e is the amount of charge on an electron, and $\bar{x}(t)$ is the location of the electron at time t . Figure 8 illustrates the geometry of the situation. Using the above expressions for \bar{J} and ρ_c and the solution of $G(\bar{r}, t | \bar{r}', t')$ given in (III-10), the equations (III-8) for \bar{A} and V become

$$(III-13) \quad \bar{A}(\bar{r}, t) = \frac{ec\mu_v}{4\pi} \int d^3\bar{r}' \int dt' \frac{\delta(t' - \{t - \frac{|\bar{r} - \bar{r}'|}{c}\})}{|\bar{r} - \bar{r}'|} \bar{\beta}(\bar{r}')\delta\{\bar{r}' - \bar{x}(t')\}$$

and

$$(III-14) \quad V(\bar{r}, t) = \frac{e}{4\pi\epsilon_v} \int d^3\bar{r}' \int dt' \frac{\delta(t' - \{t - \frac{|\bar{r} - \bar{r}'|}{c}\})}{|\bar{r} - \bar{r}'|} \delta\{\bar{r}' - \bar{x}(t')\}$$

The equations given above could be solved to obtain a closed form for \bar{A} and V . Then the operations indicated in equations (III-2) could be performed to find expressions for \bar{E} and \bar{B} . However, it is less tedious if one simply performs the operations mentioned directly on the integral forms of \bar{A} and V given in (III-13) and (III-14). Performing these operations,

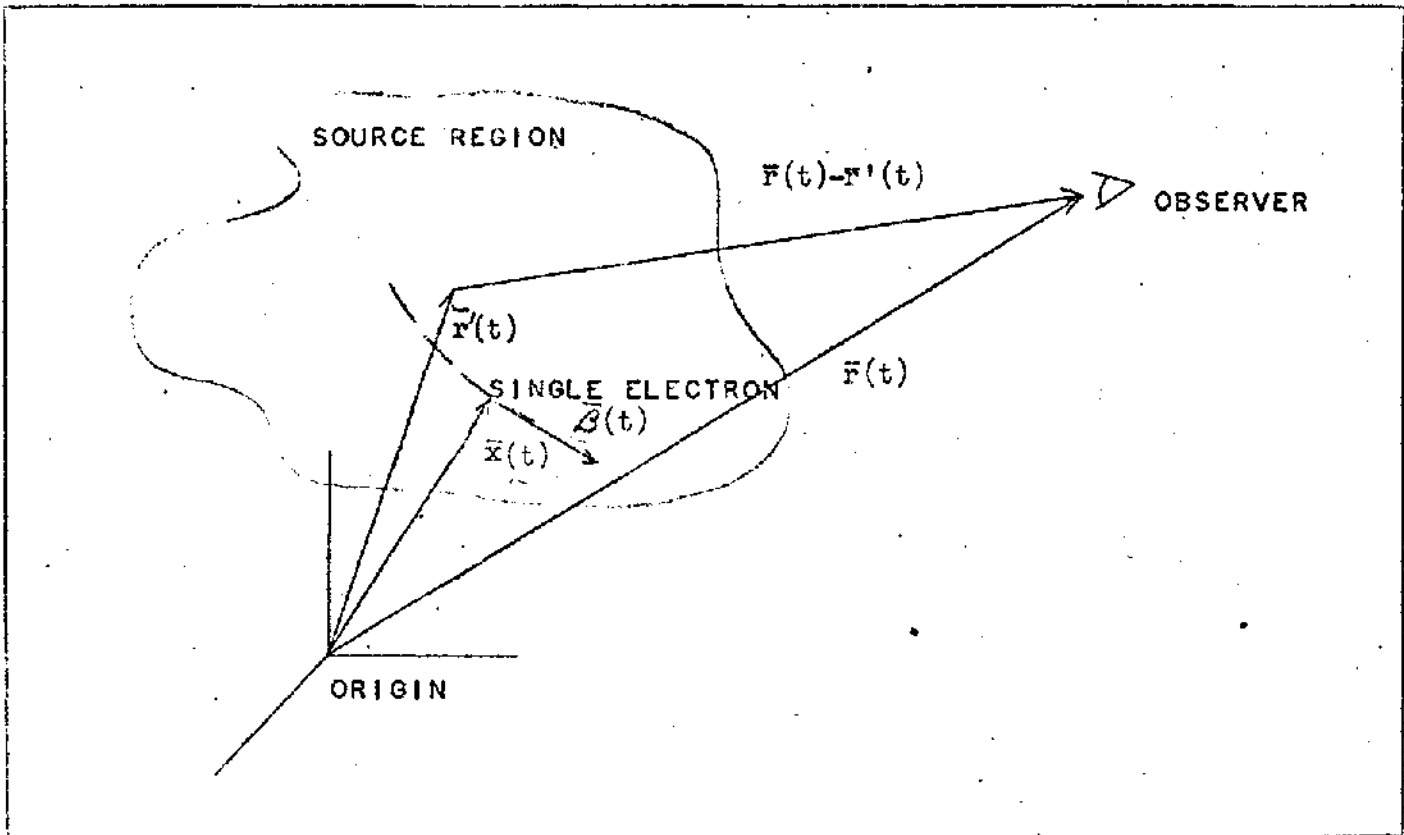


Figure 8. Geometry for a Single Electron Source. One should note that $\bar{J}(\bar{r}, t)$ and $\rho_c(\bar{r}, t)$ are zero unless $\bar{r}'(t) = \bar{x}(t)$

one obtains, after much manipulation (see Appendix B), the following relations for $\bar{E}(\bar{r}, t)$ and $\bar{B}(\bar{r}, t)$:

$$(III-15) \quad \bar{E}(\bar{r}, t) = \frac{e}{4\pi\epsilon_v} \left\{ \left| \frac{(\hat{n} - \dot{\beta})(1 - |\dot{\beta}|^2)}{\kappa^3 R^2} \right|_{\text{ret}} + \frac{1}{c} \left| \frac{\hat{n}}{\kappa^3 R} \times \{(\hat{n} - \dot{\beta}) \times \dot{\beta}\} \right|_{\text{ret}} \right\}$$

and

$$(III-16) \quad \bar{B}(\bar{r}, t) = \frac{1}{c} \{ \hat{n} \times \bar{E}(\bar{r}, t) \}$$

where $R = |\bar{R}| = |\bar{r} - \bar{r}'|$ is the distance between the source (electron) and the observer, $\hat{n} = \frac{\bar{R}}{R}$ is a unit vector indicating the direction between the source and the observer, $\dot{\beta}$ is the time derivative of the "velocity" of the electron (acceleration), and $\kappa = 1 - \hat{n} \cdot \dot{\beta}$.

The bracket with the subscript "ret" relates to the fact that the quantity in the brackets is to be evaluated at the retarded time, $t' = t - \{R(t')/c\}$. That is, what the observer "sees" at time t is that which was created at an earlier time t' where the difference is the time that is required for the signal to traverse the distance R . One should note that the fields indicated by (III-15) and (III-16) are divided into "velocity fields" which are independent of acceleration and "acceleration fields" which are dependent on $\dot{\beta}$ in a linear fashion. One can show that the velocity fields are essentially static fields falling off as R^{-2} , whereas the acceleration fields are typically radiation fields falling off as R^{-1} (Ref 10, p 467).

For long range effects of the EMP one is concerned with the radiated fields rather than the static fields since the magnitude of the radiated field represents a flow of energy. Therefore, the fields of interest for the high altitude EMP depend on the acceleration of the Compton electrons as well as their velocity. That is, in order to solve for the radiated fields one needs analytical expressions for $\dot{\beta}(t)$.

Electron Kinematics in the Atmosphere

Recall that the primary source of the high frequency, high altitude EMP is the Compton electrons created by the gamma radiation from the weapon. Since the radiated fields depend on the acceleration of the electron, we shall consider two kinds of forces which can act upon the electrons

which are created in the absorption layer (30-50 Km). The first of these is the force which results from the interaction of the electron (a charged particle) with the earth's magnetic field. The result of this interaction is a component of acceleration which is perpendicular to the instantaneous velocity of the electron. Secondly, the electron as it travels through the atmosphere, undergoes many collisions with the surrounding atoms causing it to lose energy and consequently to de-accelerated. The result of these collisions is a component of acceleration which is parallel⁹ to the instantaneous velocity. Both of these forces will be explained in greater detail in the following paragraphs.

Perpendicular Acceleration. The basic equation of motion for a charged particle under the influence of an electric or magnetic field is the Lorentz force equation or (III-17)

$$\dot{\vec{p}} = q(\vec{E} + \vec{v} \times \vec{B})$$

where $\dot{\vec{p}}$ is the time derivative of the particle's momentum, q is the particle's charge, \vec{v} is its velocity, and \vec{E} and \vec{B} represent the electric and magnetic field respectively. For the case of the electron in a magnetic field only, (III-17) becomes

$$(III-18) \quad \dot{\vec{p}} = -e(\vec{v} \times \vec{B}) \quad (\text{see Figure 9A})$$

Using relativistic mechanics¹⁰ one can easily prove the following identity between the momentum and the total

⁹For a zero order approximation

¹⁰One should be aware of the fact that the electrons which produce the EMP are energetic enough to be considered relativistic

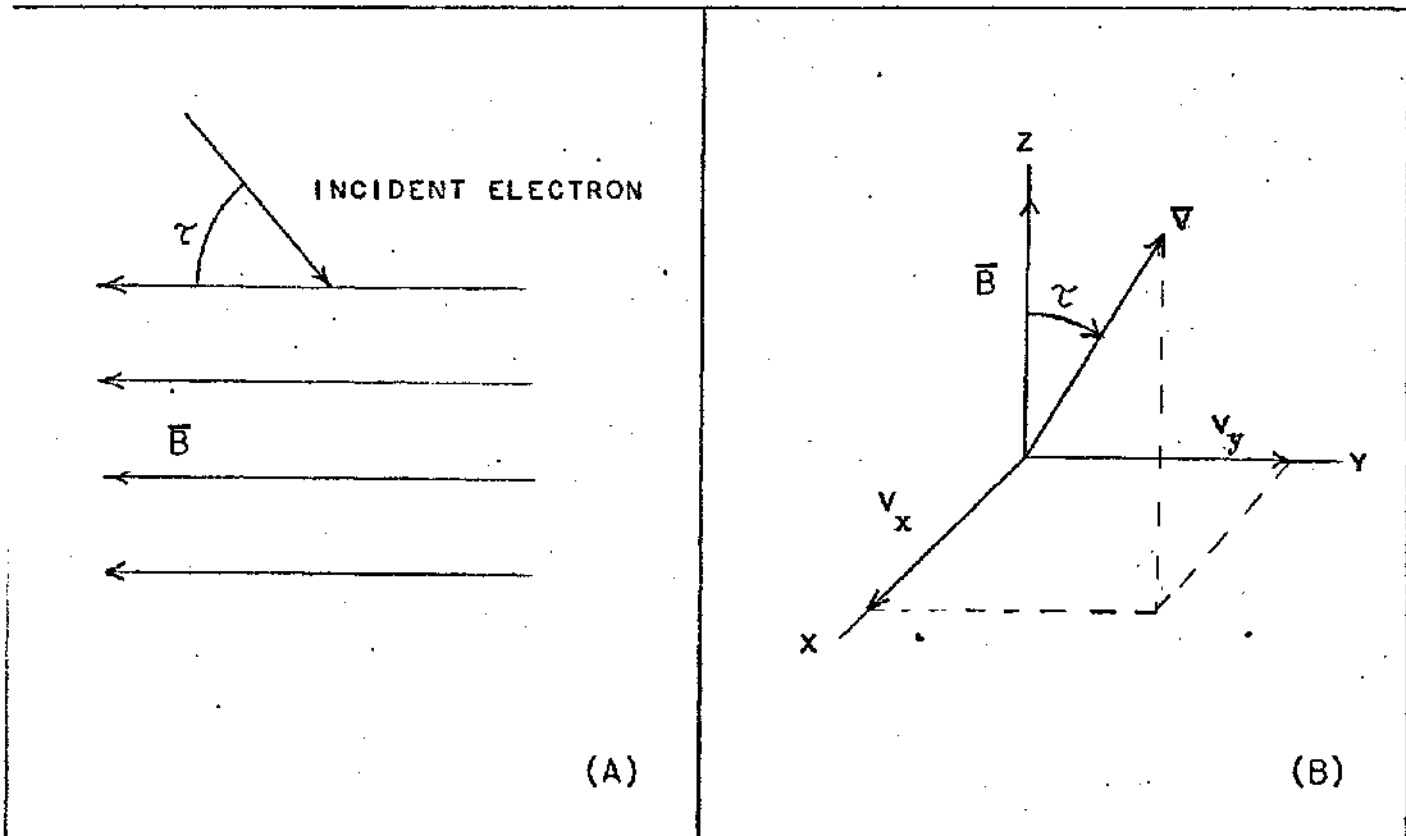


Figure 9. Electron Moving in a Magnetic Field. The (B) part of the above is the same as the (A) part except a definite set of coordinate axis has been defined.

energy (ξ_1) of a particle in a uniform magnetic field (Ref 15, p 28):

$$\vec{p} = \xi_1 \frac{\vec{v}}{c^2} \longrightarrow \frac{d\vec{p}}{dt} = \frac{\xi_1}{c^2} \frac{d\vec{v}}{dt}$$

where ξ_1 is assumed constant

Using this relation in (III-18) one finds the following:

$$(III-19) \quad \frac{\xi_1}{c^2} \frac{d\vec{v}}{dt} = -e(\vec{v} \times \vec{B})$$

If one defines the z-axis of a coordinate system in the direction of the \vec{B} field then (III-19) can be written in terms of the components of the vectors as:

$$(III-20) \quad \begin{aligned} \dot{v}_x &= -\frac{ec^2B}{\xi_1} v_y \\ \dot{v}_y &= \frac{ec^2B}{\xi_1} v_x \\ \dot{v}_z &= 0 \longrightarrow v_z = v_{oz} \text{ (constant)} \end{aligned}$$

In order to solve the two coupled equations in (III-20) one can let $\omega = \frac{ec^2 B}{\xi_1}$ and then multiply the first equation by $i = \sqrt{-1}$ and add it to the second (Ref 15, p 59). This yields

$$\frac{d}{dt} (V_y + iV_x) = -i\omega(V_y + iV_x)$$

The solution to this is of the form:

$$(III-21) \quad V_y + iV_x = g e^{-i\omega t}$$

where g is a complex constant. One can write g as $g = V_0 e^{-i\alpha_0}$

where V_0 and α_0 are real constants. Then using this in (III-20) and separating real and imaginary parts one finds that

$$(III-22) \quad V_x = -V_0 \sin(\omega t), \quad V_y = V_0 \cos(\omega t)$$

where α_0 which represents the initial phase ($t=0$) has been taken as 0 for simplicity. From (III-21) it is obvious that the following relation holds:

$$(III-23) \quad V_0 = \sqrt{V_x^2 + V_y^2} = |\bar{v}| \sin \tau \quad (\text{see Figure 9})$$

Integrating (III-21) once more ($V_x = \frac{dx}{dt}$) one finds that

$$(III-24) \quad x(t) = x_0 + r_1 \cos(\omega t), \quad y(t) = y_0 + r_1 \sin(\omega t)$$

where

$$(III-25) \quad r_1 = \frac{V_0}{\omega} = \frac{V_0 \xi_1}{ec^2 B}$$

Also if one integrates the equation for V_z in (III-20) the result is

$$(III-26) \quad z(t) = z_0 + V_{oz} t$$

Thus an electron moving in a uniform magnetic field with no other external forces will move in a helix (see Figure 10) having its axis along the direction of the magnetic field and with a radius r_1 given by (III-25). In the special case of

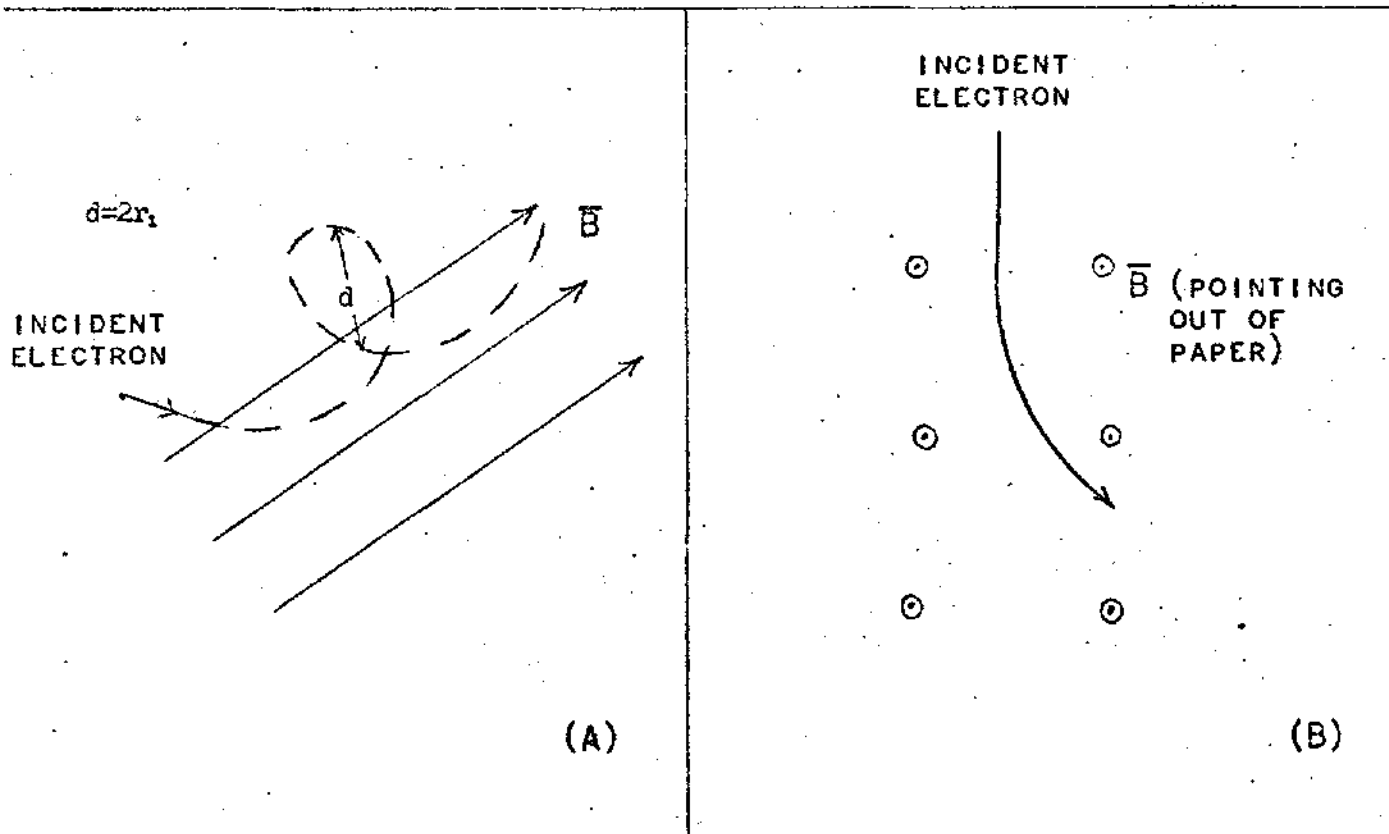


Figure 10. Trajectory of an Electron in a Uniform Magnetic Field. Part (B) is an "end on", cross-sectional view of (A).

the electron having no initial component of velocity in the direction of the \bar{B} field ($V_{Oz}=0$), it moves along a circle in the plane perpendicular to the field (Ref 15, p 60). The acceleration for the electron under these circumstances is also constant and can be found from (III-20) using (III-23) and (III-25). That is

$$|\dot{\bar{V}}|^2 = \dot{V}_x^2 + \dot{V}_y^2 + \dot{V}_z^2 = \omega^2(V_x^2 + V_y^2) = \omega^2 V_o^2$$

or

$$(III-27) \quad |\dot{\bar{V}}|^2 = \frac{V_o^4}{r_1^2} = \frac{(|\bar{V}| \sin \tau)^4}{r_1^2} \longrightarrow |\dot{\bar{B}}|^2 = \frac{V_o^4}{c^2 r_1^2}$$

One can see that for an electron of a given energy the acceleration will be maximum when the incident electron is perpendicular to the \bar{B} field ($\tau=90^\circ$). Thus the $\sin \tau$ term is seen to represent a scaling factor, the magnitude of

which depends on the angle of incidence of the electron with the magnetic field.

Parallel Acceleration. When speaking of the "slowing down" or "stopping" of an electron in a material such as air it is useful to define two quantities known as the stopping power and the range. The stopping power is defined as the amount of energy lost by an electron per unit length of path through the stopping material (Ref 6, p 185). The stopping power is symbolized by $-d\xi/dx$ since it signifies the rate of energy change with respect to distance traveled. The range of the electron, or the length of the path it travels before coming to rest, can be defined in terms of the stopping power as follows:

$$(III-28) \quad R_1 = - \int_{\xi_1}^0 dx = - \int_{\xi_1}^0 \frac{d\xi}{d\xi/dx}$$

where R_1 is the range of an electron with initial energy of ξ_1 . If one considers the case where an electron loses an increment of energy $\Delta\xi$ so that its energy becomes $\xi_2 = \xi_1 - \Delta\xi$, then one can compute the distance ($R_{1,2}$) that the electron must travel to lose this energy increment with the following relation:

$$R_{1,2} = - \int_{\xi_1}^{\xi_2} \frac{d\xi}{d\xi/dx}$$

or separating the integration into two intervals

$$R_{1,2} = \left(- \int_{\xi_1}^0 \frac{d\xi}{d\xi/dx} \right) - \left(- \int_{\xi_2}^0 \frac{d\xi}{d\xi/dx} \right)$$

or using (III-28)

$$(III-29) \quad R_{1,2} = R_1 - R_2$$

Equation (III-29) is necessary in this development because there are no simple, analytical expressions for the forces involved in the slowing down of an electron by a material. In fact, the majority of reliable information concerning this subject has been derived from experiment and is easily obtainable in the form of the total range (i.e. R_1 or R_2 and not $R_{1,2}$) of electrons with known initial energy. Therefore, in order to obtain information concerning the acceleration of an electron in such a situation it will be necessary to construct a numerical model based on physical assumptions.

The first assumption which shall be made in this model is that the electron remains on its original path while it is being slowed down and is not scattered in other directions. That is, it is assumed that the forces acting on the electron are viscous in nature, changing only the energy of the electron and not affecting its direction. This approximation is best for times soon after the creation of the Compton electron and loses its validity after the electron has lost a large portion of its energy. As was mentioned, the forces acting upon the electron are assumed to be viscous in nature also implying that the slowing down procedure is continuous and that the acceleration function is a smooth curve. An empirical relation for the range of an electron as a function of its energy has been found using these assumptions. This relation is (Ref 17, p 16-4):

$$(III-30) \quad R_1 = \frac{0.61 \xi_1^2}{\xi_1 + 0.26}$$

with ξ_1 in MeV and R_1 in gm/cm².¹¹

In order to numerically approximate the continuous slowing down of the electron it will be assumed that the electron loses small increments of energy in a point-wise manner along its path. For example, if the electron has an initial energy of ξ_1 , and the energy loss increment is $\Delta\xi$, then it will be assumed that the electron travels a distance $R_{1,2}$, given by (III-29), with a constant energy ξ_1 . After it has traveled this distance the electron then instantaneously "loses" $\Delta\xi$ amount of energy thereby acquiring an energy of $\xi_2 = \xi_1 - \Delta\xi$. This procedure is then repeated in a step-wise fashion throughout the slowing of the electron. Figure 11 gives a pictorial explanation of the situation. It should be pointed out that the accuracy of this approach increases as the magnitude of $\Delta\xi$ decreases. One should also note that the successive distances between energy increments (i.e. $R_{1,2}$, $R_{2,3}$, etc) are not necessarily equal.

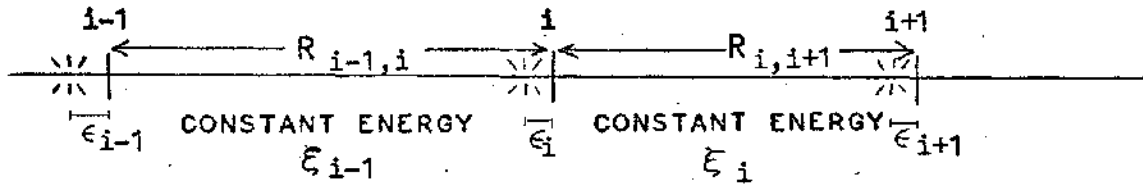
The acceleration can be approximated by giving the acceleration at the i th point (see Figure 11) such that

$$(III-31) \quad \dot{V}_i = \left\{ \frac{V_{i+1} - V_{i-1}}{x_{i+1} - x_{i-1}} \right\} \cdot \left\{ \frac{x_{i+1} - x_{i-1}}{t_{i+1} - t_{i-1}} \right\}$$

where V_i is the velocity corresponding to ξ_i which the

¹¹When measured in these units R_1 is simply the actual distance traveled in cm multiplied by the density of the stopping material. This is convenient for experimental purposes.

$$\epsilon \ll R_i$$



** SIGNIFIES INSTANTANEOUS ENERGY CHANGE

Figure 11. Approximation of Continuous Slowing Down of Electron. The i^{th} point is not at the point of energy change in order to avoid the question of infinite acceleration.

particle has at the i^{th} point, x_i is the total distance from the point $i=0$ to the i^{th} point, and t_i is the time required to traverse the distance x_i . If one realizes that the second term on the right hand side of (III-31) approximates the velocity which the electron has at the i^{th} point, then the expression for \dot{V}_i can be written as:

$$(III-32) \quad \dot{V}_i = \left\{ \frac{V_{i+1} - V_{i-1}}{x_{i+1} - x_{i-1}} \right\} \cdot \{V_i\}$$

Therefore, one can use (III-32) for an electron of initial energy ξ by incrementing the energy as indicated above and using (III-29) and (III-30) for the values of x_i while substituting the values for V_i corresponding to each energy ξ_i . This will yield a series of points for V from which a continuous

function can be implied.

In order to illustrate the method described above, the calculations were performed for 1 MeV electron at an altitude of 40 Km. Figure 12 illustrates the form of the acceleration by showing the relative velocity ($\beta=V/c$) as a function of time. Although the actual numbers are different for various altitudes, the general shape of all the curves is the same for the different altitudes. One should note that the major portion of the electron's acceleration occurs in a relatively short time at the end of the electron's trajectory.

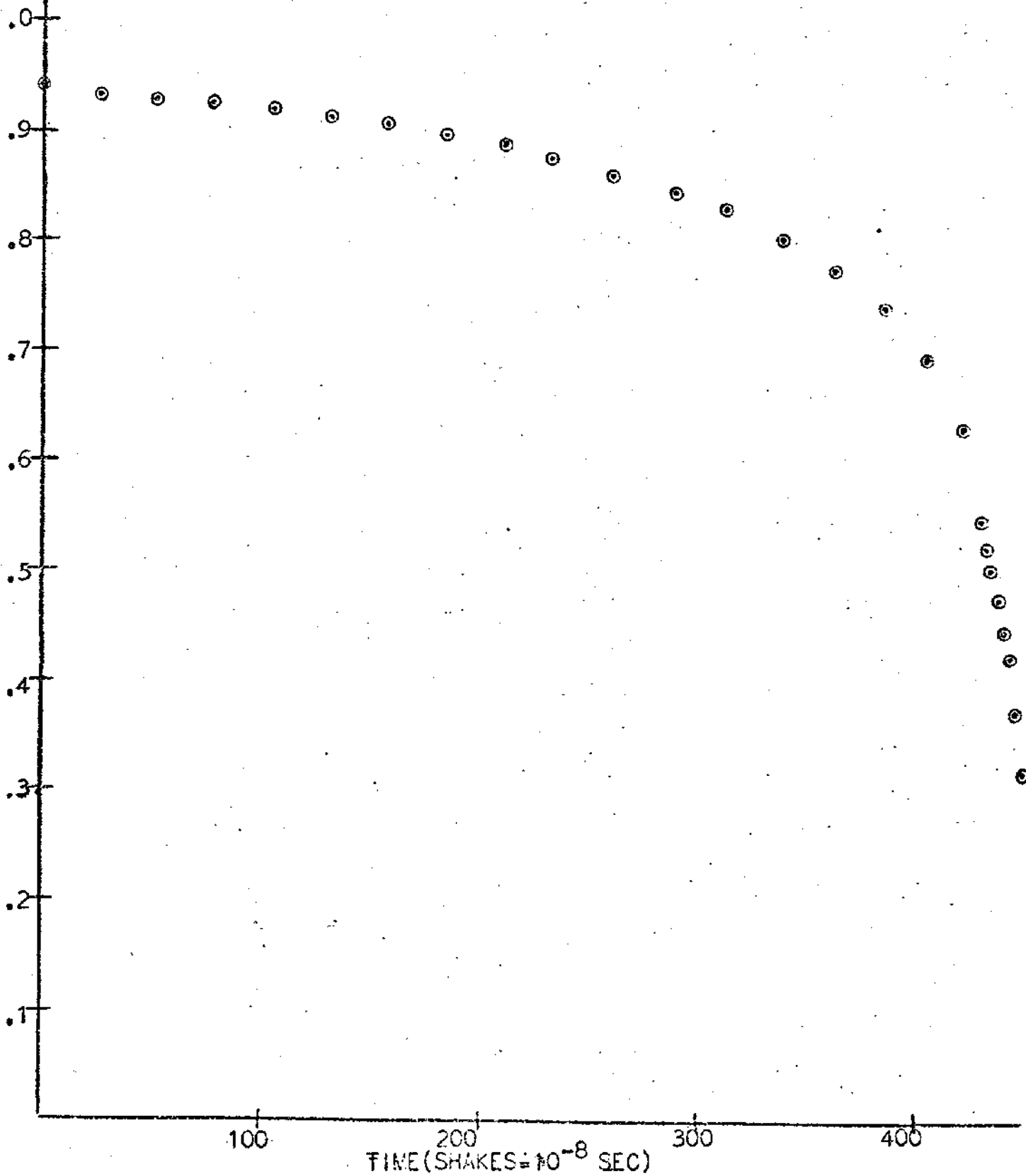
Electron trajectory. The electron in the atmosphere undergoes both the parallel and perpendicular acceleration simultaneously. Thus, the developments of the previous two sections need to be combined in some manner in order to give the electron's true trajectory. Since it is not possible to derive a self-consistent simple force equation which would simultaneously consider both effects, it is necessary to again create a numerical model based on physical assumptions.

It will be assumed that the effect of the air molecules (parallel acceleration) on the electron is the same as given in the previous section. That is, the energy of the electron changes by a definite increment at various points along its path. In between these changes, the electron moves at a constant energy and consequently at a constant speed. However, since there is a uniform magnetic field (perpendicular acceleration) acting upon the electron, the electron does not traverse a straight line in between energy changes. Rather, the path forms a segment of a helix, the radius of curvature

FIG. 12. VELOCITY VS TIME FOR
ELECTRON IN AIR.

ALTITUDE=40KM

INITIAL KINETIC ENERGY=1MEV



of which is given by equation (III-25) since the speed of the electron (and energy) is constant over this path. The arc length or actual distance the electron travels for each segment between energy changes is given by equations (III-29) and (III-30). As will be shown later, an important variable is the angle which the instantaneous velocity vector of the electron makes with the initial direction (line-of-sight) of the electron. If one measures this angle at the i^{th} point (as defined in the previous section) then it can be given in terms of previously defined quantities as follows (see Figure 13):

$$(III-33) \quad \psi_i = \frac{\sum_{i=1}^{\infty} R_{i-1,i}}{\sum_{i=1}^{\infty} r_{i-1}}$$

where ψ_i is the angle as measured at the i^{th} point. To give the reader a picture of the electron's trajectory using this model, calculations were made for the various quantities defined at 40, 30, and 20 Km.¹² These results are summarized in Table 2. One should note the differences in ranges for the various altitudes. It should also be pointed out that the electron tends to spiral inward and at higher altitudes will make several complete revolutions before coming to rest (see ψ_i column in Table 2).

¹²These calculations assumed that the density of the air varies exponentially (i.e. $\rho = \rho_0 e^{-z/z_0}$).

Table 1. Calculations for Electron Trajectory.

(| \bar{B} |= 10^{-4} weber/m²)

Electron Energy (MeV)	Total Path Traveled (meters)	Total Time Elapsed (shakes)*	Radius of Curvature (meter)	ψ_i (radians)
ABSORPTION ALTITUDE = 40 KM				
1.00	0.0	0.0	47.49	0.0
0.95	73.94	26.19	45.71	1.56
0.90	147.88	52.51	43.92	3.17
0.85	221.83	78.95	42.13	4.86
0.80	295.77	105.55	40.32	6.61
0.75	367.25	131.42	38.50	8.39
0.70	441.19	158.39	36.67	10.31
0.65	512.67	184.67	34.82	12.26
0.60	581.68	210.29	32.95	14.24
0.55	653.17	237.13	31.05	16.41
0.50	719.72	262.45	29.14	18.55
ABSORPTION ALTITUDE = 30 KM				
1.00	0.0	0.0	47.48	0.0
0.95	17.72	6.28	45.70	.37
0.90	35.44	12.58	43.92	.76
0.85	53.16	18.92	42.13	1.16
0.80	70.88	25.29	40.32	1.58
0.75	88.01	31.50	38.50	2.01
0.70	105.73	37.96	36.67	2.47
0.65	122.86	44.26	34.82	2.94
0.60	139.40	50.40	23.95	3.41
0.55	156.53	56.83	31.05	3.93
0.50	172.48	62.90	29.14	4.45
ABSORPTION ALTITUDE = 20 KM				
1.00	0.0	0.0	47.48	0.0
0.95	4.25	1.50	45.70	.09
0.90	8.49	3.02	43.92	.18
0.85	12.74	4.53	42.13	.28
0.80	16.99	6.06	40.32	.38
0.75	21.09	7.55	38.50	.48
0.70	25.34	9.10	36.67	.59
0.65	29.44	10.61	34.82	.70
0.60	33.41	12.08	23.95	.82
0.55	37.51	13.62	31.05	.94
0.50	41.34	15.07	29.14	1.07

*1 shake= 10^{-8} second

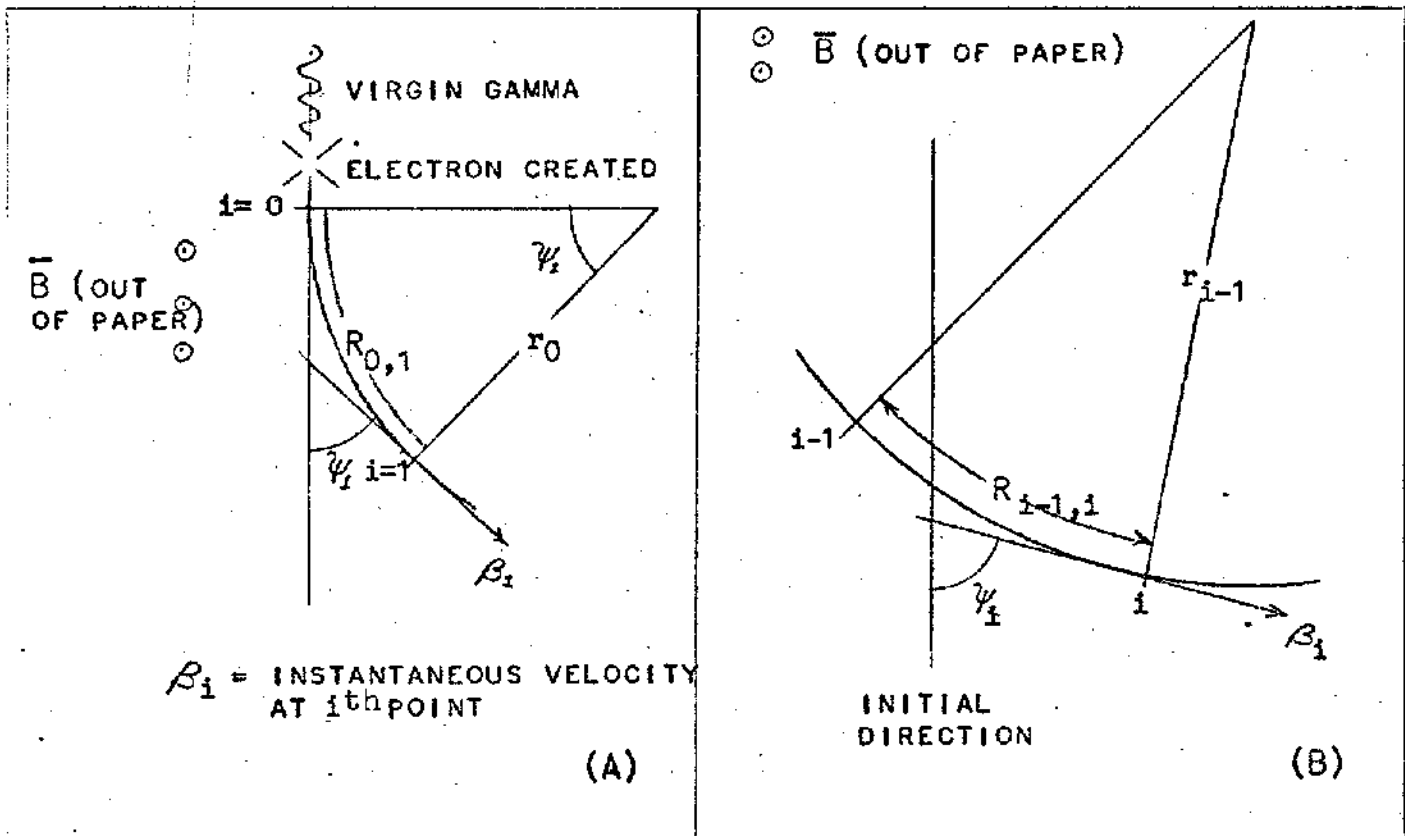


Figure 13. Electron Trajectory in Atmosphere. Part A is for the first two points. Part B is for the $i-1^{\text{th}}$ point and the i^{th} point.

Fields for Electron Moving in Specific Manner

The general field equations for an accelerated electron have been derived and are given by equation (III-15). Furthermore, it has been asserted that the electron is acted upon by a force which is perpendicular to its instantaneous velocity (\vec{B} - field) and a force which is parallel to this velocity (interaction with air molecules). Since some insight has been gained concerning the nature of the acceleration of the electron when subjected to these forces, it is now possible to arrive at relations for the fields which will be radiated by the electron as it is accelerated in this manner.

First, however, it is useful to define a quantity known as the Poynting vector \vec{S} which represents the energy which

flows across a unit area per unit time and is associated with radiated fields. If \bar{E}_a and \bar{B}_a represent the radiated portions of the fields then \bar{S} is defined as

$$(III-34) \quad \bar{S} = \frac{1}{\mu_v} (\bar{E}_a \times \bar{B}_a)$$

or using (III-16)

$$\bar{S} = \frac{1}{c\mu_v} \{\bar{E}_a \times (\hat{n} \times \bar{E}_a)\} = \frac{1}{c\mu_v} \{\hat{n}(\bar{E}_a \cdot \bar{E}_a) - \bar{E}_a(\hat{n} \cdot \bar{E}_a)\}$$

One can easily show that \bar{E}_a is perpendicular to \hat{n} which implies that

$$(III-35) \quad \bar{S} = \frac{\hat{n}}{\mu_v c} |\bar{E}_a|^2$$

Using (III-35) one can then find the energy which is flowing in the direction of the observer by the following

$$\bar{S} \cdot \hat{n} = \frac{1}{c\mu_v} |\bar{E}_a|^2$$

or, using the radiation term in (III-15)

$$(III-36) \quad \{\bar{S} \cdot \hat{n}\}_{ret} = \left(\frac{e}{4\pi\epsilon_v c}\right)^2 \left\{ \frac{c\epsilon_v}{k^6 R^2} |\hat{n} \times \{(\hat{n} - \hat{\beta}) \times \dot{\hat{\beta}}\}|^2 \right\}_{ret}$$

Using (III-36) one could then compute the amount of energy per unit area radiated during a finite period of acceleration, $t' = T_1$ and $t' = T_2$, and detected in a corresponding interval, $t = T_1 + \{R(T_1)/c\}$ and $t = T_2 + \{R(T_2)/c\}$, by the observer with the following:

$$U = \int_{T_1 + R(T_1)/c}^{T_2 + R(T_2)/c} \{\bar{S} \cdot \hat{n}\}_{ret} dt$$

or

$$(III-37) \quad U = \int_{T_1}^{T_2} (\bar{S} \cdot \hat{n}) \left(\frac{dt}{dt'}\right) dt'$$

where U is the energy measured. It is obvious from (III-37) that the quantity $(\bar{S} \cdot \hat{n}) \left(\frac{dt}{dt'} \right)$ represents the power (energy/time) radiated per unit area by the electron in terms of the "local time" of the electron rather than the retarded time defined earlier. Thus, with the definition of the solid angle in mind, one can define the power radiated per unit solid angle and measured by the observer at a distance R from the source as follows:

$$\frac{dP(t')}{d\Omega} = R^2 (\bar{S} \cdot \hat{n}) \left(\frac{dt}{dt'} \right)$$

or using the relation for retarded time (see Appendix B)

$$\frac{dP(t')}{d\Omega} = \kappa R^2 (\bar{S} \cdot \hat{n})$$

which, using the definition of κ and equation (III-36), becomes

$$(III-38) \quad \frac{dP(t')}{d\Omega} = \frac{1}{c\epsilon_v} \left(\frac{e}{4\pi} \right)^2 \left\{ \frac{|\hat{n} \times \{(\hat{n} - \bar{\beta}) \times \dot{\bar{\beta}}\}|^2}{(1 - \hat{n} \cdot \bar{\beta})^5} \right\}$$

One can reduce (III-38) to a simpler form for the case corresponding to an acceleration which is acting parallel to the instantaneous velocity by recognizing that

$$(III-39) \quad \hat{n} \times \{(\hat{n} - \bar{\beta}) \times \dot{\bar{\beta}}\} = \hat{n} \times (\hat{n} \times \dot{\bar{\beta}} - \bar{\beta} \times \dot{\bar{\beta}}) = \hat{n} \times (\hat{n} \times \dot{\bar{\beta}})$$

Since $\dot{\bar{\beta}}$ is parallel to $\bar{\beta}$. Using (III-39) and letting ψ be the angle between $\dot{\bar{\beta}}$, $\bar{\beta}$ and \hat{n} (see Figure 14 A) then one finds that

$$(III-39) \quad \frac{dP_L(t')}{d\Omega} = \frac{1}{\epsilon_v c} \left(\frac{e\dot{\bar{\beta}}}{4\pi} \right)^2 \frac{\sin^2 \psi}{(1 - \beta \cos \psi)^3}$$

where P_L signifies the power radiated which is due only to parallel acceleration. A similar reduction in form is possible for the case where the acceleration is perpendicular

to the instantaneous velocity. If one defines η as the angle between $\dot{\vec{\beta}}$ and the projection of \hat{n} into the plane perpendicular to $\vec{\beta}$ (see Figure 14 B) then one finds that

$$(III-40) \quad \frac{dP_c(t')}{d\Omega} = \frac{1}{c\epsilon_v} \left(\frac{e\dot{\beta}}{4\pi}\right)^2 \frac{1}{(1-\beta \cos \psi)^3} \left\{ 1 - \frac{\sin^2 \psi \cos^2 \eta}{\gamma^2 (1-\beta \cos \psi)^2} \right\}$$

where $\gamma^2 = (1-\beta^2)^{-1}$ and P_c signifies the power radiated which is due only to perpendicular acceleration.

With regard to the high altitude EMP the next step is to investigate the relative contributions of radiation due to parallel acceleration and perpendicular acceleration. Calculations can be made for (III-39) and (III-40) at various points along the electron's trajectory using the model outlined in the last part of the previous section to obtain values for the acceleration terms at various points. If one assumes that the observer is situated on the original line-of-sight, then $\eta=180^\circ$ and ψ at each point is the angle ψ_1 defined in the previous section. One should note that $\eta=0^\circ$ or 180° corresponds to the minimum value for (III-40) with respect to η . The calculations indicated here were performed by the author for Compton electrons created at various altitudes ranging from 60 to 20 Km. The results at 40 Km for early times are presented in Table 2 on Page 49. As one can readily see, the radiation resulting because of the electron's interaction with the magnetic field ($dP_c/d\Omega$) far outweighs that resulting from the linear slowing down of the electron ($dP_L/d\Omega$). Although Table 2 shows only the calculations at early times, and at one altitude, the results are found

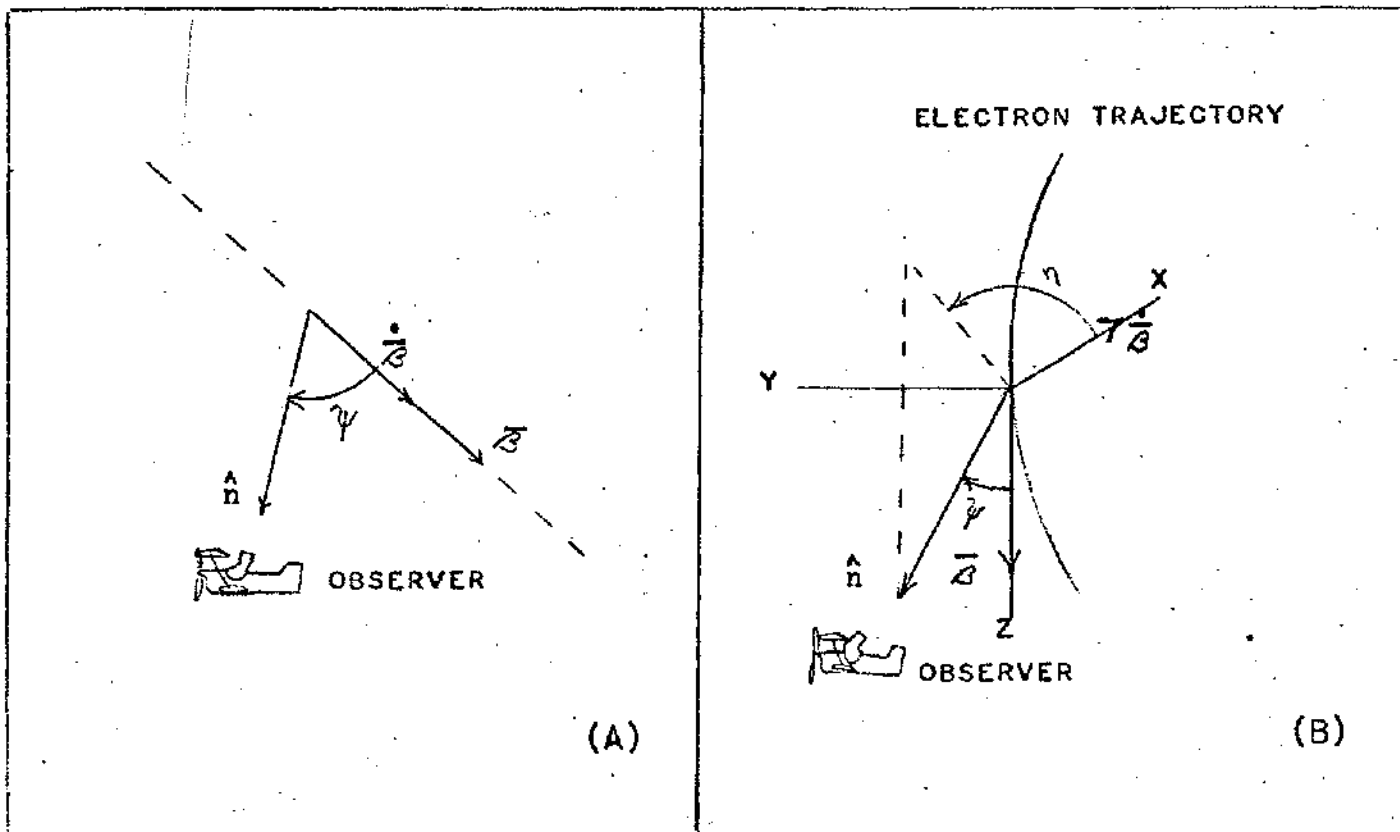


Figure 14. Geometry for Angular Distribution of Electron Radiation. Part A is for parallel acceleration; Part B concerns perpendicular acceleration.

to be the same at late times and at all altitudes. Thus, based on these calculations, one can say that the electromagnetic radiation which constitutes the high altitude EMP results from the turning of high energy Compton electrons by the earth's magnetic field.

It is beneficial to investigate even further the nature of the radiation resulting from the turning of the electron. Table 2 shows that for a period over which the radiated power drops four orders of magnitude, the velocity, β , of the electron is essentially constant to two significant figures. Thus, although much time has been devoted to the slowing of the electron in the atmosphere¹³, it is seen here that, with regard

¹³This development will be very important later, however, when discussing air conductivity.

Table 2 Comparison of $\frac{dP_L}{d\Omega}$ and $\frac{dP_C}{d\Omega}$ for Electron at 40 Km.

($|\bar{B}|=1 \times 10^{-4}$ webers/m²)

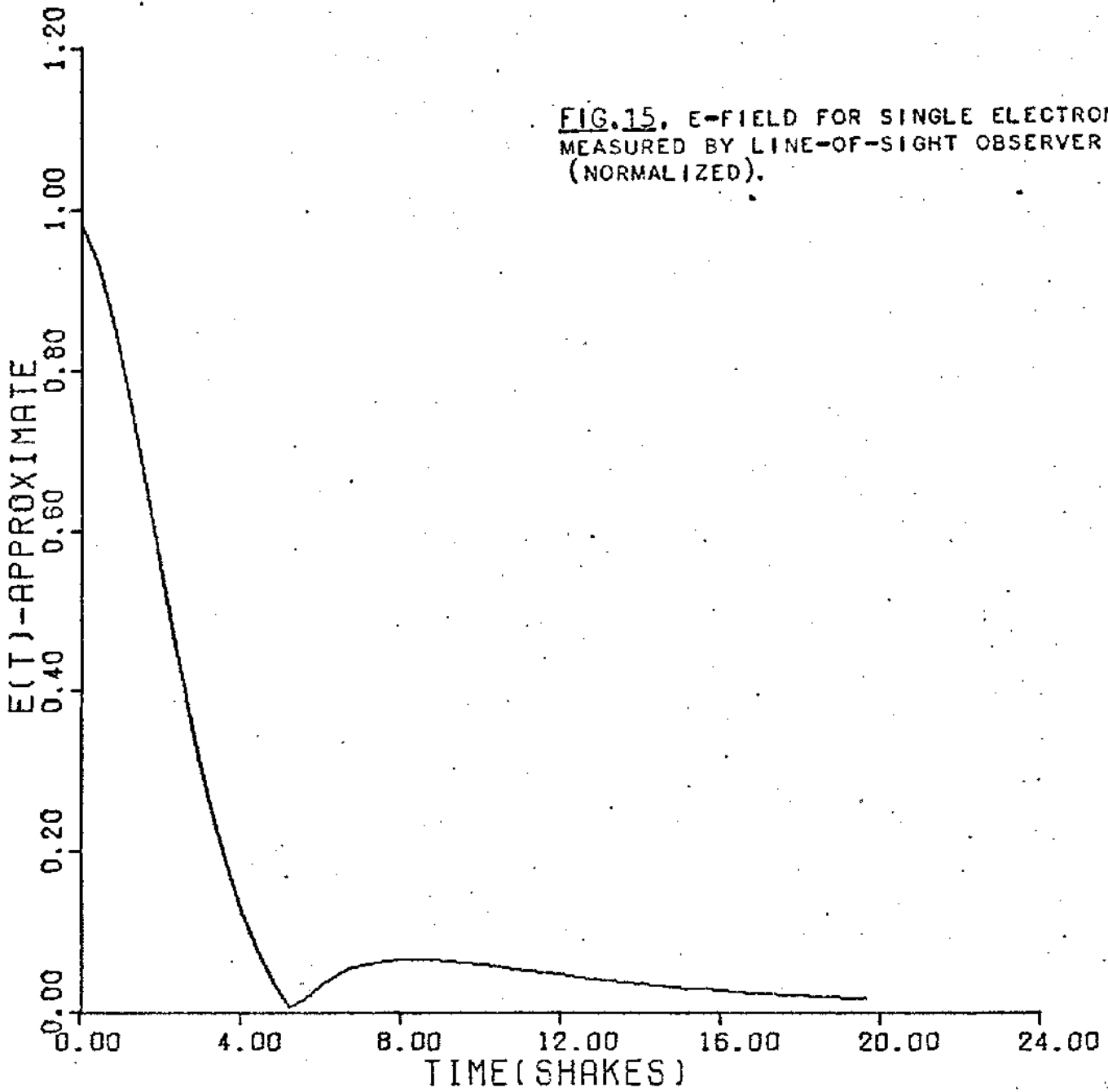
Electron Energy (MeV)	β (-)	Total Time Elapsed (shakes)	ψ_i (radians)	$\frac{dP_L}{d\Omega}$ (*)	$\frac{dP_C}{d\Omega}$ (*)
1.0000	.941	0.00	0.000	0	1.07E-13
.9964	.941	1.82	.108	1.75E-39	9.32E-14
.9929	.940	3.64	.217	2.24E-39	4.81E-14
.9893	.940	5.46	.325	1.17E-39	7.00E-15
.9857	.940	7.28	.434	4.56E-40	6.80E-17
.9821	.940	9.10	.544	1.69E-40	2.98E-16
.9786	.939	10.92	.653	6.46E-41	4.74E-16
.9750	.939	12.75	.763	2.62E-41	3.89E-16
.9714	.939	14.57	.873	1.14E-41	2.69E-16
.9679	.938	16.39	.984	5.27E-42	1.76E-16
.9643	.938	18.21	1.094	2.59E-42	1.15E-16
.9607	.938	20.03	1.205	1.34E-42	7.64E-17
.9571	.937	21.85	1.316	7.30E-43	3.63E-17
.9536	.937	23.67	1.428	4.14E-43	2.61E-17
.9500	.937	25.49	1.539	2.43E-43	1.93E-17
.9464	.936	27.32	1.651	1.47E-43	1.47E-17
.9429	.936	29.14	1.764	9.10E-44	1.14E-17
.9393	.936	30.96	1.876	5.77E-44	1.10E-18
.9357	.935	32.78	1.989	3.73E-44	7.42E-18
.9321	.935	34.60	2.102	2.41E-44	6.20E-18
.9286	.935	36.43	2.216	1.58E-44	5.28E-18
.9250	.934	38.25	2.329	1.03E-44	4.60E-18
.9214	.934	40.07	2.443	6.58E-45	4.08E-18
.9179	.934	41.89	2.558	4.10E-45	3.70E-18
.9143	.933	45.54	2.787	1.29E-45	3.21E-18
.9071	.933	47.36	2.902	5.21E-45	3.08E-18

*These calculations were performed using CGS-Gaussian units rather than MKS units.

to the high altitude EMP, the radiating electron can be considered as moving with a constant speed and being turned by the magnetic field of the earth for the time periods of interest. Making this assumption, one can then calculate the angle that the instantaneous velocity vector makes with the initial direction of the electron (the "line-of-sight" direction for example) at any time t as follows:

$$(III-41) \quad \psi(t) = \frac{\beta ct}{r_{\beta}}$$

where ψ is the indicated angle and r_{β} is the radius of curvature given by (III-25) corresponding to an electron with speed β . Using (III-41) in (III-40) one could obtain information concerning the power or the magnitude of the \bar{E} fields which an observer located along the initial direction of the electron would measure as a function of time. Such a calculation is illustrated in Figure 15 which is a graph of normalized values of the time dependence indicated by (III-40) and (III-41). An even more intuitive understanding of the distribution of this radiation is gained from Figure 16 which illustrates an iso-field line for an electron with a certain instantaneous velocity. From these two figures, one can see that a large portion of the electron's radiated energy is directed forward in the direction of its instantaneous velocity. Also, it is evident that the strength of the fields drops off rapidly as one moves away from this direction. Thus, an observer measures an initial maximum field strength which drops off drastically after the electron turns only a few degrees.



The Net Effect of Many Electrons

Line-of-Sight Effect. Since there are many Compton electrons created in the upper atmosphere by a high altitude nuclear detonation, it is necessary to know which of these contribute to the high frequency EMP measured by an observer at a particular location. It has been previously asserted that the Compton electrons which contribute to the high frequency (early time) EMP are those which are created by gamma photons moving on the "line-of-sight" direction for the observer with respect to the weapon detonation (see Figure 17).¹⁴ There are two primary reasons for this which involve the time phasing of the radiated fields and the angular distributions of the radiated energy.

The important factor with regard to the time phasing aspect is that the Compton electrons are traveling at essentially the speed of light during the time they radiate the major portion of their energy. The importance of this fact can be understood by considering two gamma photons emitted at the same time and moving together on the line-of-sight, each of which creates a Compton electron but at different times (see Figure 17). Since the first electron created is essentially moving at the same speed as the remaining gamma photon, the fields which are radiated in the time interval T_1 (T_1 small enough so that the electron has not appreciably turned off the line-of-sight) and which propagate along the

¹⁴The reader is reminded that it has been assumed that all Compton electrons initially move in the incident direction of the gamma photon.

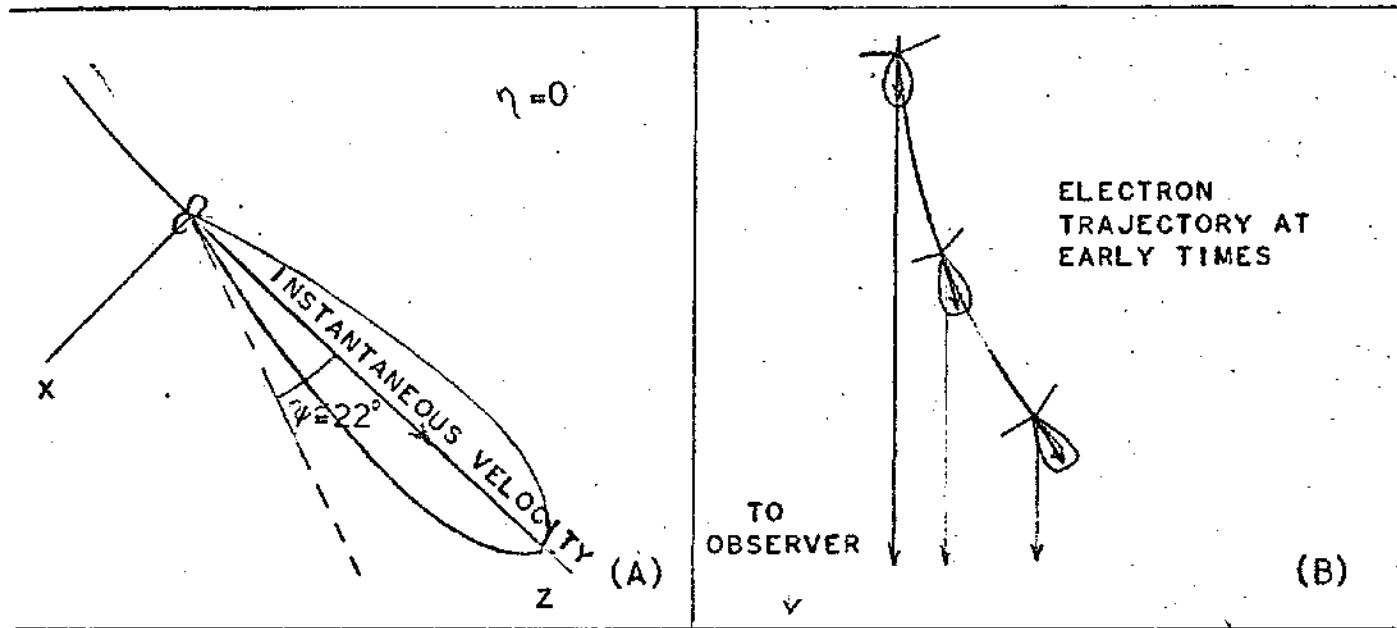


Figure 16. Radiation Pattern for Electron in Circular Motion. (Note that the coordinate system which defines ψ (and η) is constantly changing since the z-axis is defined by $\vec{\beta}(t)$.)

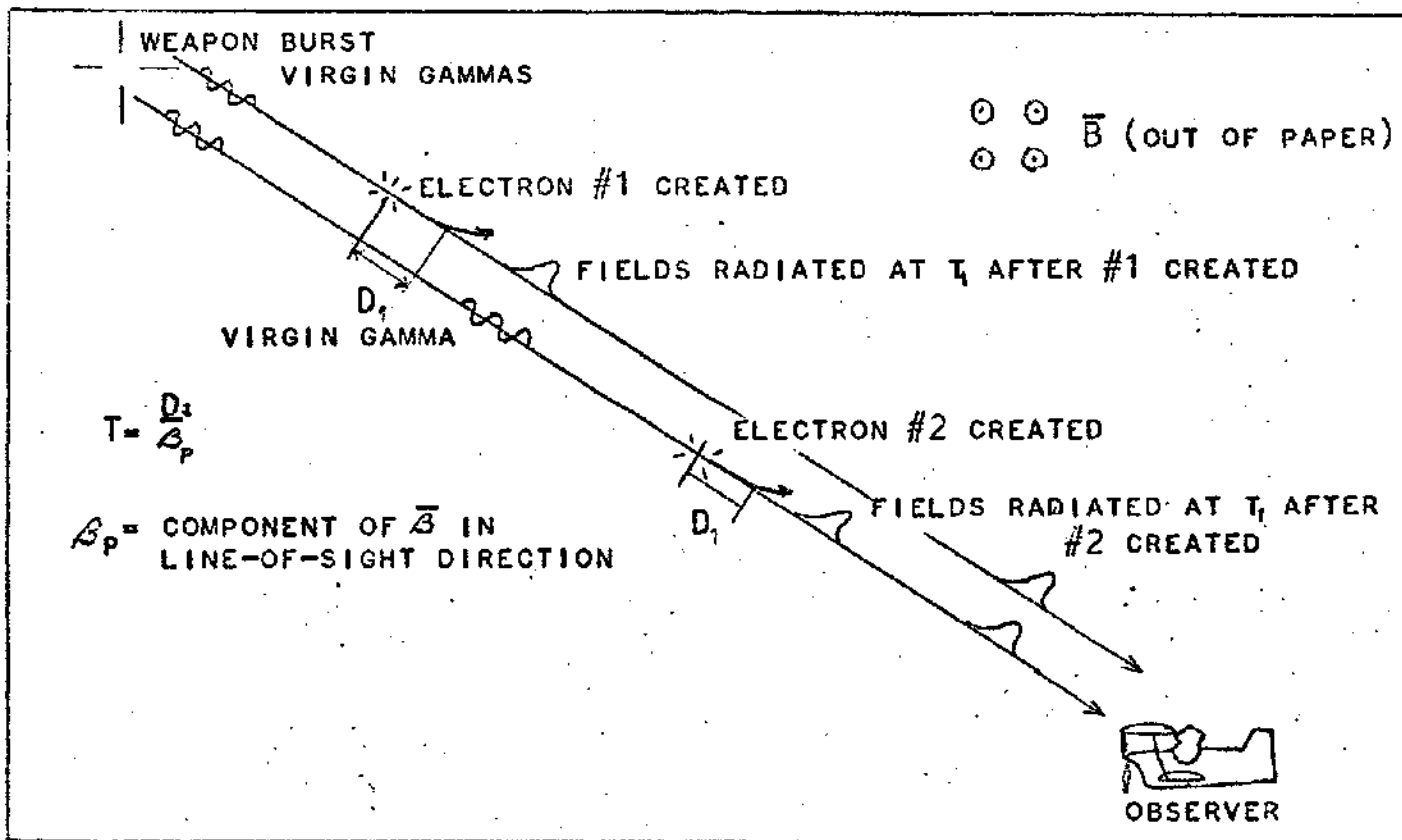


Figure 17. Time Phasing for EM Fields for High altitude EMP. If $\beta_p \approx 1$, then the two radiated fields indicated above will arrive at the observer essentially in phase with respect to time.

line-of-sight constitute a pulse the "leading edge" of which is almost even with the "leading edge" of the gamma photon. Similarly, since the electron created later by the remaining gamma photon is also moving with approximately the speed of light, the fields which it radiates in the time interval T_1 and which propagate along the line-of-sight constitute a pulse the "leading edge" of which is almost perfectly matched up to the first pulse. These two pulses, then, will arrive at the observer in such a manner as to result in almost perfect constructive interference. One can infer from this argument that the more the electron's instantaneous velocity vector deviates from the line-of-sight the less the component of velocity in the line-of-sight direction becomes and the longer the distance which the radiated energy must travel to the observer becomes. The result of this is that the contribution of the radiated pulse to that which the observer measures becomes less and less significant as compared to the contribution of the line-of-sight electrons until it is nothing more than background. Thus, when speaking of "line-of-sight" electrons with respect to time phasing one included electrons created within a small cone centered about the line-of-sight such that their velocity component parallel to the line-of-sight is approximately equal to their total velocity and such that the distance which the radiated energy travels to the observer is approximately equal to that distance which the energy radiated by actual line-of-sight electrons travels.

Independent of the time phasing and more intuitively

obvious is the effect of the angular distribution of the radiated fields. From Figure 15 and Figure 16 one can see that the electron which contributes the most to the power the observer measures is the one which is moving directly toward the observer. Referring to Table 2 one also can see that when the angle between the instantaneous velocity and the direction to the observer is just a few degrees, the radiated fields measured by the observer have dropped by an order of magnitude. Thus, the electron which is created by a gamma whose incident direction is just a few degrees from the line-of-sight direction will not significantly contribute to the early time EMP. It can be argued that an electron with initial direction away from the observer can be turned by the earth's magnetic field such that it eventually "points" at the observer. This argument is valid insofar as the motion of the electron is such that it satisfies the time phasing arguments given in the previous paragraph.

Although it has been shown that the important contribution to the high altitude, high frequency EMP is made by line-of-sight electrons, one should realize that, when speaking of the electrons which contribute to the fields measured by an observer at a particular location, some electrons which are created by gamma photons with directions slightly off the line-of-sight are to be included. The degree of deviation from the line-of-sight is determined by the constraints mentioned in the two previous sections. It is these qualifications which should be kept in mind when speaking of the high altitude,

high frequency EMP as a "line-of-sight" phenomenon.

Superimposing Effect. When computing the net effect of all the electrons which contribute to the EMP one is primarily concerned with the total field strength which the observer measures as a function of time. The variation in time of the field strength will depend, among other things, on the time nature of the gamma photon output. From equation (II-10) in Chapter II it has been shown that the number of gamma photons passing through a unit area at some distance R from the burst and at some time t" is given by

$$(III-42) \quad \Phi(R, t'') = \frac{Y}{E_{\gamma}} f(T'') F(R)$$

where

$$F(R) = \frac{\exp\{\mu_0 z_0 e^{-HOB/z_0} (1 - e^{-R/z_0})\}}{4\pi R^2}$$

and

$$T'' = t'' - \frac{R}{c}$$

Furthermore, using (II-16) one can write the number of Compton electrons which are created per unit volume per unit time at time t" as

$$\frac{dN_{\text{pri}}(R, t'')}{dt} = \frac{Y}{E_{\gamma}} \lambda(R) F(R) f(T'')$$

The number of these electrons which would be created in a time interval dt can be found from the following:

$$(III-43) \quad dN_{\text{pri}}(R, t'') = \frac{Y}{E_{\gamma}} \lambda(R) F(R) f(T'') dt$$

If $E_e(r, t_e)$ represents the general time dependence of the field strengths radiated by a single electron and measured by

an observer at a distance r away and at some time t_e ¹⁵, then for an electron created at t'' the fields measured at time t after the weapon detonation would be given by $E_e(r, t-t'')$. Thus an observer would measure the following for $(V \cdot dN_{pri})$ electrons created a distance r away from him and R from the burst:

$$E_p(r, t) = V \cdot dN_{pri}(R, t'') E_e(r, t-t'')$$

where V is the volume enclosing the electrons which contribute as earlier described. If the time origin is shifted such that $t=0$ when $T''=0$, then the above can be written as

$$E_p(r, t) = V \{dN_{pri}(R, T'') E_e(r, t-T'')\}$$

or using (III-43) and recognizing that the r dependence for E_e is $1/r$ for radiated fields,

$$(III-44) \quad E_p(r, t) = \frac{VY}{rE_Y} \lambda(R) F(R) \{f(T'') E_e(t-T'') dT''\}$$

$E_p(r, t)$ just accounts for those electrons created within an infinitesimal time increment of dT . There will be electrons created before and after this increment which will contribute to the total field strength, $E_T(r, t)$, measured by the observer. Thus, in order to obtain the total field strength caused by Compton electrons created within a finite volume¹⁶ centered about a point some distance R from the burst and measured at some time t by an observer located a distance r

¹⁵These fields were created at $t' \leq t_e - \frac{r}{c}$ (retarded time)

¹⁶For further information concerning this volume see Chapter IV.

from the electrons, one should integrate (III-44) from $T=0$ to $T=t-\frac{r}{c}$. That is,

$$(III-45) \quad E_T(r,t) = \frac{V Y_Y \lambda(R) F(R)}{E_Y r} \int_0^{t-\frac{r}{c}} f(T'') E_e(t-T'') dT''$$

As has been indicated, equation (III-45) is for the electrons created within a certain volume centered about a point some distance R from the burst. One can sum over all such points by letting $V=A \cdot dr$ where A is the cross-sectional area of V lying in a plane perpendicular to the line-of-sight¹⁷ and dR is an infinitesimal length parallel to the line-of-sight, then integrating (III-45) over the absorption layer. Letting $A=A(R)$ one can then write the following for the fields which an observer located a distance X from the burst would measure at time t .

$$(III-46) \quad E(X,t) = \frac{Y_Y}{E_Y} \int_0^X dR \frac{A(R) \lambda(R) F(R)}{(X-R)} \int_0^{t-\frac{(X-R)}{c}} dT'' f(T'') E_e(t-T'')$$

One should note that it was not necessary to make a correction for time lags between altitude because of the time phasing which was mentioned previously.

¹⁷The constraints mentioned in the previous section regarding the line-of-sight effect determine the size of A .

IV. Sample Calculations

The purpose of this chapter is to use the theory developed in the previous chapters and obtain data regarding the nature of the high altitude, high frequency EMP. The techniques used to solve the various equations and arrive at the physical quantities mentioned previously will also be demonstrated. For simplicity, all these calculations involve an observer directly beneath the burst and who is located at the magnetic equator. Thus the incident velocity of the Compton electrons will be perpendicular to the earth's magnetic field. Furthermore, it shall be assumed that the earth's magnetic field is uniform over the absorption layer and has a field strength of 1.0×10^{-4} webers/meters.

Line-of-Sight Area

As was mentioned in the previous chapter, the high frequency EMP is "almost" a line-of-sight phenomenon. That is, there are electrons just slightly off the line-of-sight which contribute significantly to the EMP measured by an observer. The first task in computing the EMP, then is to determine the number of the electrons which contribute to the observer as a function of distance from the burst. For these calculations, it shall be assumed that all the electrons which contribute, do so in exactly the same manner as the electron which is precisely on the line-of-sight. Thus, the cross-sectional area located at a certain distance R from the burst which contains all the electrons that con-

tribute will be considered to act as a point source to the observer. With regard to this approximation, it is obvious that the effect of electrons which originate with a velocity slightly off the line-of-sight yet which are turned so as to "point" at the observer will be underestimated. Similarly, the effect of the electrons originating with a velocity off the line-of-sight and which are turned away from the observer will be overestimated (see Figure 18). To obtain a measure of the error introduced by this, equation (III-40) with $\eta=180^\circ$ was integrated between an angle ψ_0 and $\psi_0 + 6^\circ$ for ψ_0 ranging between -1° and 1° . The per cent difference between each integration and the integration between $\psi_0=0^\circ$ and $\psi_0 + 6^\circ$ was then computed. These results are presented in Table 3. For the purpose of this study, it was decided that the error introduced by $\psi_0 = \pm 0.5$ was tolerable. Thus, the maximum angle between the incident direction of the electron and the line to the observer in order for the electron to be considered as a line-of-sight electron will be set at $\pm 0.5^\circ$.

If one assumes that the cross-section area $A(R)$ at each altitude is a circle, then one must find the radius of this circle in terms of ψ_0 ($=\pm 0.5^\circ$) at each altitude. Using the geometry indicated in Figure 19, with the observer at sea level and letting X_{LOS} be the sought after radius, one finds that

$$(IV-1) \quad X_{LOS}(R) = -\frac{HOB}{2\tan\psi_0} + \sqrt{\left(\frac{HOB}{2\tan\psi_0}\right)^2 + RZ}$$

Table 3
 Difference of Total Power
 Received for Electrons
 off Line-of-Sight

ψ_0	%	ψ_0	%
DEGREES	DIFF	DEGREES	DIFF
-1.0	11.2	0.1	1.3
-0.9	10.3	0.2	2.7
-0.8	9.3	0.3	4.0
-0.7	8.2	0.4	5.4
-0.6	7.2	0.5	6.9
-0.5	6.1	0.6	8.3
-0.4	4.9	0.7	9.4
-0.3	3.8	0.8	10.6
-0.2	2.5	0.9	11.1
-0.1	1.3	1.0	12.4

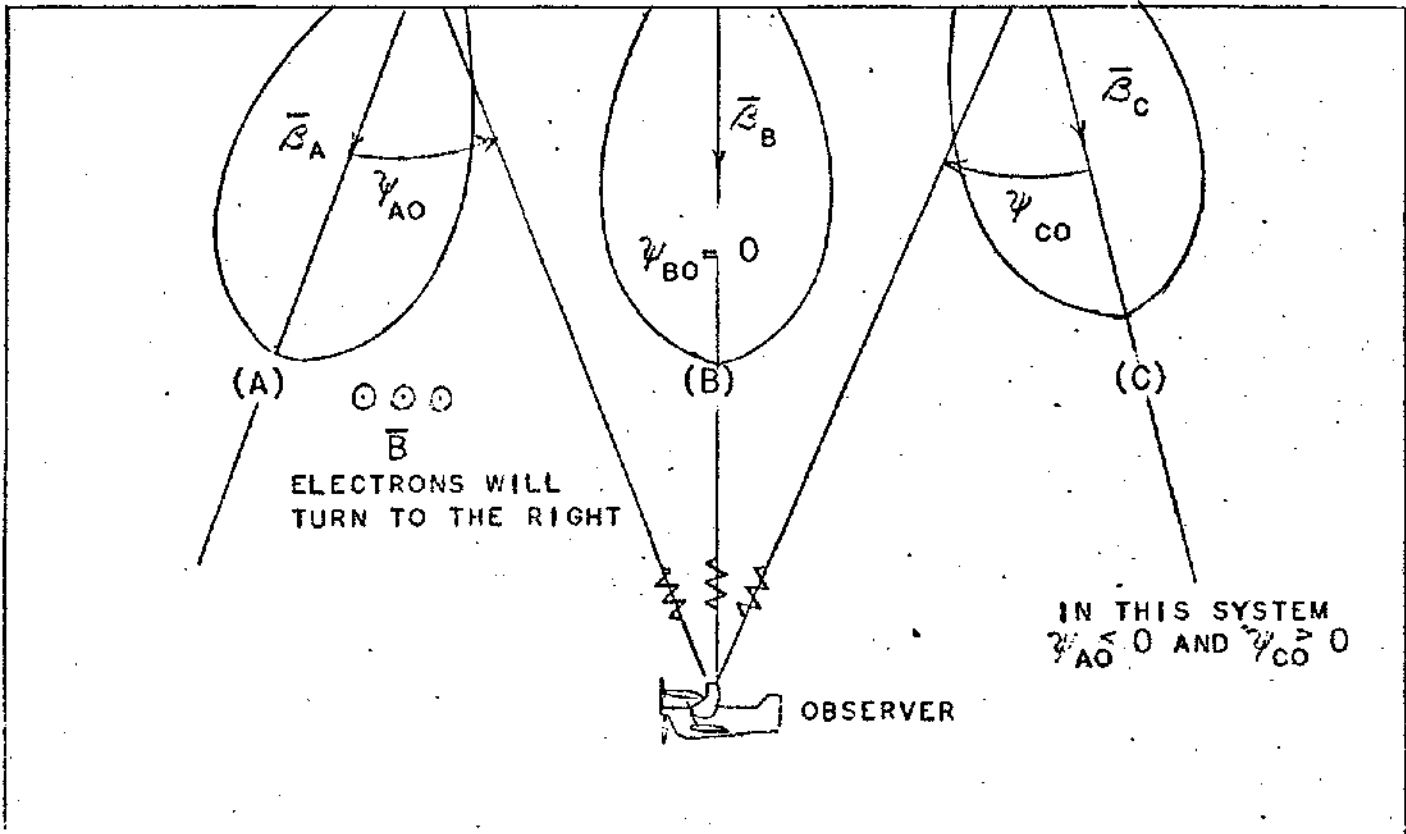


Figure 18. Iso-Power Lines for Electrons in Three Different Configurations Relative to Observer. In a set time period during which each electron turns the same distance and consequently sweeps out the same number of degrees (at least $>\psi_{AO}$) then the contribution of A will be greater than B which will be greater than C.

Therefore, for a circular cross-sectional area $A(R)$ one has,

$$A(R) = 4\pi \left\{ \frac{-\text{HOB}}{2\tan\psi_0} + \sqrt{\left(\frac{\text{HOB}}{2\tan\psi_0}\right)^2 + RZ} \right\}^2$$

A graph was made for X_{LOS} as a function of altitude for a weapon detonation occurring at 100 Km and with $\psi_0 = 0.5^\circ$. This is given in Figure 20.

The assumption that the electrons enclosed in the circular area $A(R)$ above the observer and centered on the line-of-sight act as a point source lying on the line-of-sight ignores the η dependence in equation (III-40). For the electron originating on the line-of-sight, η is always equal to 0° or 180°

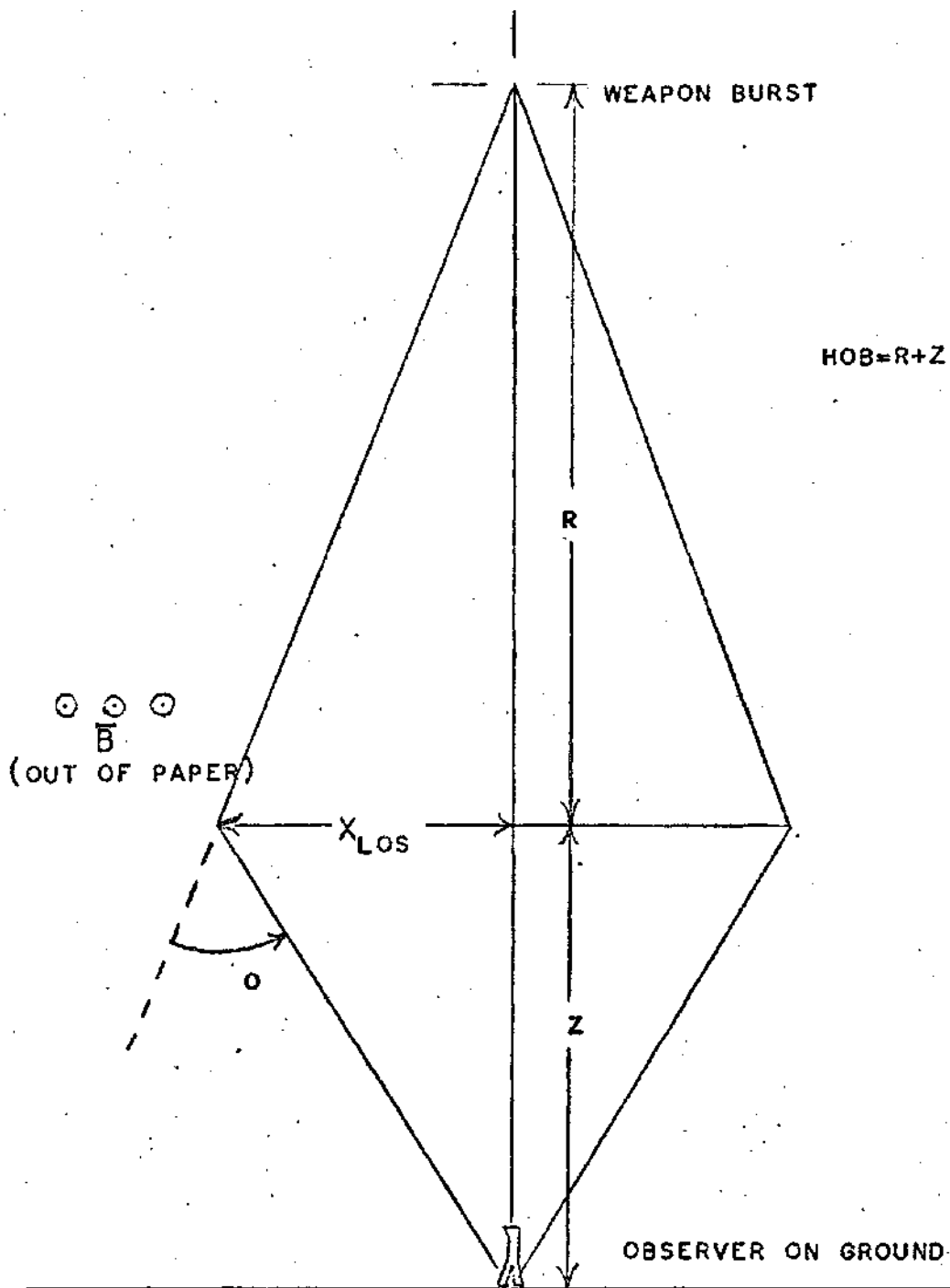
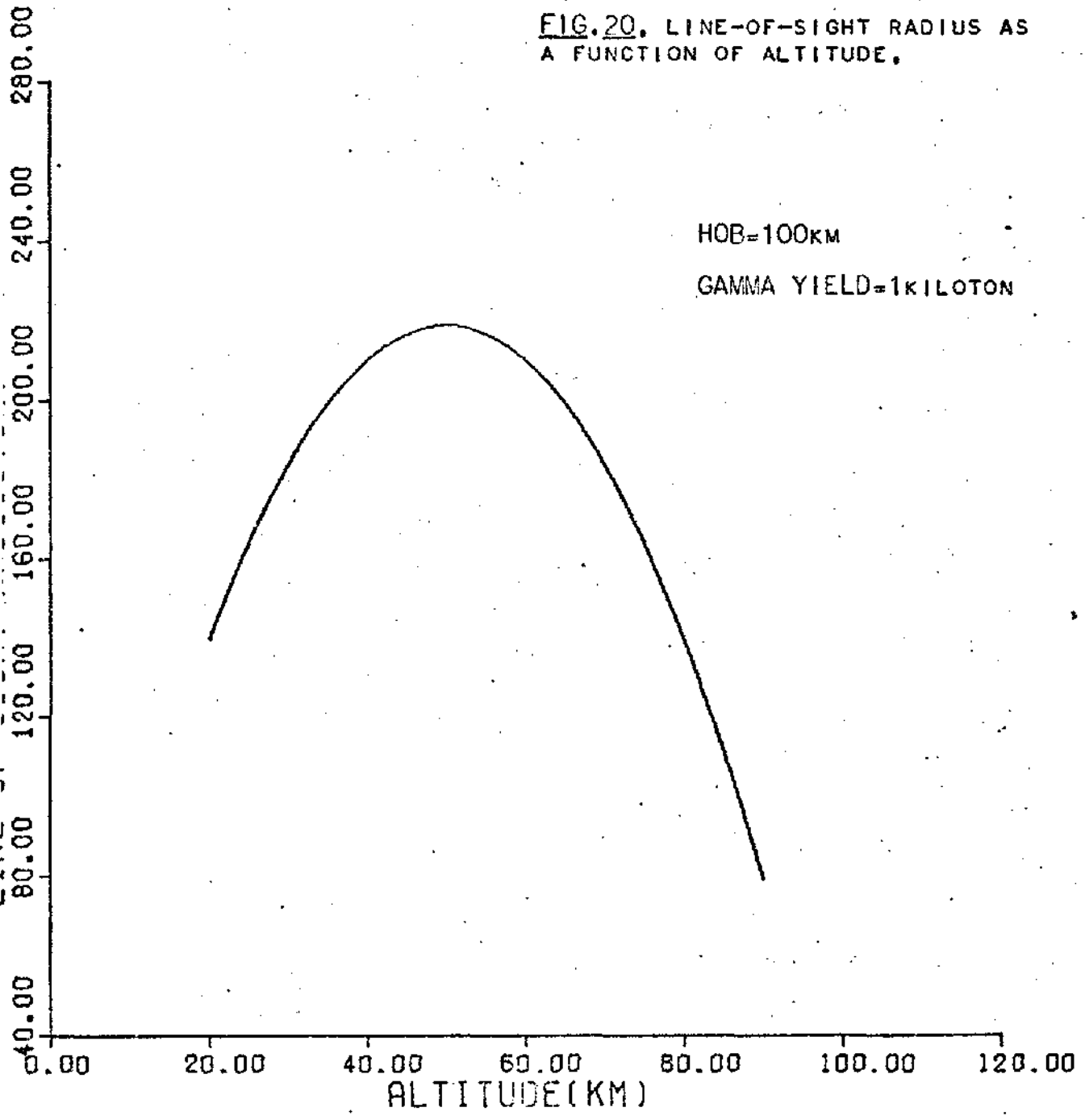


Figure 19. Geomerty for Finding the Line-of-Sight Radius.

FIG. 20. LINE-OF-SIGHT RADIUS AS A FUNCTION OF ALTITUDE.



and $\cos^2\eta=1$. However, there are electrons included in $A(R)$ which have values of η ranging from 0° to $\pm 180^\circ$ (see Figure 21). By saying that the disk with area $A(R)$ appears as a point to the observer, one is implying that the distance X_{LOS} cannot be revolved. Therefore, as far as the observer is concerned, the electrons all appear at a point and have a value of $\eta=0^\circ$ or 180° depending on the orientation of the magnetic field. To test the validity of this assumption one can compare the magnitude of $X_{LOS}(R)$ at various altitudes to the magnitude of the distance to the observer. For example, using Figure 20 one can see that at an altitude of 50 Km the value of X_{LOS} is about 0.22 Km. The ratio between this and the distance to the observer is .004 so that one could say that $X_{LOS} \ll z$ where z , in this case, is the distance to the observer. Similarly, at 20 Km the ratio is .007. Therefore, the assumption of a point source is a relatively good one. One should note that the $A(R)$ which meets the point source specifications falls well within the line-of-sight requirements mentioned in the previous chapter.

Integration Over Absorption Layer

The integration over R in equation (III-46) can be approximated by summing over segments of the absorption layer each centered about some distance R_i and having a depth of ΔR . The quantity ΔR must be such that the macroscopic cross sections and all other quantities depending on R are constant over the interval, since all quantities in this interval will be assumed to have the value given at R_i . It was found that

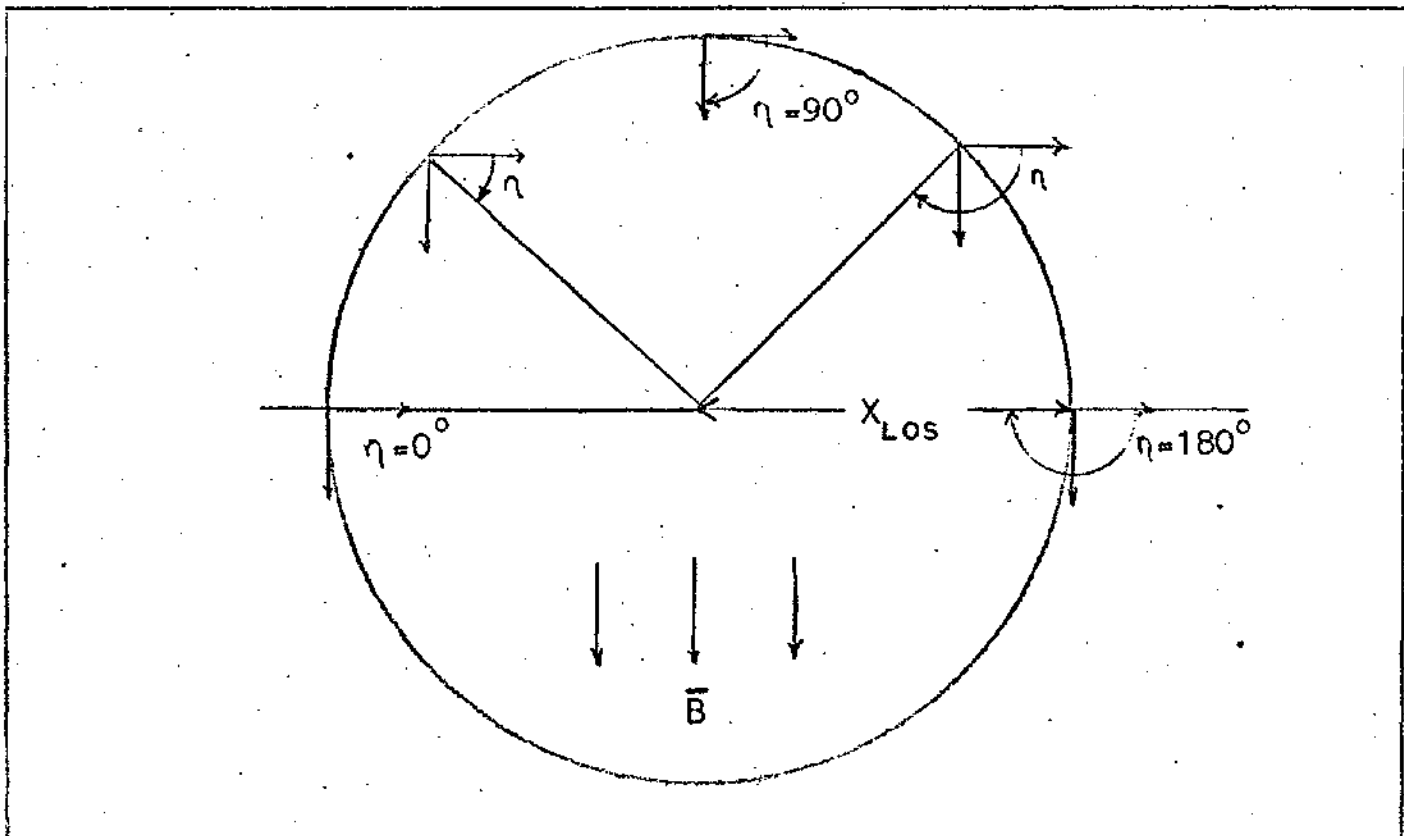


Figure 21. Top View of Electron in Line-of-Sight Area $A(R)$.

$\Delta R=1$ Km was a relatively good approximation. Using this one can now compute the magnitude of the fields resulting from a single electron at R_i which an observer would measure at a certain time, multiply that number by the Compton electrons per unit volume formed at R_i at an appropriate earlier time, and then multiply by $A(R_i)\Delta R$ to get the total effect of a cylindrical volume of electrons centered at R_i . This procedure could then be repeated for all other R_i in the absorption layer and the various contributions summed up in order to obtain the net effect.

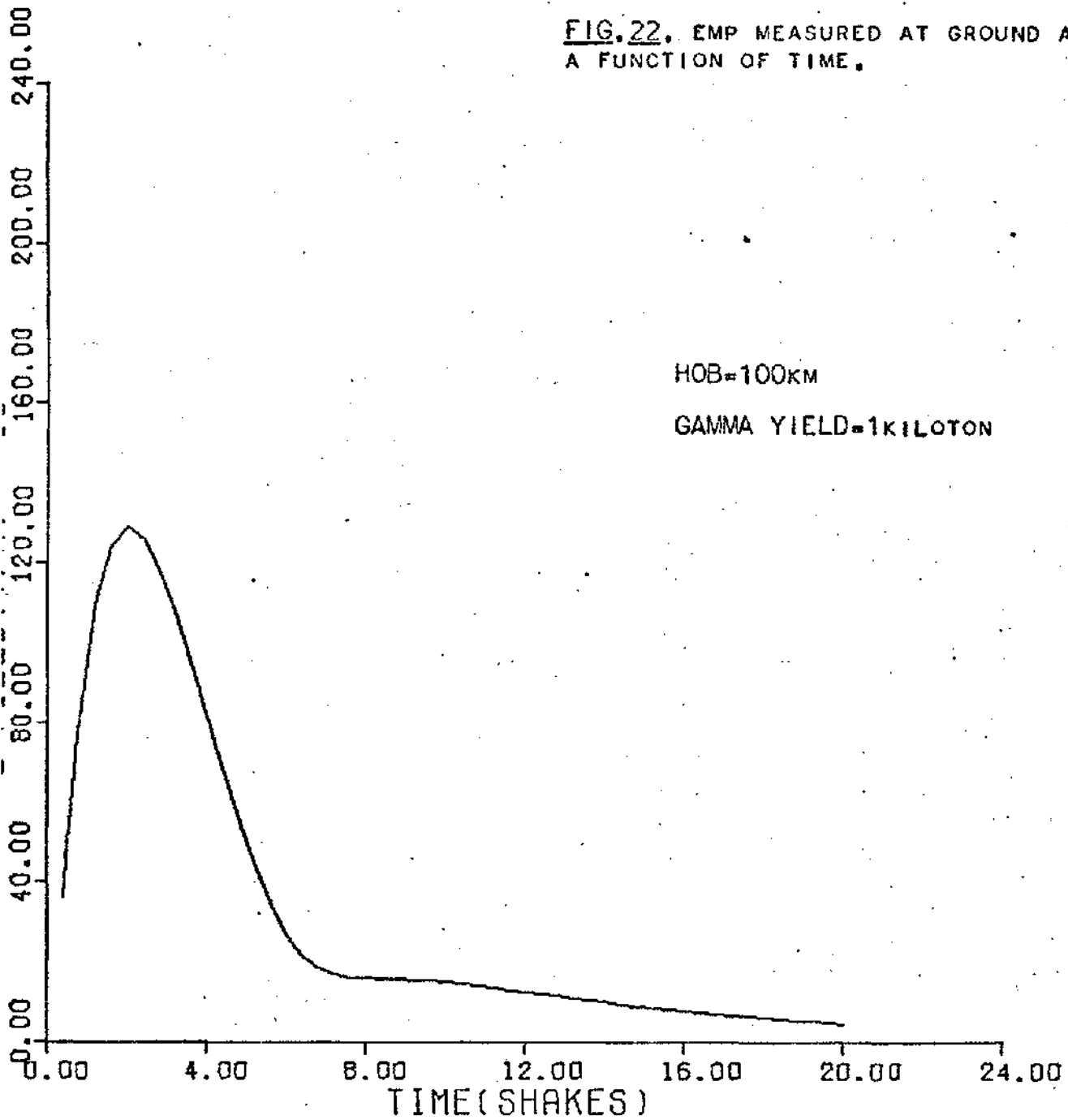
Discussion of Results

The calculations which have been previously discussed were performed for a nuclear detonation occurring at 100 Km with a gamma yield of one kiloton. The magnitude of the \vec{E}

fields which an observer, located directly beneath the burst at sea level and at the magnetic equator, would measure, based on these calculations, is presented in Figure 22. The length of the pulse is about 5 shakes (1 shake = 10^{-8} sec) and reaches peak fields of the order of 12.0×10^4 volts/meter. The validity of the section of the graph for times after ten shakes is doubtful since by this time many of the electrons have slowed considerably below the value of $\beta=0.94$ which was assumed for the calculation. In a paper by Karzas and Latter (Ref 11) using a macroscopic approach with similar weapon parameters, peak field values of 6.0×10^4 volts/meter are reported. Thus, the microscopic approach does give answers which are in the same order of magnitude as accepted theories. The difference between the two could be accounted for by the fact that conductivity has been ignored here but was accounted for in the Karzas and Latter paper.

Although the previous calculations were done for the case where the electron's incident velocity is perpendicular to the earth's magnetic field, it is a simple matter to show the effects of different orientations using this microscopic model. Equations (III-35) and (III-40) indicate that the magnitude of the \bar{E} fields measured by an observer are proportional to the acceleration, $\dot{\beta}$. From equation (III-27) one can see that for an electron of a given energy the acceleration is proportional to $\sin^2\tau$ where τ is the angle between the incident direction and the magnetic field. Thus, the magnitude of the fields measured by an observer will vary as $\sin^2\tau$ according to his

FIG. 22. EMP MEASURED AT GROUND AS A FUNCTION OF TIME.



magnetic bearing with respect to the weapon burst. This point is illustrated by Figure 23 on the next page. The observer at point E will measure the maximum field magnitudes since the angle, τ , between the initial direction of the electrons and the magnetic field is 90° . However, the observer at point A will not measure any fields since the direction of the electrons' motion is parallel to the magnetic field ($\tau=0^\circ$). The field strengths measured by the observers at points B, C and D increase as $\sin^2\tau$ according to the respective values of τ in each case.

One should be aware of the potential range of the high altitude EMP which can be inferred from its "line-of-sight" nature and the facts of the previous paragraph. Since the high altitude, high frequency EMP is essentially a line-of-sight phenomenon, the effects of a burst located at a proper location with respect to the earth's magnetic field could be detected from "horizon to horizon". This fact is illustrated in Figure 24. As one can see from this figure, the size of the area in which the EMP could be detected, for a given orientation with respect to the earth's magnetic field, depends on the height of the weapon burst.

Calculations similar to that mentioned at the beginning of this section were performed for various gamma yields and heights of burst for the weapon. These calculations also ignored conductivity and considered only the gamma induced (ignoring x-ray induced) EMP. The results of these are presented on the following pages in graph form.

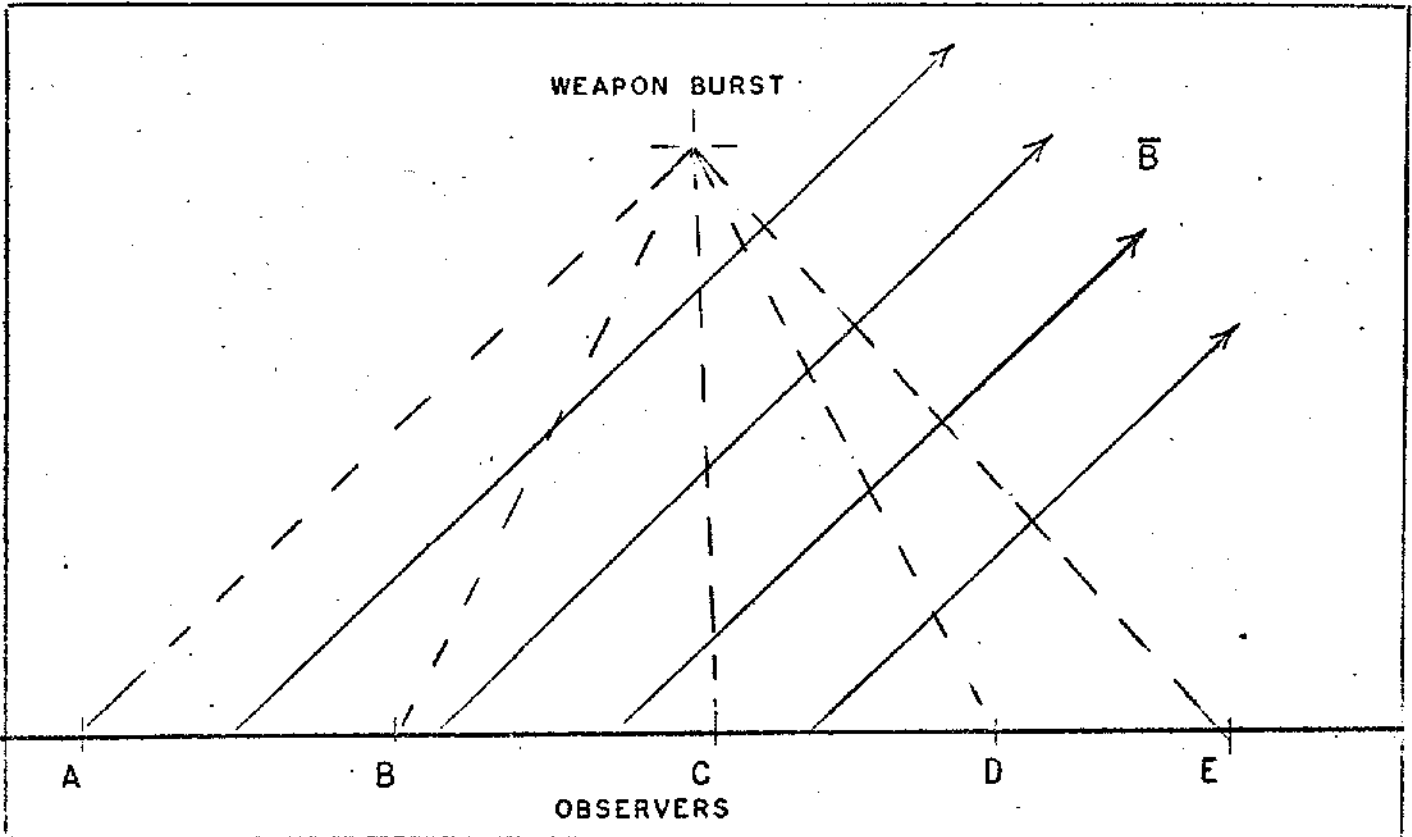


Figure 23. Effect of the Earth's Magnetic Field Orientation on the High Altitude EMP.

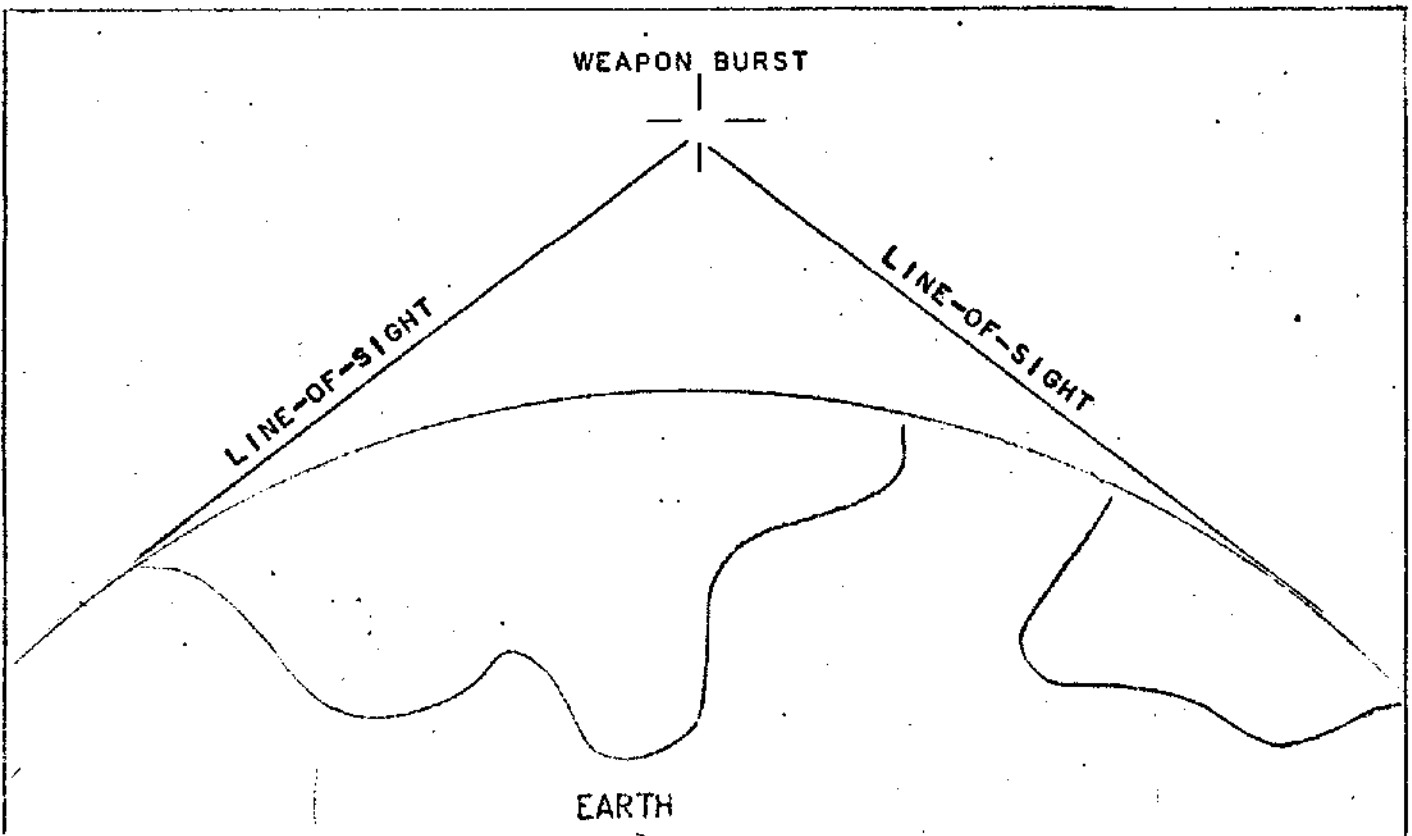


Figure 24. The Horizon-to-Horizon Nature of the EMP.

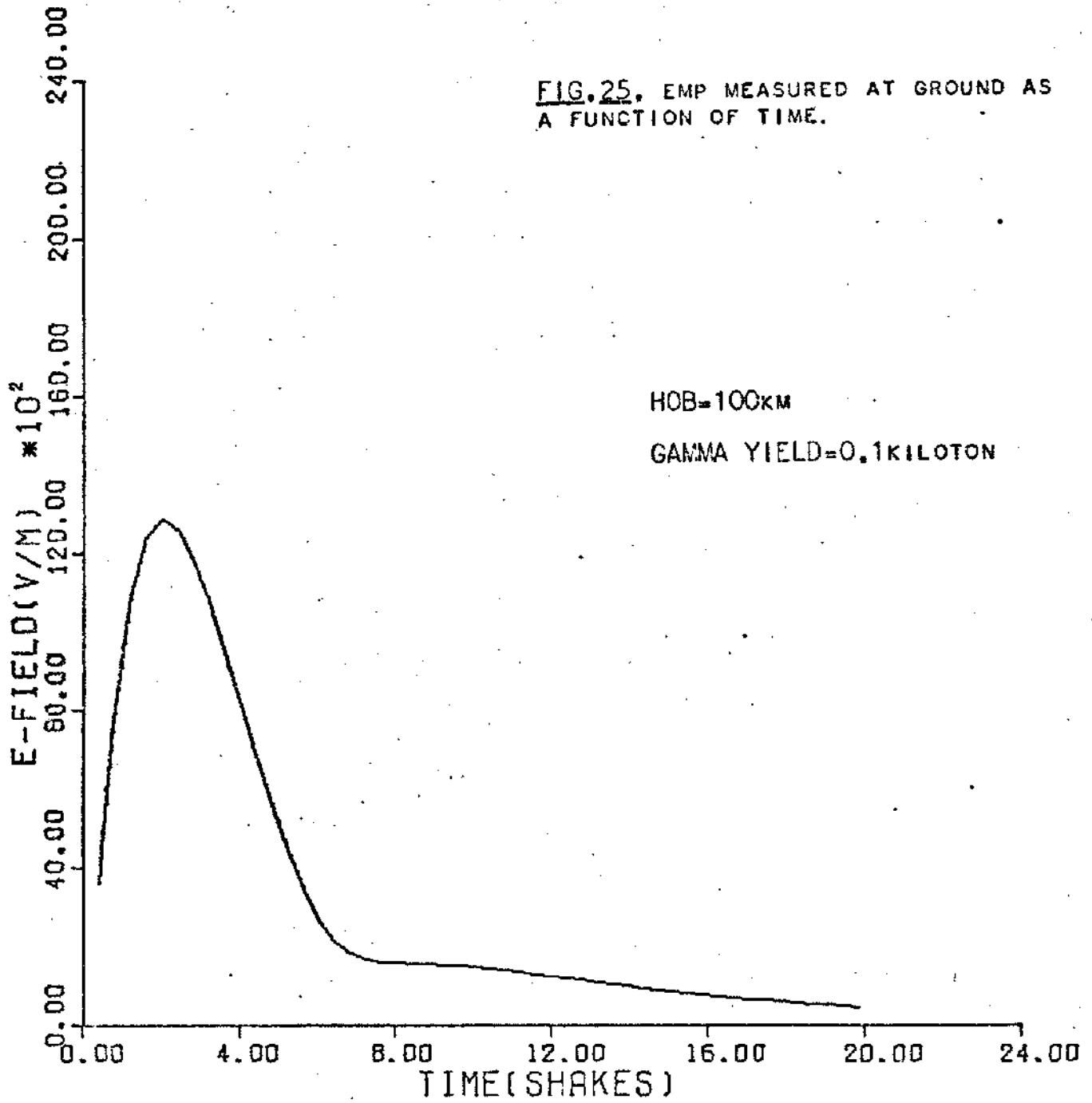


FIG.26. EMP MEASURED AT GROUND AS A FUNCTION OF TIME.

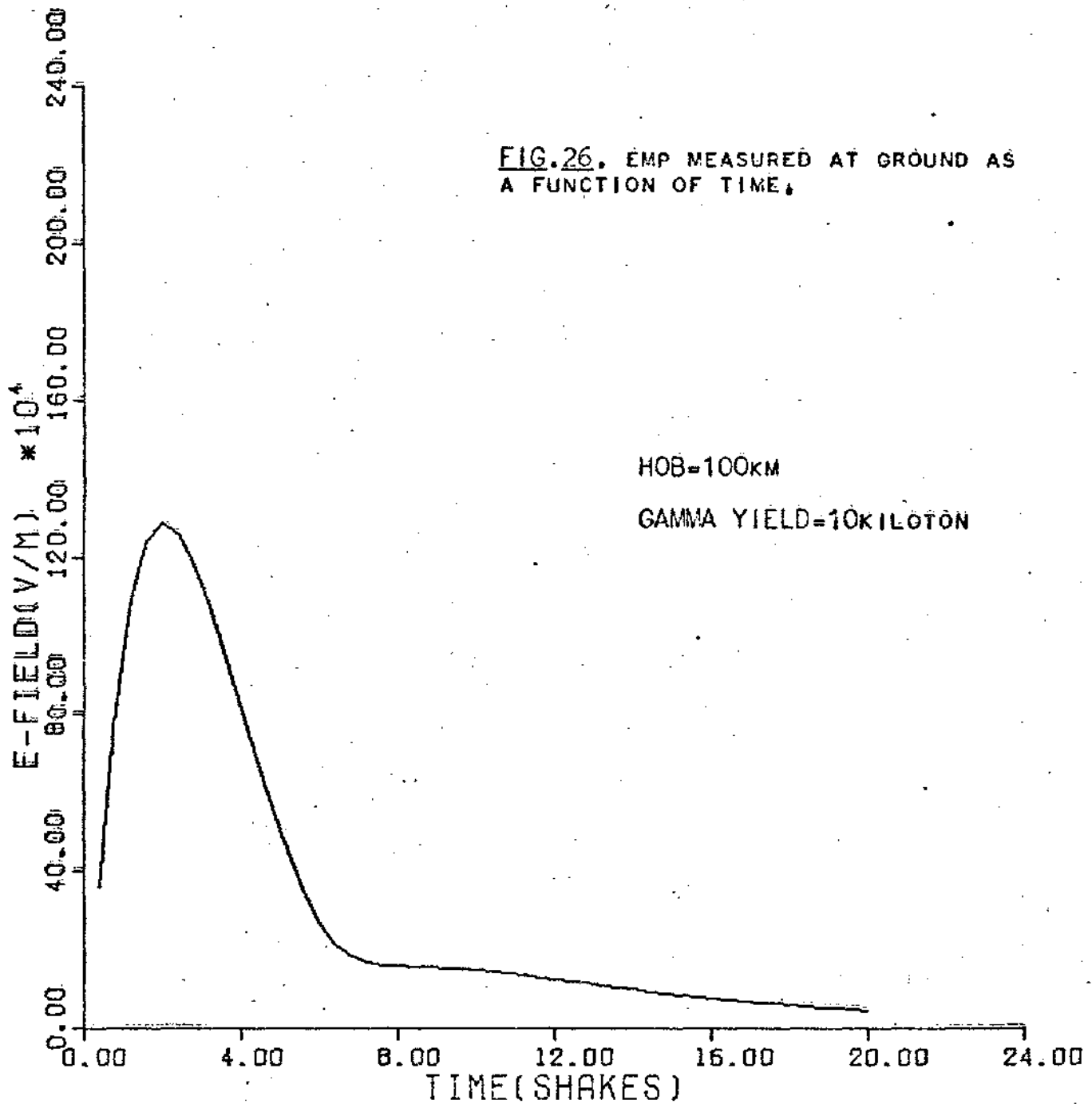
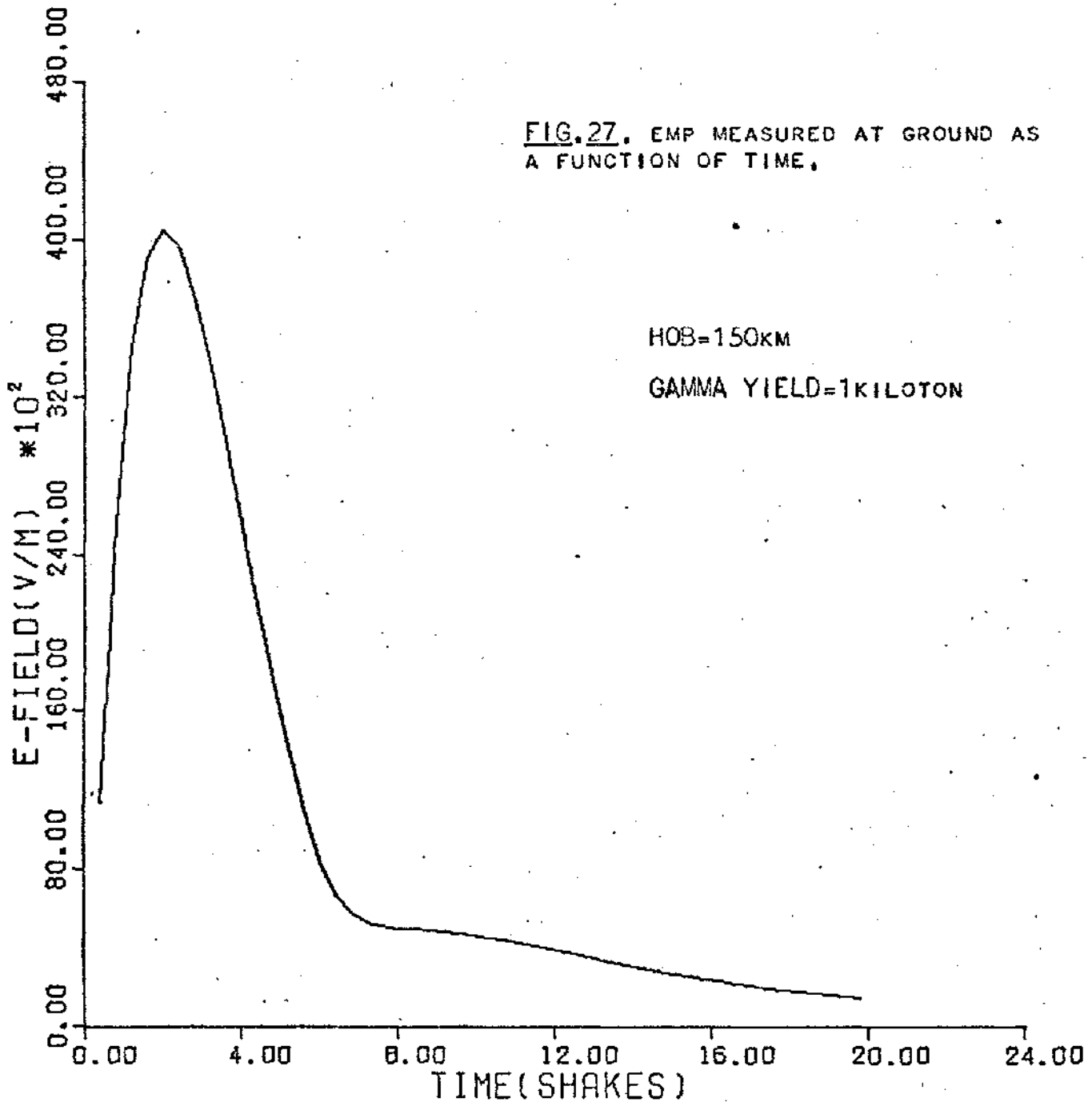


FIG. 27. EMP MEASURED AT GROUND AS A FUNCTION OF TIME.



V. Effects of Air Conductivity

In the previous chapters it was assumed that the conductivity of the air surrounding the radiating electron could be neglected. The purpose of this chapter is to study the validity of this assumption. This will be done by briefly studying the physics involved in air conductivity with respect to the mechanisms relating to the creation of the conductivity and its subsequent buildup in time. There will also be a short section included to indicate the equations which must be solved in order to obtain the fields radiated within a conducting media.

Formation and Buildup of Conductivity

The basic cause of conductivity in the air is the ionization of the molecules of the air caused by the high energy Compton electrons. The result of this ionization is to release large numbers of low energy electrons (secondary electrons) into the media. Although these electrons are not energetic enough to add appreciably to the radiated fields, they do cause the environment to act as a conductor since they are free electrons. One can express the conductivity of the air in terms of the number density of these secondary electrons as follows (Ref 13, p 101):

$$(V-1) \quad \sigma(R,t) = \frac{N_{\text{sec}}(R,t)e^2}{m_0 v_c(z)}$$

where σ is the conductivity measured at a distance R from the weapon detonation at time t , N_{sec} is the secondary electron

density, e is the magnitude of the charge on a single electron, m_0 is the mass of an electron, and ν_c is the frequency of collisions at an altitude z above the ground. It should be mentioned that, in general, the conductivity depends on the density of negative and positive ions as well as free electrons. However, in this case the contribution of the ions is negligible as compared to that of the electrons. The reason for this is that the conductivity is proportional to the sum of the inverses of the mass of the electron, positive ions, and negative ions. Since the ions are orders of magnitude more massive than the electron, the terms involving the inverse of their mass will be negligible compared to the term involving the inverse of the electron mass.

If one assumes that ν_c is constant with respect to time, then the only time dependence in (V-1) is that in the N_{sec} term. There are several mechanisms which affect the time dependency of the density of the secondary electrons. One such mechanism is, of course, the rate at which energy is deposited by the Compton electrons to ionize the air, thereby creating the secondary electrons. However, the chemistry of the air is such that there are also mechanisms whereby these secondary electrons may be removed. The mechanisms include the attachment of a free secondary electron to an O_2 atom to form an O_2^- ion and the recombination of an O_2^+ ion and a N_2^+ ion with a free electron. Since the main purpose of this chapter is to test the validity of ignoring the conductivity, the removal mechanisms for secondary electrons will be ignored in order to arrive at a "worst possible

case" for conductivity. Thus, a lower limit for the time during which conductivity can be ignored will be developed.

In order to relate the number of secondary electrons created to a given amount of energy deposited by the Compton electrons, one can define an average ionization energy W which is defined as the ratio of the energy lost by the Compton electron to the total ionization produced by it. That is, W represents the average energy required to be deposited in order to create a secondary electron. An accepted value for W in air is 34 eV (Ref 19, p 5-6). If a Compton electron was created at some time T and if $\xi_{DEP}(t_c)$ represents the amount of energy which this electron has deposited at some time t_c after its creation, then the number of secondary electrons at time t is given by

$$(V-2) \quad N_{sec}(t) = \frac{\xi_{DEP}(t-T)}{W}$$

It is obvious from this argument that the number density of secondary electrons at a distance R from the burst at a given time t will be dependent upon the number density of the Compton electrons at this point in space and time. That is, at any time t after detonation the number of secondary electrons at a certain R will depend on the number of all the Compton electrons which have been created previous to t and the amount of energy which each has deposited between the time of its creation and t . If $\frac{dN_{pri}(R,T)}{dt}$ represents the rate of change of the primary electron number density at R and T , then one can express the secondary electron number density at any time

t as follows:

$$(V-3) \quad N_{\text{sec}}(R,t) = \int_0^t \left\{ \frac{dN_{\text{pri}}(R,t)}{dt} \right\} \left\{ \frac{\xi_{\text{DEP}}(R,t-T)}{W} \right\} dt$$

where an R dependence has been included in ξ_{DEP} to account for any variation with altitude.

In order to obtain numerical values for (V-1) one needs an expression for $v_c(z)$. The expression for v_c can be shown to vary with altitude primarily as the density of the air varies with altitude. Thus, if one assumes that the atmospheric density varies exponentially with altitude then one can write:

$$(V-4) \quad v_c(z) = v_0 e^{-z/Z_0}$$

where v_0 is the collision frequency at sea level and Z_0 is the scale factor introduced in Chapter II. Using geometry indicated in Chapter II one can write the following for

$$(V-4) \quad v_c(z) = v_0 e^{-(HOB-R)/Z_0}$$

Using (V-1), (V-3), and (V-4) calculations were made for the conductivity as a function of time at various altitudes and for weapons with different amounts of gamma yields. A functional dependence for $\xi_{\text{DEP}}(R,t)$ was obtained at each altitude from data such as that indicated in Table 3. The data was "fit" using a least squares technique and the resulting functional form was used in the integral in (V-3). The results of these calculations for an altitude of 40 Km and varying gamma yields are presented in Table 4 on the following page. To illustrate the variation in altitude,

Table 4
 Conductivity as a Function of Time
 (Altitude = 40 Km)

Time (shakes)	ξ_{DEP} (eV)	σ (Mho/Meter)	$\sigma/\epsilon_v \omega$ (-)
GAMMA YIELD = 1 KILOTON			
0.4	0	0	0
1.2	1.403E02	0	0
2.0	1.865E03	5.314E-09	3.002E-05
2.8	3.586E03	1.082E-07	6.115E-04
3.6	5.302E03	2.303E-07	1.301E-03
4.4	7.014E03	3.627E-07	2.049E-03
5.2	8.721E03	5.010E-07	2.830E-03
6.0	1.042E04	6.427E-07	3.631E-03
6.8	1.212E04	7.867E-07	4.445E-03
7.6	1.382E04	9.320E-07	5.265E-03
8.4	1.551E04	1.078E-06	6.091E-03
9.2	1.720E04	1.225E-06	6.920E-03
10.0	1.888E04	1.372E-06	7.750E-03
GAMMA YIELD = 5 KILOTONS			
0.4	0	0	0
1.2	1.403E02	0	0
2.0	1.865E03	2.657E-08	1.501E-04
2.8	3.586E03	5.410E-07	3.058E-03
3.6	5.302E03	1.152E-06	6.505E-03
4.4	7.014E03	1.814E-06	1.025E-02
5.2	8.721E03	2.505E-06	1.415E-02
6.0	1.042E04	3.214E-06	1.816E-02
6.8	1.212E04	3.934E-06	2.223E-02
7.6	1.382E04	4.660E-06	2.633E-02
8.4	1.551E04	5.390E-06	3.046E-02
9.2	1.720E04	6.125E-06	3.460E-02
10.0	1.888E04	6.860E-06	3.875E-02
GAMMA YIELD = 10 KILOTONS			
0.4	0	0	0
1.2	1.403E02	0	0
2.0	1.865E03	5.314E-08	3.002E-04
2.8	3.586E03	1.082E-06	6.115E-03
3.6	5.302E03	2.303E-06	1.301E-02
4.4	7.014E03	3.627E-06	2.049E-02
5.2	8.721E03	5.010E-06	2.830E-02
6.0	1.042E04	6.427E-06	3.631E-02
6.8	1.212E04	7.867E-06	4.445E-02
7.6	1.382E04	9.320E-06	5.265E-02
8.4	1.551E04	1.078E-05	6.091E-02
9.2	1.720E04	1.225E-05	6.920E-02
10.0	1.888E04	1.372E-05	7.750E-02

* $\omega = 2.0 \times 10^{-7} \text{ sec}^{-1}$

the conductivity at a given instant of time is plotted as a function of altitude in Figure 28.

Relative Significance of Conductivity

To gain a deeper understanding for the significance of the values listed in Table 5, it is necessary to consider Maxwell's equations as applied to a conducting media. With regard to the equation which involves the current density,

$$(V-5) \quad \nabla \times \bar{B} = \mu_V \bar{J} + \frac{1}{c^2} \frac{\partial \bar{E}}{\partial t}$$

one can express the current density as the sum of the Compton current density and the current density of the secondary electrons as follows:

$$\bar{J} = \bar{J}_{\text{comp}} + \bar{J}_{\text{sec}}$$

In the previous chapters, it has been assumed that $\bar{J}_{\text{sec}} = 0$.

If one assumes that Ohm's law applies to the secondary electron current density, namely that

$$\bar{J}_{\text{sec}} = \sigma \bar{E}$$

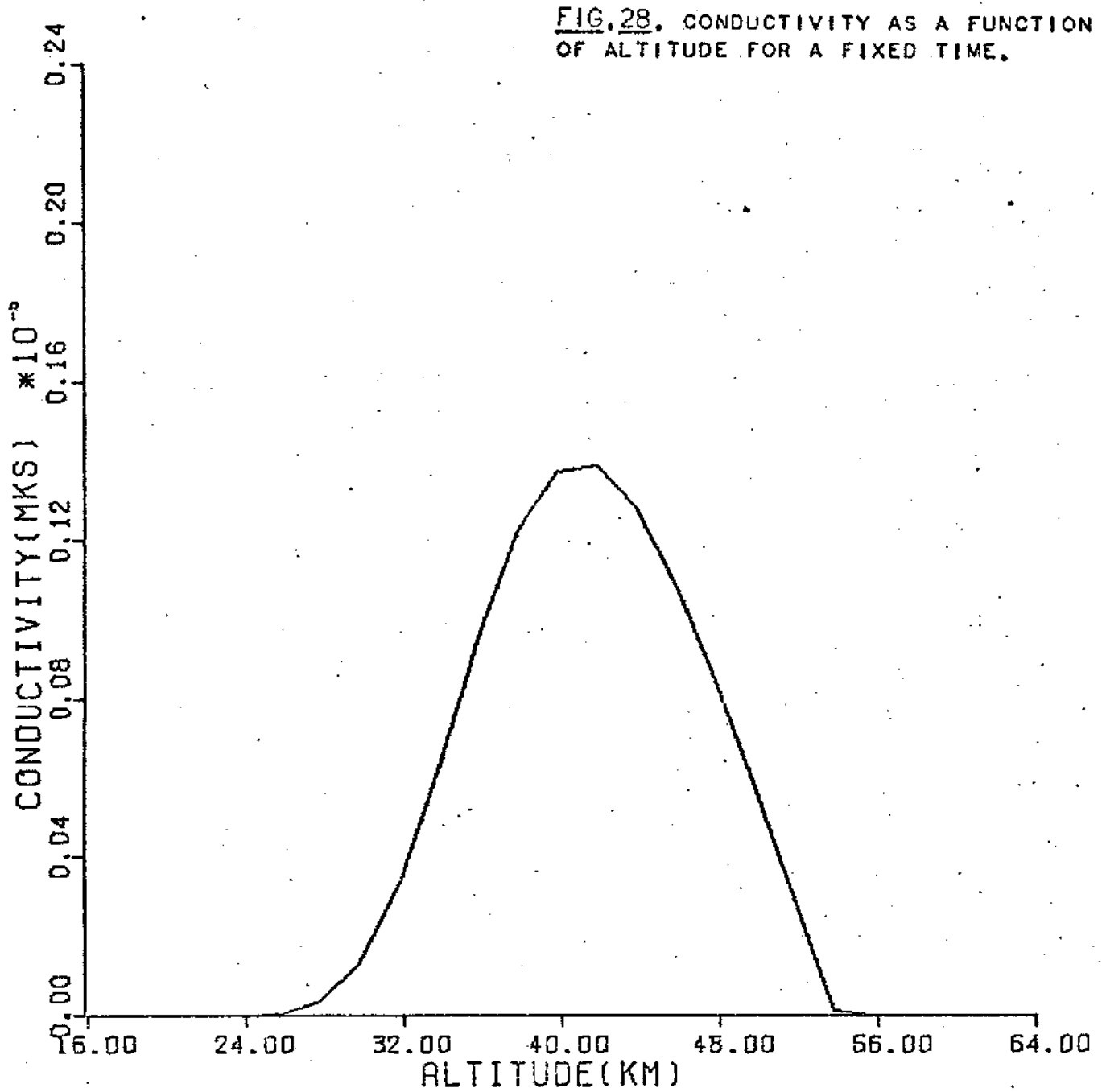
then (V-5) can be written as:

$$(V-6) \quad \nabla \times \bar{B} = \mu_V \bar{J}_{\text{comp}} + \mu_V \sigma \bar{E} + \frac{1}{c^2} \frac{\partial \bar{E}}{\partial t}$$

Using (V-6) and the remainder of Maxwell's equations as indicated in Chapter III and Appendix B, one can obtain wave equations for the vector potential \bar{A} and the scalar potential V such that:¹⁸

$$(V-7) \quad \left\{ \nabla^2 - \mu_V \sigma \frac{\partial}{\partial t} - \frac{1}{c^2} \frac{\partial^2}{\partial t^2} \right\} \left| \frac{\bar{A}}{V} \right| = \left| \frac{\bar{A}}{V} \right| = \left[\begin{array}{l} -\mu_V \bar{J}_{\text{comp}} \\ -\frac{1}{\epsilon_V} \rho_C \end{array} \right]$$

¹⁸ Assuming that σ is constant with respect to space and time.



If one applies a Fourier transform with respect to time to the left hand side of (V-7) the time derivatives can be done explicitly to yield the following for the operator \hat{L} enclosed in the brackets:

$$(V-8) \quad \hat{L}_{FT} = \left\{ \nabla^2 - i\omega\mu_V\sigma - \frac{(i\omega)^2}{c^2} \right\}$$

where \hat{L}_{FT} indicates that the Fourier transform has been applied, $i = \sqrt{-1}$, and ω is the transformation variable. It can be shown that ω corresponds physically to the frequency of the radiated fields. If one divides (V-8) by $\frac{(i\omega)^2}{c^2}$ the results are:

$$\frac{c^2}{(i\omega)^2} \hat{L}_{FT} = \left\{ \frac{c^2}{(i\omega)^2} \nabla^2 + i \left(\frac{\sigma}{\epsilon_V \omega} \right) - 1 \right\}$$

where $c^2 = 1/\mu_V \epsilon_V$ has been used. Thus, one can obtain an estimation of the relative importance of the term involving conductivity by comparing the magnitude of the term $\frac{\sigma}{\epsilon_V \omega}$ to 1. Since the actual fields which are radiated form a pulse which consists of many frequencies, it is necessary to arrive at some "characteristic frequency" of the pulse in order to obtain numbers for the $\frac{\sigma}{\epsilon_V \omega}$ term for various values of σ . A crude approximation which is consistent with the Uncertainty Principle is to let ω be equal to the inverse time width of the radiated pulse. In Chapter IV it was shown that the pulse was about 5×10^{-8} seconds long. Thus, $\omega = 2 \times 10^7$ inverse seconds. The results of such calculations are indicated in the last column of Table 4. If the number .01 is arbitrarily set as the level at which $\frac{\sigma}{\epsilon_V \omega}$ is to be considered significant, then one can see from Table 4 that the conductivity can be

ignored for a gamma yield of one kiloton during the times which the high frequency EMP is being radiated. However, as the gamma yield is increased to five and then ten kilotons, the conductivity does become significant at relatively early times. Therefore, it is fairly safe to ignore the conductivity for weapons with relatively low gamma yields (≤ 1 KT). One should be aware that this last statement is based on ignoring .01 as compared to 1.

Field Equations for a Conducting Media

Equation (V-7) can be solved formalistically as was indicated in Chapter III using the Green's function approach. That is,

$$(V-9) \quad \begin{vmatrix} \bar{A}(\bar{r}, t) \\ \bar{V}(\bar{r}, t) \end{vmatrix} = \int dt' \int d^3\bar{r}' G(\bar{r}, t | \bar{r}', t') \begin{vmatrix} -\mu_v \bar{J}_{comp}(\bar{r}', t') \\ -\frac{1}{\epsilon_v} \rho_c(\bar{r}', t') \end{vmatrix}$$

where $G(\bar{r}, t | \bar{r}', t')$ is the Green's function and which must satisfy the following:

$$(V-10) \quad \left\{ \nabla^2 - \mu_o \sigma \frac{\partial}{\partial t} - \frac{1}{c^2} \frac{\partial^2}{\partial t^2} \right\} G(\bar{r}, t | \bar{r}', t') = \delta(\bar{r} - \bar{r}') \delta(t - t')$$

Equation (V-10) can be solved using Laplace transform techniques to yield (see Appendix C)

$$(V-11) \quad G(\bar{r}, t | \bar{r}', t') = \frac{1}{4\pi r} \left\{ e^{\frac{-\sigma}{2\epsilon_v}(t-t')} \frac{\frac{\sigma r}{2\epsilon_v c} I_1 \left| \frac{\sigma}{2\epsilon_v} \sqrt{(t-t')^2 - \left(\frac{r}{c}\right)^2} \right.}{\sqrt{(t-t')^2 - \left(\frac{r}{c}\right)^2}} \right. \\ \left. \times U\left|t-t' - \frac{r}{c}\right| + \delta\left(t-t' - \frac{r}{c}\right) \right\}$$

where $I_1|x|$ is the modified Bessel function with argument x and $U|x|$ is the unit step function with argument x ($U|x|=0$ for

$x < 0$ and $U|x| = 1$ for $x \geq 0$). The reader should note that the above expression was derived assuming that σ was constant with respect to time which, from Table 4, is seen not to be the case. Yet, even with this simplifying assumption, the author was unable to successfully integrate (V-9) using (V-11). This result was included to indicate to the reader the difficulties involved in applying the microscopic model of the high frequency EMP to conducting media.

VI. Final Remarks

The purpose of this thesis has been to present a model for the high altitude, high frequency EMP which could be used as a pedagogical tool. As such, the emphasis has been placed on developing and outlining the theory rather than obtaining state-of-the-art numerical values for threat levels of the EMP. However, this author feels that this model has great potential for application in this area. The reason for this is that this model allows one to see the effect of changing a greater number of physical parameters than does the macroscopic approach which was briefly described in Chapter I. For this reason, the following recommendations have been made to anyone interested in following up on the work presented in this thesis:

- 1) An attempt should be made to solve the field equations for a conducting media as indicated in Chapter V. The approach to this might involve:
 - a) finding a numerical solution to the integral involving Green's function given in Chapter V in equations (V-9) and (V-11) or
 - b) approaching the problem using a technique other than that presented in Chapter V.
- 2) If one is able to solve Recommendation #1, then it will become necessary to make more precise calculations for conductivity than were included in Chapter V. One should include the various loss mechanisms for the secondary electrons such as attachment and recombination.
- 3) More study should be made regarding the cross-sectional line-of-sight area $A(R)$. This could include sensitivity studies with respect to increasing or decreasing $A(R)$ and the possibility of including the η dependence indicated in (III-40).

Bibliography

1. Bridgman, C. J. Physics of Nuclear Explosives. AFIT Class Notes, NE 6.05, Winter 1973.
2. Case, Carl T. Introduction to Plasma Physics. AFIT Class Notes, PH 5.50, Spring 1973.
3. - - - -. The Electromagnetic Pulse. AFIT Class Notes, EE 6.30, Summer 1973.
4. - - - -. Electromagnetic Waves. AFIT Class Notes, PH 5.31, Winter 1973.
5. Curtis, L. F. "Nuclear Physics" in American Institute of Physics Handbook, edited by Dwight E. Gray. New York: McGraw-Hill, 1963.
6. Enge, Harold A. Introduction to Nuclear Physics. Massachusetts: Adison-Wesley Publishing Company Inc, 1966.
7. Evans, R. D. The Atomic Nucleus. New York: McGraw-Hill, Inc, May 26, 1972.
8. Gaskell, R. E. "The Laplace Transform" in CRC-Standard Mathematical Tables, edited by Samuel M. Selby. Cleveland, Ohio, 1972.
9. Glasstone, Samuel. The Effects of Nuclear Weapons. Washington D. C.: United States Atomic Energy Commission, April 1962.
10. Jackson, John D. Classical Electrodynamics. New York: John Wiley and Sons, 1967.
11. Karzas W. J. and Latter. Detection of the EM Radiation from Nuclear Explosions in Space. AFWL EMP Theoretical Note 40 (AFWL-EMP 2-2). Air Force Weapons Laboratory, April 1971.
12. - - - -. Electromagnetic Radiation from a Nuclear Explosion in Space. AFWL EMP Theoretical Note 27 (AFWL-EMP 2-2). Air Force Weapons Laboratory, April, 1971.
13. Kaufman, Allan N. "Dissipative Effects" in Plasma Physics in Theory and Application, edited by Wulf B. Kunkel. New York: McGraw-Hill, 1966.
14. Kinsley, Otho. Introduction to the Electromagnetic Pulse. Unpublished thesis. Wright-Patterson AFB, Ohio: Air Force Institute of Technology, GNE/PH/71-4.

15. Landau, L. O. and Lifshitz, E. M. The Classical Theory of Fields. Massachusetts: Adison-Wesley Publishing Company Inc, 1962.
16. Leighton, Robert B. Principles of Modern Physics. New York: McGraw-Hill, 1959.
17. Malik, J. S. The Compton Current. AFWL EMP Theoretical Note 16 (AFWL-EMP 2-1). Air Force Weapons Laboratory, April 1971.
18. Pomraning, G. C. Early Time Air Fireball Model for a Near-Surface Burst. Science Application Inc Report SAI-72-588-LJ). March, 1973.
19. Price, Wm. J. Nuclear Radiation Detection. New York: McGraw-Hill, 1964.
20. Theobald, J. K. Fast Electromagnetic Signals Produced by Nuclear Explosions in the Troposphere. LA-2808. Los Alamos Scientific Laboratories, New Mexico; November 1962.

Appendix A

Gamma Ray Interaction with MatterAttenuation Law

The probability of a photon interacting with the atoms of its environment can be expressed in terms of either the microscopic cross section or the macroscopic cross section of the material which constitutes the environment. The microscopic cross section (σ_c) is defined as the effective cross sectional area which an atom presents to a gamma photon for interaction. The macroscopic cross section (μ) is a more useful quantity than the microscopic cross section than driving a law for the attenuation of gamma radiation. The macroscopic cross section is defined as the probability of reaction per unit length of photon path and is related to the microscopic cross section by the relation

$$(A1) \quad \mu = N\sigma_c \quad (\text{Ref 1, p 1-61})$$

where N is the atom density of the environment. Since σ_c has units of area and N has units of inverse volume, then μ must have units of inverse length. It is obvious from (A1) that μ will depend upon the physical state of the environment at any given time, whereas σ_c is a fundamental quantity which is constant for a given material regardless of the physical state. The quantity N can be found from the following relation

$$(A2) \quad N = \frac{N_a \rho}{AW}$$

where N_a is Avogadro's number, ρ is the material density, and AW is the atomic weight of the matter making up the environment.

For the purpose of this study an attenuation law with

respect to a spherical geometry (see Figure 29) will be developed. As shown in Figure 29, the source shall be considered a point source such that photons emanate from it equally in all directions. Thus the only variation in the photon intensity (photons/unit area) is with respect to the distance from the source r . If ϕ_0 represents the number of photons which originate from the source and if one assumes that there is no removal mechanism for the photons in the transport media then the number of photons crossing a unit area at a distance r from the source (intensity - $\phi(r)$) is given by

$$(A3) \quad \phi(r) = \frac{\phi_0}{4\pi r^2}$$

since $4\pi r^2$ represents the surface area of a sphere of radius r . If a material of cross section μ is placed around the source as a shell with an inner radius of r and thickness dr (see Figure 29A) then the intensity of unreacted photons (virgin intensity) at $r + dr$ will be

$$(A4) \quad \phi(r+dr) = \phi(r) + d\phi(r) \quad (\text{see Figure 29B})$$

In the previous equation $d\phi$ represents the change in the virgin photon intensity across dr because of interaction with the material shell. Since μ represents the probability of an interaction per unit photon path length, this change $d\phi$ must satisfy the relation

$$(A5) \quad d\phi(r) = -\phi(r)\mu dr$$

That is, the number of photons which interact in the thickness dr is equal to the total probability of photon interaction in the shell (μdr) multiplied by the number of photons "entering"

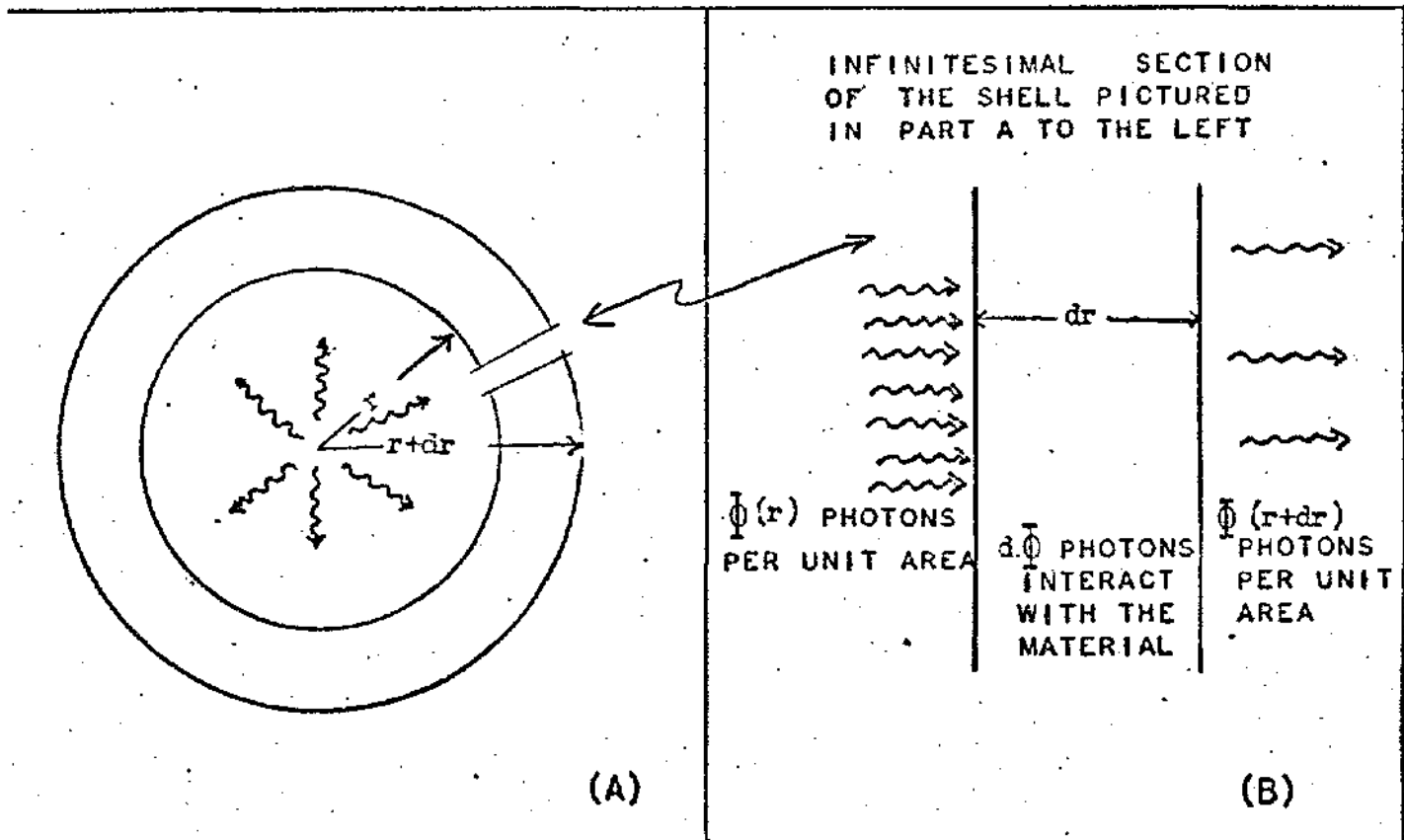


Figure 29. Spherical Geometry for Attenuation Law.

the shell. The equation (A5) can be rewritten such that

$$(A6) \quad \frac{d\phi(r)}{\phi(r)} = -\mu dr$$

If one pictures the gamma source as completely surrounded by an infinite number of shells of infinitesimal thicknesses such that the inner most shell has an inner radius of zero and the outermost shell has an outer radius of R then the virgin flux at R can be obtained by integrating the left hand side of (A6) between $\frac{\phi_0}{4\pi R^2}$ and $\phi(R)$ and the right hand side between 0 and R. That is

$$\int_{\phi_0/4\pi R^2}^{\phi(R)} \frac{d\phi}{\phi} = - \int_0^R \mu dr \{ \text{assume } \mu = \mu(r) \}$$

or

$$\ln \left\{ \frac{\phi(R) 4\pi R^2}{\phi_0} \right\} = - \int_0^R \mu dr$$

or equivalently

$$\frac{\Phi(R) 4\pi R^2}{\Phi_0} = e^{-\int_0^R \mu dr}$$

or solving for $\Phi(R)$

$$(A7) \quad \Phi(R) = \frac{\Phi_0}{4\pi R^2} e^{-\int_0^R \mu dr}$$

The last expression above represents the attenuation law which is used in this thesis for the virgin intensity of gamma photons.

Compton Effect (Ref 16, p 432)

The primary gamma photon interaction with respect to the high altitude EMP is the Compton effect. The analysis of this effect is performed by applying the energy and momentum conservation laws to a collision between an electromagnetic quantum (gamma photon) and an electron. If E_γ is the energy of the incident gamma, E_γ' the energy of the scattered gamma, $m_0 c^2$ the rest energy of the electron, and W_e the total energy of the recoil electron (see Figure 6, Chapter II) then the energy conservation law can be expressed as

$$E_\gamma + m_0 c^2 = E_\gamma' + W_e$$

Using the substitutions indicated in Figure 6 in Chapter II one obtains for the above

$$(A8) \quad h\nu + m_0 c^2 = h\nu' + W_e$$

Similarly, the momentum conservation laws for this situation can be written as

$$(A9) \quad \frac{h\nu}{c} = \frac{h\nu'}{c} \cos \theta + P_e \cos \phi$$

and

$$(A10) \quad 0 = \frac{hv'}{c} \sin \theta - P_e \sin \phi$$

where the variables used above are those indicated in Figure 6. The variable ϕ can be eliminated by rearranging (A9) and (A10), squaring both sides and adding. The results of this are

$$\frac{h^2 v^2}{c^2} - \frac{2h^2 vv'}{c^2} \cos \theta + \frac{h^2 v'^2}{c^2} = P_e^2$$

If one multiplies the above by c^2 and then rearranges terms, the equation becomes

$$(A11) \quad h^2(v-v')^2 + 2h^2 vv'(1-\cos \theta) = P_e^2 c^2$$

Equation (A8) can be solved for W_e^2 whereupon one finds

$$(A12) \quad h^2(v-v')^2 + 2h(v-v')m_0 c^2 + m_0^2 c^4 = W_e^2$$

If one subtracts equation (A11) from (A12) and eliminates W_e and P_e through the relativistic relation

$$W_e^2 - P_e^2 c^2 = m_0^2 c^4$$

then one obtains

$$(A13) \quad 2h(v-v')m_0 c^2 = 2hvv'(1-\cos \theta)$$

Equation (A13) can then be easily solved for hv' with the result that

$$hv' = \frac{hv}{\left\{1 + \frac{hv}{m_0 c^2} (1 - \cos \theta)\right\}}$$

or

$$E_{\gamma'} = \frac{E_{\gamma}}{\left\{1 + \frac{E_{\gamma}}{m_0 c^2} (1 - \cos \theta)\right\}}$$

Appendix B

Derivation of E and B for an Accelerated ElectronThe Wave Equation (Ref 4)

Maxwell's equations are the starting point for finding relations for \bar{E} and \bar{B} for a given source. These equations are

$$(B1) \quad \nabla \times \bar{E}(\bar{r}, t) = - \frac{\partial \bar{B}(\bar{r}, t)}{\partial t}$$

$$(B2) \quad \nabla \times \bar{B}(\bar{r}, t) = \mu_v \bar{J}(\bar{r}, t) + \mu_v \epsilon_v \frac{\partial \bar{E}(\bar{r}, t)}{\partial t}$$

$$(B3) \quad \nabla \cdot \bar{E}(\bar{r}, t) = \frac{1}{\epsilon_v} \rho_c(\bar{r}, t)$$

$$(B4) \quad \nabla \cdot \bar{B}(\bar{r}, t) = 0$$

where the variables are as indicated in Chapter III. Henceforth it shall be assumed that the conductivity of the media surrounding the current source is zero. Because (B4) is always true one can say that

$$(B5) \quad \bar{B} = \nabla \times \bar{A}$$

where \bar{A} is an arbitrary vector at this point. Substituting (B5) into (B1) and assuming that \bar{A} is such that the curl operator and time derivative operator can be interchanged, one obtains the following:

$$(B6) \quad \nabla \times \left\{ \bar{E}(\bar{r}, t) + \frac{\partial \bar{A}(\bar{r}, t)}{\partial t} \right\} = 0$$

Since for any scalar V it is true that $\nabla \times \nabla V = 0$, one can make the following assertion without loss of generality:

$$\bar{E} + \frac{\partial \bar{A}}{\partial t} = - \nabla V$$

or

$$(B7) \quad \bar{E} = - \frac{\partial \bar{A}}{\partial t} - \nabla V$$

where V is an arbitrary scalar. If one substitutes (B7) into (B3) and again assumes that \bar{A} is such that the spatial derivative ($\nabla \cdot$) can be interchanged with the time derivative then the following relation is found:

$$(B8) \quad \nabla^2 V(\bar{r}, t) + \frac{\partial}{\partial t} \{ \nabla \cdot \bar{A}(\bar{r}, t) \} = - \frac{\rho_c(\bar{r}, t)}{\epsilon_v}$$

Also, if one substitutes (B7) and (B5) into (B2) and uses the identities $\nabla_x(\nabla_x \bar{A}) = \nabla(\nabla \cdot \bar{A}) - \nabla^2 \bar{A}$ and $\mu_v \epsilon_v = \frac{1}{c^2}$ then one obtains

$$(B9) \quad \nabla^2 \bar{A} - \frac{1}{c^2} \frac{\partial^2 \bar{A}}{\partial t^2} = -\mu_v \bar{J} + \nabla \left\{ \nabla \cdot \bar{A} + \frac{1}{c^2} \frac{\partial V}{\partial t} \right\}$$

At this point there is still a certain "arbitrariness" with respect to \bar{A} . Since any vector is uniquely defined when both its curl and divergence are specified, the arbitrariness in \bar{A} can be removed by specifying its divergence or the gauge. By studying (B8) and (B9) one observes that a convenient gauge for this problem is the Lorentz gauge or

$$(B10) \quad \nabla \cdot \bar{A} = - \frac{1}{c^2} \frac{\partial V}{\partial t}$$

Substituting (B10) into (B8) and (B9) one finds the following relations for the wave equations of \bar{A} and V :

$$(B11) \quad \nabla^2 V(\bar{r}, t) - \frac{1}{c^2} \frac{\partial^2 V(\bar{r}, t)}{\partial t^2} = - \frac{\rho_c(\bar{r}, t)}{\epsilon_v}$$

and

$$(B12) \quad \nabla^2 \bar{A}(\bar{r}, t) - \frac{1}{c^2} \frac{\partial^2 \bar{A}(\bar{r}, t)}{\partial t^2} = - \mu_v \bar{J}(\bar{r}, t)$$

The Green's Function (Ref 4)

Solutions to (B11) and (B12) can be written formally using the Green's function approach such that the

following is true:¹⁹

$$(B13) \quad \begin{vmatrix} \bar{A}(\bar{r}, t) \\ \bar{V}(\bar{r}, t) \end{vmatrix} = \int d^3\bar{r}' \int dt' G(\bar{r}, t | \bar{r}', t') \begin{vmatrix} -\mu_V \bar{J}(\bar{r}', t') \\ \frac{1}{\epsilon_V} \rho_C(\bar{r}', t') \end{vmatrix}$$

where $G(\bar{r}, t | \bar{r}', t')$ is known as the Green's function and which must satisfy the following equation

$$(B14) \quad \nabla^2 G(\bar{r}, t | \bar{r}', t') - \frac{1}{c^2} \frac{\partial^2 G(\bar{r}, t | \bar{r}', t')}{\partial t^2} = \delta(\bar{r} - \bar{r}') \delta(t - t')$$

One should note that the derivative operators (∇^2 and $\frac{\partial^2}{\partial t^2}$) are both with respect to the unprimed coordinates. To solve (B14) one can use the Laplace transform technique to remove the time derivative from the problem. Thus, if one lets Λ denote the Laplace transform operator with respect to time then the Laplace transform of G becomes

$$(B15) \quad \tilde{G}(\bar{r}, s | \bar{r}', t') = \Lambda\{G\} = \int_0^\infty dt e^{-st} G(\bar{r}, t | \bar{r}', t')$$

Using the property for Laplace transforms of the p^{th} derivative of a function $F(t)$ which is as follows (Ref 8, p 490)

$$\Lambda\{F^{(p)}(t)\} = s^p f(s) - \sum_{n=0}^{p-1} s^{p-1-n} F^{(n)}(0) \quad (+0)$$

where $f(s) = \Lambda\{F(t)\}$, one can then write for the Laplace transform of the second time derivative of G the following:

$$\Lambda\left\{\frac{\partial^2 G(\bar{r}, t | \bar{r}', t')}{\partial t^2}\right\} = s^2 \tilde{G}(\bar{r}, s | \bar{r}', t') - sG(\bar{r}, 0 | \bar{r}', t') - \left.\frac{\partial G(\bar{r}, t | \bar{r}', t')}{\partial t}\right|_{t=0}$$

If one demands that the Green's function and its first time

¹⁹This is just a short hand notation to avoid writing both equations.

derivative satisfy homogeneous boundary conditions at $t=0$ then the previous equation becomes:

$$(B16) \quad \Lambda \left\{ \frac{\partial^2 G(\bar{r}, t | \bar{r}', t')}{\partial t^2} \right\} = s^2 \tilde{G}(\bar{r}, s | \bar{r}', t')$$

One can find the Laplace transform of the right hand side of equation (B14) directly by solving the equation:

$$\Lambda \{ \delta(\bar{r} - \bar{r}') \delta(t - t') \} = \int_0^{\infty} dt e^{-st} \delta(t - t')$$

which, if one applies the properties of the Dirac delta function, becomes

$$(B17) \quad \Lambda \{ \delta(\bar{r} - \bar{r}') \delta(t - t') \} = \delta(\bar{r} - \bar{r}') e^{-st'}$$

Using equations (B15), (B16) and (B17) one can see that if the Laplace operator is applied to both sides of equation (B14) that this equation becomes

$$(B18) \quad \nabla_{\bar{r}}^2 \tilde{G}(\bar{r}, s | \bar{r}', t') - \frac{s^2}{c^2} \tilde{G}(\bar{r}, s | \bar{r}', t') = \delta(\bar{r} - \bar{r}') e^{-st'}$$

where the \bar{r} subscript to the $\nabla_{\bar{r}}^2$ operator is used to emphasize that the derivative is with respect to the unprimed \bar{r} . By translating the origin from 0 to \bar{r}' and letting $\bar{R} = \bar{r} - \bar{r}'$ one can write (B18) as

$$(B19) \quad \nabla_{\bar{R}}^2 \tilde{G} - \frac{s^2}{c^2} \tilde{G} = \delta(\bar{R}) e^{-st'}$$

where the argument of \tilde{G} has been dropped for brevity's sake and where it has been assumed that $\nabla_{\bar{r}}^2 \leftrightarrow \nabla_{\bar{R}}^2$ (this is easily shown). If one multiplies (B19) by $e^{st'}$ on both sides and lets $\tilde{G} = \tilde{G} e^{st'}$ then this equation can be written as follows:

$$(B20) \quad \nabla_{\bar{R}}^2 \tilde{G} - \frac{s^2}{c^2} \tilde{G} = \delta(\bar{R})$$

Since $\delta(\bar{R})$ represents essentially a point source at $\bar{R}=0$, one can argue that there is spherical symmetry in the problem and

the only spatial dependence which \tilde{G} has is with respect to the distance from the source and not on direction. That is,

$$\tilde{G} = \tilde{G}(|\vec{R}|) = \tilde{G}(R)$$

Thus for $\nabla_R^2 \tilde{G}(R)$ one can write the following

$$\nabla_R^2 \tilde{G} = \frac{1}{R^2} \frac{d}{dR} \left(R^2 \frac{d\tilde{G}}{dR} \right)$$

Using the above and letting $\tilde{G}=g/R$ one can rewrite (B20) as

$$\frac{1}{R} \frac{d^2 g}{dR^2} - \frac{s^2}{c^2} \frac{g}{R} = \delta(R)$$

or

$$(B21) \quad \frac{d^2 g}{dR^2} - \frac{s^2}{c^2} g = R\delta(R)$$

If $R > 0$ then $\delta(R) = 0$ and the right hand side of (B20) is zero; if $R = 0$ then the integral of the right hand side is zero. Thus, without loss of generality, one can solve the following instead of (B21):

$$(B22) \quad \frac{d^2 g}{dR^2} - \frac{s^2}{c^2} g = 0$$

Equation (B22) has the following general solution:

$$g(R) = C_1 e^{-sR/c} + C_2 e^{+sR/c}$$

Since it is desired that the fields go to zero as R approaches infinity, then C_2 must be zero in the above. Also, in order that the final solutions would reduce to the electrostatic solution for $V(\vec{r}, t)$ it is seen that C_1 must equal $\frac{-1}{4\pi}$.²⁰ Thus

²⁰This is stated without proof. The interested reader can carry C_1 through the derivation to find V and then match the solution to the electrostatic one to find C_1 .

one has for $g(R)$ that

$$g(R) = -\frac{1}{4\pi} e^{-sR/c}$$

then for \tilde{G} ,

$$\tilde{G} = \frac{g(R)}{R} = \frac{-e^{-sR/c}}{4\pi R}$$

and for \tilde{G} ,

$$(B23) \quad \tilde{G}(\bar{r}, s | \bar{r}', t') = e^{-st'} \tilde{G} = \frac{-e^{-s(t' + \frac{|\bar{r}-\bar{r}'|}{c})}}{4\pi |\bar{r}-\bar{r}'|}$$

A general identity concerning Laplace transforms is that

$$(B24) \quad \Lambda^{-1}\{e^{-s\tau}\} = \delta(t-\tau)$$

where Λ^{-1} denotes the inverse transform. Therefore, if one lets $\tau = t' + \frac{|\bar{r}-\bar{r}'|}{c}$ and applies equation (B24) to (B23) the result is

$$\begin{aligned} G(\bar{r}, t | \bar{r}', t') &= \Lambda^{-1}\{\tilde{G}(\bar{r}, t | \bar{r}', t')\} \\ G(\bar{r}, t | \bar{r}', t') &= \frac{-1}{4\pi |\bar{r}-\bar{r}'|} \Lambda^{-1}\left\{e^{-s(t' + \frac{|\bar{r}-\bar{r}'|}{c})}\right\} \\ (B25) \quad G(\bar{r}, t | \bar{r}', t') &= \frac{-1}{4\pi |\bar{r}-\bar{r}'|} \delta\left\{t - \left(t' + \frac{|\bar{r}-\bar{r}'|}{c}\right)\right\} \end{aligned}$$

Since the Dirac delta function is an even function and since $t - (t' + \frac{|\bar{r}-\bar{r}'|}{c}) = -\{t' - (t - \frac{|\bar{r}-\bar{r}'|}{c})\}$, equation (B25) can be re-written as

$$(B26) \quad G(\bar{r}, t | \bar{r}', t') = \frac{-1}{4\pi |\bar{r}-\bar{r}'|} \delta\left\{t' - \left(t - \frac{|\bar{r}-\bar{r}'|}{c}\right)\right\}$$

Going back to equation (B13) one then has for $\bar{A}(\bar{r}, t)$ and

$V(\vec{r}, t)$ the following relation:

$$(B27) \quad \left| \begin{array}{l} \bar{A}(\vec{r}, t) \\ V(\vec{r}, t) \end{array} \right| = \frac{1}{4\pi} \int d^3\vec{r}' \int dt' \frac{\delta\{t' - (t - \frac{|\vec{r} - \vec{r}'|}{c})\}}{|\vec{r} - \vec{r}'|} \left| \begin{array}{l} \mu_v \bar{J}(\vec{r}', t') \\ \frac{1}{\epsilon_v} \rho_c(\vec{r}', t') \end{array} \right|$$

\bar{E} and \bar{B} Solution

Before one can find a solution for $\bar{E}(\vec{r}, t)$ and $V(\vec{r}, t)$ from (B27) one must have an analytical expression for $\bar{J}(\vec{r}', t')$ and $\rho_c(\vec{r}', t')$. For an electron with charge e and velocity $\vec{v}(t)$ at the point $\vec{x}(t)$ the current and charge density are given by the following:

$$\bar{J}(\vec{r}', t') = e c \bar{\beta}(t) \delta\{\vec{r}' - \vec{x}(t')\}$$

and

$$\rho_c(\vec{r}', t') = e \delta\{\vec{r}' - \vec{x}(t')\}$$

where $\bar{\beta}(t') = \vec{v}(t')/c$. Thus one can write for the vector and scalar potential the following:

$$\left| \begin{array}{l} \bar{A}(\vec{r}, t) \\ V(\vec{r}, t) \end{array} \right| = \frac{e}{4\pi} \int d^3\vec{r}' \int dt' \frac{\delta\{t' - (t - \frac{|\vec{r} - \vec{r}'|}{c})\}}{|\vec{r} - \vec{r}'|} \delta\{\vec{r}' - \vec{x}(t')\} \left| \begin{array}{l} \mu_v c \bar{\beta}(t') \\ \frac{1}{\epsilon_v} \end{array} \right|$$

Using the properties of the Dirac delta function the integration over the spatial coordinates (\vec{r}') can be immediately performed to yield:

$$(B28) \quad \left| \begin{array}{l} \bar{A}(\vec{r}, t) \\ V(\vec{r}, t) \end{array} \right| = \frac{e}{4\pi} \int dt' \frac{\delta\{t' + \frac{R(t')}{c} - t\}}{R(t')} \left| \begin{array}{l} \mu_v c \bar{\beta}(t') \\ \frac{1}{\epsilon_v} \end{array} \right|$$

where $R(t') = |\vec{r} - \vec{x}(t')|$

One should observe that the only spatial dependence in (B28) is in the term R . Further, since the forms of \bar{E} and \bar{B} given by equation (B5) and (B7) require the use of the spatial

operator ∇_r it is convenient to express this operator in terms of its effect of R rather than r . Using the Einstein summation notation ²¹ the vector R can be written as

$$\bar{R} = x_i \hat{e}_i \quad (i = 1, 2, 3)$$

where the x_i represent the coordinates of \bar{R} in the cartesian basis \hat{e}_i . One can also represent the ∇_r operator by

$$(B29) \quad \nabla_r \rightarrow \hat{e}_i \frac{\partial}{\partial x_i}$$

so that for some function $f(R) = f\{R(x_i)\}$ one can write that

$$\nabla_r \bar{f}(R) = \hat{e}_i \frac{\partial f(R)}{\partial x_i}$$

or, using the chain rule

$$\nabla_r \bar{f}(R) = \hat{e}_i \frac{\partial f(R)}{\partial R} \frac{\partial R}{\partial x_i}$$

$$\nabla_r \bar{f}(R) = \hat{e}_i \frac{\partial R}{\partial x_i} \frac{\partial f(R)}{\partial R}$$

or, using (B29)

$$(B30) \quad \nabla_r \bar{f}(R) = \nabla \bar{R} \frac{\partial f(R)}{\partial R}$$

Since $R = (x_i x_i)^{1/2}$ one can write for $\nabla \bar{R}$ that

$$\nabla \bar{R} = \hat{e}_j \frac{\partial}{\partial x_j} (x_i x_i)^{1/2} = e_j \frac{2x_i \delta_{ij}}{2(x_i x_i)^{1/2}}$$

or

$$(B31) \quad \nabla \bar{R} = \frac{x_j \hat{e}_j}{(x_i x_i)^{1/2}} = \frac{\bar{R}}{R} \equiv \hat{n}$$

where, because of the definition of \bar{R} , \hat{n} is a unit vector

²¹In this notation a repeated index signifies a sum. Thus $a_i b_i = \sum_i a_i b_i = a_1 b_1 + a_2 b_2 + \dots$

pointing from the source to the observer. Thus one can write, using (B30) and (B31), that

$$(B32) \quad \nabla_{\mathbf{r}} \rightarrow \hat{\mathbf{n}} \frac{\partial}{\partial R}$$

Using the relation for $\bar{\mathbf{E}}$ given in (B7) as applied to (B28) and letting $\nabla_{\mathbf{r}}$ be as given in (B32) one finds the following for $\bar{\mathbf{E}}(\bar{\mathbf{r}}, t)$

$$\begin{aligned} \bar{\mathbf{E}}(\bar{\mathbf{r}}, t) = & \frac{e}{4\pi} \int dt' \left(\frac{\hat{\mathbf{n}}}{\epsilon_{\mathbf{v}} R^2(t')} \delta\left\{t' + \frac{R(t')}{c} - t\right\} \right. \\ & \left. - \frac{\hat{\mathbf{n}}}{\epsilon_{\mathbf{v}} R(t')} \left\{ \delta'\left(t' + \frac{R(t')}{c} - t\right) \frac{\partial\left(t' + \frac{R(t')}{c} - t\right)}{\partial R} \right\} \right) \\ & - \frac{\bar{\beta}(t') \mu_{\mathbf{v}} c}{R(t')} \left\{ \delta'\left(t' + \frac{R(t')}{c} - t\right) \frac{\partial\left(t' + \frac{R(t')}{c} - t\right)}{\partial t} \right\} \end{aligned}$$

where $\delta'(x)$ denotes the first derivative of the Dirac delta function with respect to its argument. After terms are rearranged and the indicated derivatives performed the above expression for $\bar{\mathbf{E}}(\bar{\mathbf{r}}, t)$ can be written as

$$(B33) \quad \bar{\mathbf{E}}(\bar{\mathbf{r}}, t) = \frac{e}{4\pi\epsilon_{\mathbf{v}}} \int dt' \left(\frac{\hat{\mathbf{n}}}{R^2(t')} \delta\left\{t' + \frac{R(t')}{c} - t\right\} \right. \\ \left. + \frac{1}{R(t')c} (\bar{\beta}(t') - \hat{\mathbf{n}}) \delta'\left\{t' + \frac{R(t')}{c} - t\right\} \right)$$

where the fact that $\mu_{\mathbf{v}} \epsilon_{\mathbf{v}} = \frac{1}{c^2}$ has been used. In order to evaluate the integral in (B33) it will be divided into the following two parts:

$$(B34) \quad I_1 = \int dt' \left(\frac{\hat{\mathbf{n}}}{R^2(t')} \delta\left\{t' + \frac{R(t')}{c} - t\right\} \right)$$

$$(B35) \quad I_2 = \int dt' \frac{1}{R(t')c} (\bar{\beta}(t') - \hat{\mathbf{n}}) \left\{ \delta'\left(t' + \frac{R(t')}{c} - t\right) \right\}$$

It should be noted that the argument of the delta function in I_1 (and I_2) contains a function of the variable of integration

rather than simply the variable itself. In order to evaluate this particular situation the following general integral will be considered:

$$I = \int g(t') \delta\{f(t') - c\} dt'$$

where g and f are arbitrary functions of x each of which has an inverse²² and first derivative and where c is some constant with respect to the integration variable. If one lets $f(t')=u$ and then makes a change of variable in the integral such that $t'=f^{-1}(u)$ then

$$du = \frac{df}{dt'} dt' \rightarrow dt' = \frac{du}{df/dt'}$$

and I becomes

$$I = \int \frac{g(f^{-1})}{df/dt'} \delta(u-c) du$$

or using the delta function properties

$$I = \frac{g(f^{-1})}{df/dt'} \Big|_{u=c}$$

or

$$(B36) \quad I = \int g(x) \delta\{f(t')-c\} dt' = \sum_i \frac{g(t_i')}{df/dt'} \Big|_{f(t')=c}$$

where the t_i' are those values of t' which satisfy $f(t')=c$. Applying (B36) to (B34) one can see first that $f(t')=t'+\frac{1}{c}R(t')$ which implies the following:

$$(B37) \quad \frac{df}{dt'} = 1 + \frac{1}{c} \frac{dR}{dt'}$$

If one represents R by $(\bar{R} \cdot \bar{R})^{1/2}$ then $\frac{1}{c} \frac{dR}{dt'}$ can be written as:

$$\frac{1}{c} \frac{dR}{dt'} = \frac{1}{c} \frac{d}{dt'} (\bar{R} \cdot \bar{R})^{1/2} = \frac{1}{c} \frac{\bar{R} \cdot d\bar{R}}{\bar{R}}$$

or using the definition of \bar{R} and letting $\hat{n} = \frac{\bar{R}}{R}$

²²For example if $f(x)=u$, then $x=f^{-1}(u)$ where f^{-1} is the inverse function of f.

$$(B38) \quad \frac{1}{c} \frac{dR}{dt'} = \hat{n} \cdot \frac{1}{c} \frac{d}{dt'} \{ \bar{r} - \bar{x}(t') \} = -\hat{n} \cdot \frac{\bar{v}(t')}{c} = -\hat{n} \cdot \bar{\beta}(t')$$

Thus one has for (B37)

$$(B39) \quad \frac{df}{dt'} = 1 - \hat{n} \cdot \bar{\beta}(t') \equiv \kappa$$

Using (B38) and the relation defined in (B36) one finds that

(B34) can be written as follows

$$I_1 = \frac{\hat{n}}{\kappa R^2(t')} \left|_{t' + \frac{R(t')}{c}} = t$$

or

$$(B40) \quad I_1 = \frac{\hat{n}}{\kappa R^2(t')} \left|_{t' = t - \frac{R(t')}{c}} = \left| \frac{\hat{n}}{\kappa R^2} \right|_{\text{ret}}$$

The brackets with the subscript "ret" means that the quantity which they enclose is to be evaluated at the retarded time,

$$t' = t - \frac{R}{c}$$

The expression (B35) and I_2 can be evaluated similarly to I_1 if one makes the following substitutions:

$$f(t') = t' + \frac{R(t')}{c} \equiv u \rightarrow t' = f^{-1}(u)$$

$$(B41) \quad dt' = \frac{du}{df/dt'} \equiv \frac{du}{\kappa} \quad (\text{as before})$$

$$g(u) = \frac{\bar{\beta}(f^{-1}) - \hat{n}}{R(f^{-1})}$$

Then one has for I_2 that

$$I_2 = \frac{1}{c} \int \frac{g(u)}{df/dt'} \delta'(u-t) du$$

The above can be integrated by parts on the derivative of the delta function to yield:

$$I_2 = -\frac{1}{c} \int \delta(u-t) \frac{d}{dt'} \left\{ \frac{g(u)}{\kappa} \right\} \frac{dt'}{du} du$$

This can then be integrated in the same manner as I_1 to yield

$$I_2 = - \frac{1}{c} \left(\frac{dt'}{du} \frac{d}{dt'} \left\{ \frac{g(u)}{\kappa} \right\} \right) \Big|_{u=t}$$

or using the substitutions indicated in (B40)

$$(B42) \quad I_2 = - \left[\frac{1}{\kappa c} \frac{d}{dt'} \left(\frac{\hat{\beta} - \hat{n}}{\kappa R} \right) \right]_{\text{ret}}$$

The equation (B33) for $\bar{E}(\bar{r}, t)$ can be written in a closed form if one employs (B40) and (B41). The results of this are

$$\bar{E}(\bar{r}, t) = \frac{e}{4\pi\epsilon_v} \left[\frac{\hat{n}}{\kappa R^2} + \frac{1}{\kappa c} \frac{d}{dt'} \left(\frac{\hat{n} - \bar{\beta}}{\kappa R} \right) \right]_{\text{ret}}$$

To perform the differentiation $-\frac{1}{c} \frac{d\hat{n}}{dt'}$ one can use the following identity presented here without proof or justification²³

$$(B43) \quad \frac{1}{c} \frac{d\hat{n}}{dt'} = \frac{1}{R} \{ (\hat{n} \cdot \bar{\beta}) \hat{n} - \bar{\beta} \}$$

Using the substitution indicated by (B43) and performing the necessary algebra, one finds the following relation for $\bar{E}(\bar{r}, t)$:

$$(B44) \quad \bar{E}(\bar{r}, t) = \frac{e}{4\pi\epsilon_v} \left[\frac{\hat{n}}{\kappa^2 R^2} + \frac{\hat{n}}{c\kappa} \frac{d}{dt'} \left(\frac{1}{\kappa R} \right) - \frac{\bar{\beta}}{\kappa^2 R^2} - \frac{1}{c\kappa} \frac{d}{dt'} \left(\frac{\bar{\beta}}{\kappa R} \right) \right]_{\text{ret}}$$

If one had performed similar calculations to those performed up to this point on $\bar{B}(\bar{r}, t)$ where $\bar{B} = \nabla \times \bar{A}$ then the following relation would have been found for $\bar{B}(\bar{r}, t)$:

$$(B45) \quad \bar{B}(\bar{r}, t) = \frac{ec\mu_v}{4\pi} \left\{ \left(\frac{\bar{\beta}}{\kappa^2 R^2} + \frac{1}{c\kappa} \frac{d}{dt'} \left\{ \frac{\bar{\beta}}{\kappa R} \right\} \right) \times \hat{n} \right\}$$

One can easily show using (B44) and vector algebra that the following relation exist between E and B:

$$(B46) \quad \bar{B}(\bar{r}, t) = \frac{1}{c} \{ \hat{n} \times \bar{E}(\bar{r}, t) \}$$

²³To verify this relation one should realize that $r = \bar{x}(t') + \bar{R}(t')$ and that for a fixed observer $\frac{dr}{dt} = 0$. Also use the definition of $\hat{n} = \bar{R}(\bar{R} \cdot \bar{R})^{-1/2}$.

In order to obtain a more explicit form for $\bar{E}(\bar{r}, t)$ than that given by (B44) the following relation is noted:

$$\frac{1}{c} \frac{d}{dt'} (\kappa R) = \frac{1}{c} \frac{d}{dt'} \left[(1 - \hat{n} \cdot \bar{\beta}) R \right]$$

$$(B47) \quad \frac{1}{c} \frac{d}{dt'} (\kappa R) = -\frac{R}{c} (\hat{n} \cdot \dot{\bar{\beta}}) - \frac{R}{c} \bar{\beta} \cdot \frac{d\hat{n}}{dt'} + \frac{1}{c} \frac{dR}{dt'} (1 - \hat{n} \cdot \bar{\beta})$$

where

$$(B48) \quad \dot{\bar{\beta}} = \frac{d\bar{\beta}}{dt}$$

Equation (B47) can be rewritten using the substitutions indicated by (B38) and (B43) such that

$$(B49) \quad \frac{1}{c} \frac{d}{dt'} (\kappa R) = \beta^2 - (\bar{\beta} \cdot \hat{n}) - \frac{R}{c} (\hat{n} \cdot \dot{\bar{\beta}})$$

Therefore, if one uses the substitutions given by equations (B48) and (B49) and rearranges the terms using vector algebra then equation (B44) can be written as follows:

$$(B50) \quad \bar{E}(\bar{r}, t) = \frac{e}{4\pi\epsilon_v} \left\{ \left| \frac{\hat{n} - \bar{\beta}}{\kappa^3 R^2} (1 - |\bar{\beta}|^2) \right|_{\text{ret}} + \frac{1}{c} \left| \frac{\hat{n}}{\kappa^3 R} \times \{ (\hat{n} - \bar{\beta}) \times \dot{\bar{\beta}} \} \right|_{\text{ret}} \right\}$$

Appendix C

Derivation of the Green's Function for Conducting Media

If one assumes that a conducting media obeys Ohm's law and that the conductivity is uniform throughout space and constant with respect to time then the following wave equation for the vector and scalar potential can be derived (see Chapter V)

$$(C1) \quad \left\{ \nabla^2 - \mu_V \sigma \frac{\partial}{\partial t} - \frac{1}{c^2} \frac{\partial^2}{\partial t^2} \right\} \begin{vmatrix} \bar{A}(\bar{r}, t) \\ \bar{V}(\bar{r}, t) \end{vmatrix} = \begin{vmatrix} -\mu_V \bar{J}(\bar{r}, t) \\ \frac{1}{\epsilon_V} \rho_C(\bar{r}, t) \end{vmatrix}$$

The Green's function associated with this must satisfy the following equation

$$(C2) \quad \left\{ \nabla^2 - \mu_V \sigma \frac{\partial}{\partial t} - \frac{1}{c^2} \frac{\partial^2}{\partial t^2} \right\} G(\bar{r}, t | \bar{r}', t') = \delta(\bar{r} - \bar{r}') \delta(t - t')$$

One can solve (C2) in exactly the same manner as indicated in the second section of Appendix B using Laplace transform techniques. Doing this one finds the following for the Laplace transform of $G(\bar{r}, t | \bar{r}', t')$:

$$(C3) \quad \tilde{G}(\bar{r}, s | \bar{r}', t') = \frac{1}{4\pi r} e^{-\frac{r}{c} \sqrt{s \left(\frac{\sigma}{\epsilon_V} + s \right)}} e^{-st'}$$

It will be necessary to rearrange some of the terms and use some transform identities in order to get (C3) into a form which can be found in a table of Laplace transforms. The following identity shall be employed (Ref 8, p 491):

$$(C4) \quad \Lambda^{-1} \{ f(s) e^{-st'} \} = F(t - t')$$

where

$$\Lambda^{-1} \{ f(s) \} = F(t) \text{ and } F(t) = 0 \text{ for } t < 0$$

Therefore it is only necessary to find the inverse transform of the following for (C3):

$$(C5) \quad g(s) = e^{-\frac{r}{c} \sqrt{s \left(\frac{\sigma}{\epsilon_v} + s \right)}}$$

If one lets $K \equiv \frac{\sigma}{\epsilon_v}$ then one can write that

$$s \left(s + \frac{\sigma}{\epsilon_v} \right) = s(s + K)$$

or

$$s(s + K) = s^2 + sK + \left(\frac{K}{2} \right)^2 - \left(\frac{K}{2} \right)^2$$

or

$$(C6) \quad s(s + K) = \left(s + \frac{K}{2} \right)^2 - \left(\frac{K}{2} \right)^2$$

Using (C6) one can then write the following for (C5):

$$(C7) \quad g(s) = e^{-\frac{r}{c} \sqrt{\left(s + \frac{K}{2} \right)^2 - \left(\frac{K}{2} \right)^2}}$$

If $F(t) = \Lambda^{-1}\{h(s)\}$ then the following identity is true

(Ref 8, p 491):

$$(C8) \quad \Lambda^{-1}\{h(s - b)\} = e^{bt} f(t)$$

where b is a constant with respect to the transform. Thus, if one lets $h(s)$ be the following:

$$h(s) = e^{-\frac{r}{c} \sqrt{s^2 - \left(\frac{K}{2} \right)^2}}$$

then from (C7)

$$h(s-b) = g(s) = e^{-\frac{r}{c} \sqrt{\left(s + \frac{K}{2} \right)^2 - \left(\frac{K}{2} \right)^2}}$$

where, in this case, $b = -\frac{K}{2}$. Thus, using (C8) one finds

$$(C9) \quad \Lambda^{-1}\{g(s)\} = \Lambda^{-1}\{h(s-b)\} = e^{-\frac{K}{2}t} \Lambda^{-1}\left\{ e^{-\frac{r}{c} \sqrt{s^2 - \left(\frac{K}{2} \right)^2}} \right\}$$

The last term in (C9) can be written as follows by adding 0 to both sides:

$$(C10) \quad \Lambda^{-1} \left\{ e^{-\frac{r}{c} \sqrt{s^2 - \left(\frac{K}{2}\right)^2}} \right\} = \Lambda^{-1} \left\{ e^{-\frac{r}{c} \sqrt{s^2 - \left(\frac{K}{2}\right)^2}} - e^{-\frac{rs}{c}} \right\} + \Lambda^{-1} \left\{ e^{-\frac{rs}{c}} \right\}$$

The inverse transforms of each term on the right hand side of (C10) are common in tables of Laplace transforms. Using such a table the following is found:

$$(C11) \quad \Lambda^{-1} \left\{ e^{-\frac{r}{c} \sqrt{s^2 - \left(\frac{K}{2}\right)^2}} \right\} = \frac{Kr}{2c} \frac{I_1 \left| \frac{K}{2} \sqrt{t^2 - \left(\frac{r}{c}\right)^2} \right|}{\sqrt{t^2 - \left(\frac{r}{c}\right)^2}} U \left| t - \frac{r}{c} \right| + \delta \left(t - \frac{r}{c} \right)$$

where $I_1|x|$ is the modified Bessel's function with argument x and $U|x|$ is the unit step function with argument x . Substituting (C11) into (C9) one finds that:

$$(C12) \quad \Lambda^{-1} \{g(s)\} = e^{-\frac{\sigma}{2\epsilon_v} t} \left\{ \frac{\sigma r}{2\epsilon_v c} \frac{I_1 \left| \frac{\sigma}{2\epsilon_v} \sqrt{t^2 - \left(\frac{r}{c}\right)^2} \right|}{\sqrt{t^2 - \left(\frac{r}{c}\right)^2}} U \left| t - \frac{r}{c} \right| + \delta \left(t - \frac{r}{c} \right) \right\}$$

Finally if one applies (C12) with the identity given in (C4) to (C3) the result is as follows:

$$(C13) \quad G(\bar{r}, t | \bar{r}', t') = \Lambda^{-1} \{ \tilde{G}(\bar{r}, s | \bar{r}', t') \}$$

$$G(\bar{r}, t | \bar{r}', t') = \frac{1}{4\pi r} \left\{ e^{-\frac{\sigma}{2\epsilon_v} (t-t')} \left(\frac{I_1 \left| \frac{\sigma}{2\epsilon_v} \sqrt{(t-t')^2 - \left(\frac{r}{c}\right)^2} \right|}{\sqrt{(t-t')^2 - \left(\frac{r}{c}\right)^2}} \right. \right.$$

$$\left. \times U \left| t-t' - \frac{r}{c} \right| + \delta \left(t-t' - \frac{r}{c} \right) \right\}$$

Vita

John R. Lillis was born on 4 November 1950 in Frankfort, Kentucky. He was graduated from Madison High School in Richmond, Kentucky in 1968. He attended Virginia Polytechnical Institute, Georgia Institute of Technology, and received the degree of Bachelor of Science with a major in physics and a regular commission in the United States Air Force from the University of Kentucky in May, 1972. After graduation he was assigned to the Air Force Institute of Technology where he received a Master of Science degree in Nuclear Engineering in March, 1974. He is a member of Phi Beta Kappa and Tau Beta Pi academic honoraries.

Permanent mailing address: 1421 Fairlane Drive
Richmond, Kentucky 40475

This thesis was typed by Mrs. Laura Reams.